Interaction of alpha-melanocyte stimulating hormone and its analogues with the human melanocortin receptor subtypes: MC1-R and MC4-R

Doherty, Rachel Veronica Mary

Award date:
1996

Awarding institution:
University of Bath

Interaction of α-Melanocyte Stimulating Hormone and its Analogues with the Human Melanocortin Receptor Subtypes: MC1-R and MC4-R

submitted by Rachel Veronica Mary Doherty

for the degree of Doctor of Philosophy

of the University of Bath

1996

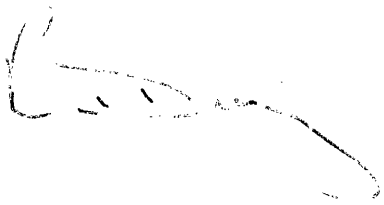

ProQuest LLC
789 East Eisenhower Parkway
P.O. Box 1346
Ann Arbor, MI 48106-1346

For Mum and Dad

ACKNOWLEDGEMENTS

I should like to acknowledge Dr. Colin Pouton for his help as a supervisor, together with his motivation throughout the course of this study.

I also thank Dr. Steve Moss for his administrative support, Dr. Graham Smith for his FACS expertise, Dr. Anthony Smith for helpful chats on molecular biology, Dr. George Olivier for peptide synthesis, Dr. Ulrike Sahm for further peptide synthesis along with immense practical input and Alan Russell for computing assistance.

I am grateful to Prof. D.J. Davies for providing the facilities for this work and to many other people within the department for their day to day assistance.

Sincere thanks go to my family for their constant encouragement and multifaceted help, with particular recognition for Dad who battled his way through this text to perform invaluable services as a proof-reader. The 'endurance award' however, unquestionably belongs to Steve with his remarkable patience and unfailing support.

There are so many others whose cheery presence and friendship helped make the last three years fly by, those within Bath including Ulrike, Martine, Dave, and housemates Su, Gwen and especially Em.

A final 'big-hand' must go to all past and present lab members who, each in their own inimitable way, contributed to the general insanity and camaraderie that made 2.29 a unique place to work in. Particular mention must go to Bev, Al, Pete, Paul, Ady, Aima, Dave, Heidi, Heather and Niamh, without whom lab-life would have been so much less colourful.

TABLE OF CONTENTS

ABBREVIATIONS

ACTH	adrenocorticotropic hormone
BSA	bovine serum albumin
cAMP	cyclic adenosine 3'-5' monophosphate
cDNA	complementary deoxyribonucleic acid
Ci	Curie
CLIP	corticotrophin-like intermediate lobe peptide
CMV	cytomegalovirus
CNS	central nervous system
cpm	counts per minute
Da	Daltons
DHI	dihydroxyindole
DHICA	dihydroxyindole carboxylic acid
DMF	dimethylformamide
DMSO	dimethylsulphoxide
DNA	deoxyribonucleic acid
DOPA	3,4-dihydroxyphenylalanine
dpm	decays per minute
EDTA	ethylenediaminetetraacetic acid
EC_{50}	concentration of ligand required for 50% maximal response
F	Farad
FAB-MS	fast atom bombardment mass spectroscopy
FACS	fluorescence activated cell sorting
FBS	foetal bovine serum
FITC	fluorescein isothiocyanate
g	acceleration due to gravity (9.81 ms^{-1})
G418	geneticin
HEK	human embryonic kidney (cells)
HEPES	*N*-(2-hydroxyethyl)piperazine-*N*-2-ethane sulphonic acid
hMC-R	human melanocortin receptor
HPLC	high pressure liquid chromatography
IBMX	1-methyl-3-isobutylxanthine
IC_{50}	concentration of ligand required to inhibit 50% maximal response
IL	interleukin
IPTG	isopropyl β-D-thiogalactopyranoside
K_d	dissociation constant of radioligand
K_i	dissociation constant of competitor
LPH	lipotropin
μ	micro (10^{-6})
M	mole(s) per litre
MBq	mega (10^6) Becquerel(s)
MC	melanocortin
mMC-R	murine melanocortin receptor
mRNA	messenger ribonucleic acid
MSH	melanocyte-stimulating hormone
MTT	1-[4,5-dimethylthiazol-2-yl]-3,5-diphenylformazan

MW	molecular weight
n	nano (10^{-9})
NMR	nuclear magnetic resonance
NO	nitric oxide
OD	optical density
PAGE	polyacrylamide gel electrophoresis
PBS	phosphate buffered saline
PCA	perchloric acid
PCR	polymerase chain reaction
PKA	protein kinase A
POMC	pro-opiomelanocortin
RER	rough endoplasmic reticulum
RNA	ribonucleic acid
rpm	revolutions per minute
SDS	sodium dodecyl sulphate
TEMED	*N,N,N,N*-tetramethylethyldiamine
TFA	trifluoroacetic acid
TPA	12-*O*-tetradecanoyl phorbol-13-acetate
Tris	tris(hydroxymethyl) aminomethane
TRP	tyrosinase-related protein
UV	ultraviolet
V	volt(s)
v/v	volume by volume
w/v	weight by volume
X-gal	5-bromo-4-chloro-3-indoyl-β-D-galactopyranoside

SUMMARY

The melanocortin (MC) receptors form a subgroup within the G-protein-coupled receptor superfamily. To date five receptor subtypes have been characterised, differing in their melanocortin peptide specificities and main sites of expression.

The work presented in this thesis involved an investigation into the structure-activity relationships of the interaction of α-MSH with two of the human melanocortin receptor subtypes: MC1-R and MC4-R which have been shown previously to exhibit similar ligand binding profiles. Transient and stable receptor expression took place in COS7 and HEK 293 cells, respectively, to overcome problems associated with relatively low level native expression. Attention was focused on the tryptophan-9 residue within the central core and the C-terminal of α-MSH, both regions being regarded as important for receptor binding and activation. Appropriate α-MSH analogues were synthesised by solid-phase techniques and assayed for both receptor binding and stimulation as determined by cAMP quantification.

Aromaticity of the tryptophan-9 residue was found to be of prime importance, and the requirement for the presence of the C-terminal for full activity confirmed. Partial delineation of the structural requirements for high affinity binding to and stimulation of the two receptor subtypes was achieved with the discovery that [Pro^{12}] and [Gly^{10}] of α-MSH appear critical for conferring peptide selectivity on the human MC1-R and MC4-R, respectively.

A preliminary attempt was made at site-directed mutagenesis of the human MC1-R with the aim of validating a model for hormone-receptor interaction as proposed by this laboratory using molecular modelling techniques.

Taken together, this two-pronged approach aims to yield further information about melanocortin receptor subtype specificities. Such a fundamental understanding is a prerequisite for the development of both subtype specific agonists and antagonists. Given the pleiotropic nature of these peptides, such compounds may have important therapeutic implications.

CHAPTER 1: INTRODUCTION

Interest in the melanotropic peptides, or melanocortins, was first stimulated early this century when Fuchs (1912) demonstrated that pituitary extracts darken the skin of frogs. Shortly afterwards it was shown that amphibian pituitary gland removal leads to a loss of pigmentation, thus illustrating how control of amphibian skin colour is dependent on an intact pituitary gland. This led to extensive investigation into the pigmentation effects of these peptides in lower vertebrates. Further research into these peptides disclosed the functional relationship between the melanocortins, adrenocorticotropin, lipotropin and endorphin, which culminated in the isolation of their common precursor, pro-opiomelanocortin, POMC.

More recent discoveries of peripheral sites of melanocortin synthesis together with their apparent multiple roles in the central nervous system and the cloning of their receptor subtypes have established the importance of these peptides in mammals, including man.

1.1. Production of POMC

Active peptides produced by eukaryotic cells are usually synthesised as fragments of large precursor proteins. The prohormone, pro-opiomelanocortin, was the first polypeptide to be discovered as a precursor for several functionally distinct peptides. Biologically active POMC cleavage products include the α-, β- and γ-melanocyte-stimulating hormones (MSHs), adrenocorticotropic hormone (ACTH), and β-endorphin (Figure 1.1.).

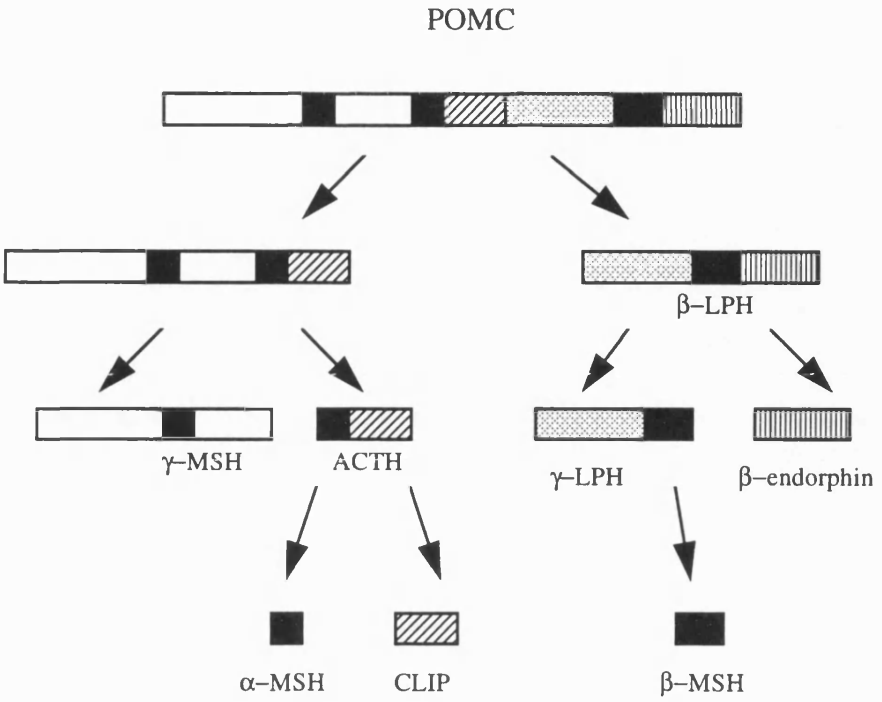

Figure 1.1. Diagrammatic representation of POMC cleavage giving rise to melanocortin, lipotropin and β-endorphin fragments.

Nakanishi *et al.* (1979) determined the 1091 base pair nucleotide sequence of cloned cDNA of the mRNA encoding for bovine POMC and by 1980, the gene structure for POMC in several mammalian species, including man (Chang, 1980), had been determined. The POMC gene probably evolved by duplication of ancestral genes as suggested by the three MSH sequences contained within it. This evolution by duplication may have been directed by the pleiotropic function of POMC as a prohormone for a number of actions. As all vertebrates investigated to date have a POMC gene containing all three sequences, this duplication must have occurred at an early stage in evolution (Eberle, 1988).

As with other precursor proteins, biosynthesis begins on the rough endoplasmic reticulum (RER). Cleavage of the signal peptide occurs within the RER with subsequent passage to the Golgi apparatus. Further post-translational modifications take place within the Golgi, including glycosylation and phosphorylation, (Zimmerman *et al.*, 1980). From the Golgi complex the protein passes to storage secretory vesicles where upon concomitant vesicle maturation and acidification, the processing proteolytic enzymes are activated (Orci, 1986). These specific trypsin-like endopeptidases cleave at sites of paired basic amino acids, namely -Lys-Lys-, -Arg-Arg-, -Lys-Arg-, and -Arg-Lys-, and, together with further enzymes that modify the initial cleavage products generate the various POMC fragments.

Tissue-specific post-translational processing mechanisms for POMC observed in the pituitary of adult mammals result in the production of ACTH(1-39) by corticotropes and α-MSH, (N-acetyl-ACTH(1-13)amide), by melanotropes as major end-products.

1.2. The Melanocyte-Stimulating Hormone Family

1.2.1. α-Melanocyte-Stimulating Hormone

Figure 1.1. illustrates the cleavage pattern of POMC and the formation of α-MSH from ACTH. In 1957, Harris and Lerner determined the amino acid sequence of porcine α-MSH and described it as having a blocked N-terminal and amidated C-terminal. The amino acid sequence of α-MSH corresponds to ACTH(1-13), the final composition (Figure 1.2.) of which was elaborated by Harris (1959) and led to the characterisation of α-MSH as a tridecapeptide with an isoelectric point of 10.5-11. It

is now known that the N^{α}-amino group of [Ser^{1}] is either free (desacetyl-α-MSH) or blocked with one or two acetyl groups, depending on the tissue of synthesis .

It would be predicted that a minimum of three enzymes would be required for the conversion of ACTH(1-39) to ACTH(1-13)amide and ACTH(18-39), the latter fragment being known as CLIP. An endopeptidase would first be required to cleave the -Arg-Arg- residues at positions 17 and 18 in ACTH(1-39). A carboxypeptidase-like enzyme would then be required to remove sequentially the -Lys-Lys-Arg- residues at positions 15, 16 and 17. Finally, an alpha-amidating enzyme is needed to convert ACTH(1-14) into ACTH(1-13)amide (Dores, 1990). A fourth enzyme, N-acetyltransferase, is required to convert ACTH(1-13)amide into α-MSH. This enzyme is localised in secretory granules in mammals and the reaction occurs prior to secretion (Glembotski, 1982).

Isolation and structural analysis of this peptide from a number of mammals shows a high sequence conservation of this peptide during evolution.

Ac-Ser^{1}-Tyr^{2}-Ser^{3}-Met^{4}-Glu^{5}-His^{6}-Phe^{7}-Arg^{8}-Trp^{9}-Gly^{10}-Lys^{11}-Pro^{12}-Val^{13}-NH_2

Figure 1.2. Amino acid sequence of α-MSH as determined by Harris (1959).

1.2.2. β-Melanocyte-Stimulating Hormone

The carboxy-terminal of POMC produces the cleavage fragment β-lipotropin (β-LPH), which undergoes further processing to give γ-lipotropin (γ-LPH), β-endorphin and β-MSH (Figure 1.1.).

β-MSH is an octadecapeptide and corresponds with the sequence γ-LPH(41-58) (Bertagna *et al.*, 1986). The peptide shows considerably more inter-species variation than α-MSH with some species expressing more than one form (Lee *et al.*, 1963), indicating the expression of two different genes or alternative post-translational modifications. In common with α-MSH, mammalian β-MSH contains the heptapeptide sequence: Met-Glu-His-Phe-Arg-Trp-Gly.

1.2.3. γ-Melanocyte-Stimulating Hormone

Analysis of the POMC sequence showed the presence of the tetrapeptide His-Phe-Arg-Trp within its N-terminal region. Three possible cleavage sites are present which would give rise to three fragments corresponding to the sequences (51-61), (51-62), and (51-77) of bovine N-POMC (Ling *et al.*, 1979). These potential fragments were named γ_1-, γ_2- and γ_3-MSH respectively (Figure 1.3.). The search for the naturally occurring fragments first resulted in the isolation of N-POMC(1-76/77) or pro-γ-MSH, from the human pituitary which is the precursor for the smaller peptides, (Estivariz *et al.*, 1980). The presence of these peptide products in mammalian pituitary extracts has since been determined (Böhlen *et al.*, 1981; Tanaka *et al.*, 1980), and all were found to have an additional lysine residue at the N-terminus end, indicating alternative cleavage patterns to those predicted.

γ_1-**MSH** Tyr-Val-**Met**-Gly-**His-Phe-Arg-Trp**-Asp-Arg-Phe-NH_2

γ_2-**MSH** Tyr-Val-**Met**-Gly-**His-Phe-Arg-Trp**-Asp-Arg-Phe-Gly-OH

γ_3-**MSH** Tyr-Val-**Met**-Gly-**His-Phe-Arg-Trp**-Asp-Arg-Phe-Gly-Arg-Arg-Asn-Gly-Ser-Ser-Ser-Ser-Gly-Val-Gly-Gly-Ala-Ala-Gln-OH

Figure 1.3. Structure of mammalian γ-MSH peptides as proposed from analysis of the POMC gene (Eberle, 1988).

1.3. Distribution of α-MSH and other POMC Products

1.3.1. Pituitary

POMC is synthesised in the corticotropic cells of the *pars distalis* and in the melanotropic cells of the intermediate lobe, or *pars intermedia,* of the pituitary gland (Eipper and Mains, 1980). The *pars intermedia* of the pituitary gland is therefore the major biosynthetic source of α-MSH in most species, including the rat (Vaudry *et al.*, 1978). Adult humans, however, lack an anatomically distinct *pars intermedia.* The *pars intermedia* present in the foetal human pituitary undergoes regressive development after birth and intermingles with the *pars distalis* (Daniel and Pritchard, 1975). This modified region along the neural tube is termed the *zona intermedia.*

Only low concentrations of α-MSH can be detected in the human pituitary gland, most of which is in the desacetylated form (Tilders *et al.*, 1981). However, the human foetus contains high α-MSH bioactivity which decreases dramatically after

birth. This may be a consequence of the human foetus, unlike the adult, having a well-developed intermediate lobe. β-MSH is not normally produced by the human pituitary gland as adult melanotrophs lack the enzyme required for cleavage of γ-LPH into β-MSH (Scott and Lowry, 1974).

1.3.2. Brain

It has been known for many years that MSH bioactivity exists in the brain (Rudman *et al.*, 1973). It was postulated that these peptides are synthesised in the CNS rather than being transported from the pituitary gland as α-MSH and β-endorphin in the brain are not depleted by hypophysectomy (Vaudry *et al.*, 1978). Distribution of α-MSH in both its acetylated and desacetylated forms within the human brain is uneven with the highest concentration found in the hypothalamus. β-MSH has also been identified in the hypothalamus, suggesting that the human pituitary is an exception in its inability to cleave γ-LPH into β-MSH (Bertagna *et al.*, 1986).

1.3.3. Placenta

Opiomelanogenic peptides, including ACTH and α-MSH have been identified in human placental extracts (Clark *et al.*, 1978). The foetal pituitary may be the source although it is improbable that α-MSH can cross the placental barrier. The maternal pituitary may produce α-MSH during pregnancy, but the placenta cannot be ruled out as a site of production. Indeed, biosynthesis of opiomelanotropinergic peptides similar to that described in the pituitary has been demonstrated in cultured

human placental trophoblastic cells (Liotta and Krieger, 1980). This suggests a trophic function during foetal development, although Chen *et al.* (1986) found placental POMC mRNA content to remain unchanged during pregnancy. In addition, the close interrelationship of the foetal brain and pituitary with the placenta together with the synthesis of a wide range of hormones and growth factors, makes it difficult to assess the relative importance of MSH and other POMC peptides for foetal development.

1.3.4. Gastrointestinal Tract

POMC products have been found by immunoreactive detection studies in endocrine cells of the human gastrointestinal tract and pancreas and were not eliminated by hypophysectomy (Feurle *et al.*, 1980). Their presence suggests local synthesis and processing but a precise physiological role is still uncertain.

1.3.5. Skin

POMC mRNA and its melanocortin products have been detected in the skin (Slominski *et al.*, 1993; Thody *et al.*, 1983), including constitutive expression in keratinocytes (Wintzen *et al.*, 1996). Keratinocyte-derived factors have been shown to affect human melanocyte growth and melanogenesis *in vitro* (Gordon *et al.*, 1989), emphasising the importance of these cells as regulators of melanocyte behaviour and suggesting a paracrine role for the melanocortins in pigmentation.

1.3.6. Ectopic Tumours

MSH bioactivity has been found in various tumour tissues. For example, α-MSH and β-MSH largely account for melanocortin bioactivity detected in patients with ectopic ACTH syndrome (Abe *et al.*, 1967; McLoughlin *et al.*, 1980).

Elevated plasma levels of α-MSH have also been detected in melanoma patients with Ghanem *et al.* (1986) reporting increased values for about one third of their patient sample as compared to controls.

As can be seen from the above summary, MSH peptides occur widely throughout the body. This suggests that the melanocortins have multiple endocrine regulatory functions mediated by various responsive tissues expressing receptors for these hormones.

1.4. Functions of α-MSH

1.4.1. Amphibians

MSH was so-termed after discovery of its pigmentation role in lower vertebrates (Lerner *et al.*, 1954). It causes rapid dispersion of melanin granules stored within the melanosomes of melanophores thereby causing the colour changes commonly seen in these animals. This observation led to the development of assay methods involving visual detection of changes in amphibian skin pigmentation (Tilders *et al.*, 1975; Carter and Shuster, 1978), most commonly in the lizard (Anolis) and frog (Rana).

This research has been reviewed by Eberle (1988) and is only considered within this work in terms of the relevant insights and conclusions drawn.

1.4.2. Mammals

1.4.2.1. Mammalian pigmentation

Melanin pigmentation is recognised as being the most important factor in determining hair and skin colour and is formed from specialised pigment-producing cells known as melanocytes. Melanocytes originate from neural crest cells which in turn are derived from the embryonic ectodermal germ layer. Most melanocytes migrate during embryogenesis to the epidermis, where they differentiate towards epidermal or follicular melanocytes. Each melanocyte is associated with approximately 36 keratinocytes. The established function of epidermal melanocytes is the production and transfer of melanin granules to surrounding keratinocytes with subsequent degradation. Follicular melanocytes, however, undergo cyclical proliferative and melanogenic activity which is coupled to the growing phase of the hair follicles and determines the colour of the mature hair shaft (Fitzpatrick *et al.*, 1979).

Although administration of α-MSH causes skin darkening in man (Lerner and McGuire, 1961) and specific α-MSH binding sites have been demonstrated on human melanocyte cell surfaces (Donatien *et al.*, 1992; De Luca *et al.*, 1993), early data suggested that MSH peptides fail to stimulate tyrosinase activity and hence melanin production in cultured human melanocytes (Halaban *et al.*, 1983). However, Hunt *et al.* (1994) proposed that these results were a consequence of mitogens such as TPA and cholera toxin routinely included in the culture media, which were found to affect basal melanogenesis levels. Exclusion of these agents produced significant, although variable increases in tyrosinase activity and melanin content on α-MSH stimulation (Hunt, 1995).

1.4.2.1.1. Mechanism of action

The complex formed on interaction of MSH with its receptor appears to be rapidly internalised (García-Bórron *et al.*, 1992), with lysosomal degradation (Adams, 1993) and subsequent recycling of the receptor within a few minutes (Orlow *et al.*, 1990).

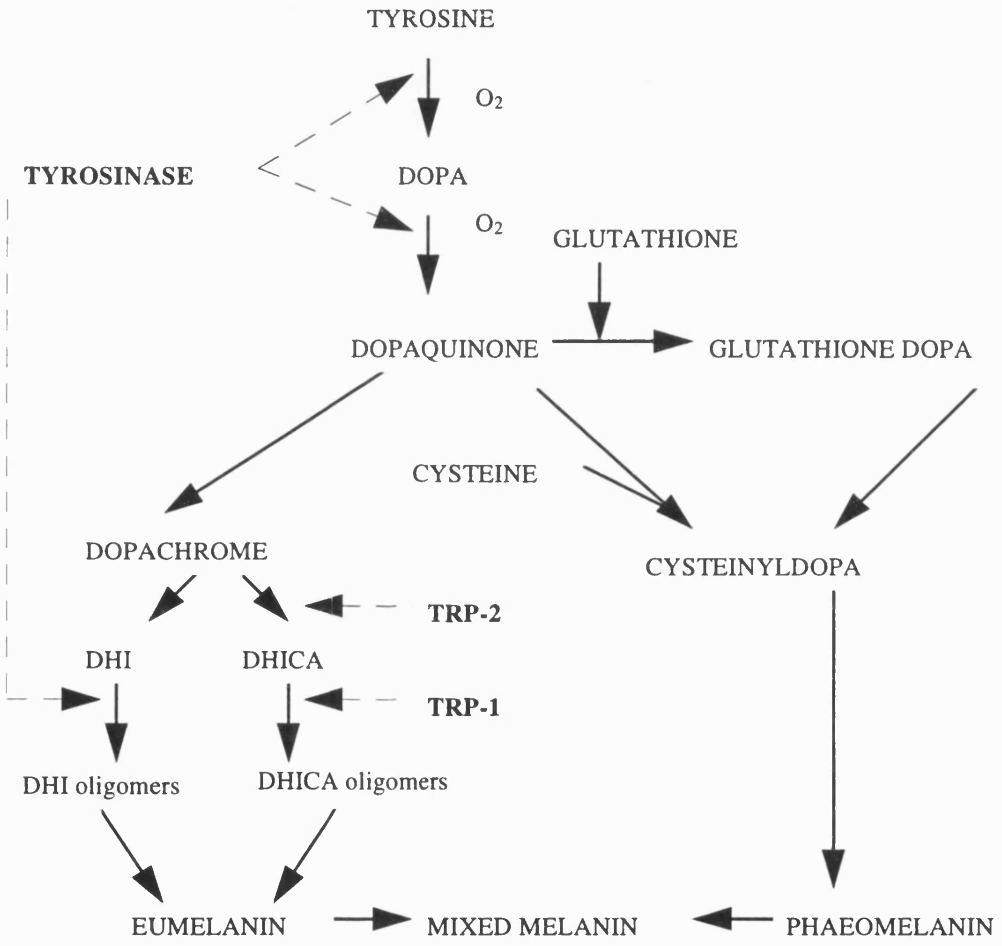

Figure 1.4. Schematic representation of the metabolic pathway of tyrosine to melanin (adapted from Thody, 1995).

The mechanism of action of α-MSH on pigment production in mammalian melanocytes and melanoma cells is thought to be via receptor-mediated induction of the second messenger, cAMP, since both dibutyryl cAMP and theophylline, a phosphodiesterase inhibitor, mimic MSH action (Bitensky and Demopoulos, 1970; Wong. and Pawelek, 1973; Fuller and Lebowitz, 1980). MSH stimulation of the enzyme adenylate cyclase via G-protein activation (Kreiner *et al.*, 1973) is responsible for this increase in cAMP which in turn induces protein phosphorylation via protein kinase A (PKA) stimulation (de Graan *et al.*, 1987). However, Buffey *et al.* (1991) proposed the involvement of a second system. They found that whereas the melanogenic response to MSH is dependent on cell density, cAMP production is not. Further work established a role for protein kinase C, whose effect appears to be at least partially mediated by PKA-induced phosphorylation of the receptor itself (Buffey *et al.*, 1992).

Although these molecular events are still unclear, they culminate in tyrosinase activation and melanin production. Tyrosinase is the rate-limiting enzyme in the melanin biosynthetic pathway depicted in Figure 1.4. and is a multifunctional copper-containing glycoprotein which exists as a single chain. Synthesis occurs on ribosomes, followed by transfer through the endoplasmic reticulum to the Golgi complex, where glycosylation takes place. It is then packaged into vesicles which fuse with the pre-melanosomes where the enzyme becomes functionally active and where melanogenesis occurs (reviewed Hearing and Tsukamoto, 1991). The human tyrosinase gene has been cloned and mapped to the albino locus on the long arm of chromosome 11 (Kwon *et al.*, 1987).

Tyrosinase catalyses three reactions in this pathway: (1) the hydroxylation of L-tyrosine to L-dopa, generally considered to be the most critical reaction as the subsequent stages can proceed spontaneously at physiological pH; (2) the oxidation of dopa to dopaquinone, an extremely reactive compound that rapidly enters the eumelanin or phaeomelanin pathway; (3) the hydroxylation of 3,6-dihydroxyindole (DHI) to indole-quinone leading to eumelanin production (Körner and Pawelek, 1982). This last enzymatic role may explain why eumelanogenesis is more dependent on tyrosinase than is phaeomelanin production, as discussed below. The first and third reactions require dopa as a co-factor whereas in the second, dopa is a substrate.

Tyrosinase activity is regulated by α-MSH, which induces a 2-5 fold increase in the transcription of its gene (Kwon *et al.*, 1988; Hoganson *et al.*, 1989) and a 5-50 fold increase in tyrosinase activity (Wong and Pawelek, 1975; Halaban *et al.*, 1984). However, the precise molecular mechanisms underlying tyrosinase induction were debated for some time. Wong and Pawelek (1975) proposed that MSH acts on Cloudman S91 mouse melanoma cells by converting pre-existing tyrosinase molecules from an inactive to an active state. Jiménez *et al.* (1988) found a large increase in tyrosinase activity which preceded the necessary time lag for *de novo* tyrosinase synthesis, thereby lending weight to this proposal. However, Halaban *et al.* (1983, 1984) found an approximately linear correlation between tyrosinase mRNA abundance and tyrosinase activity produced by MSH stimulation in both mouse melanoma cells and cultured human melanocytes. They therefore suggested that the increase in tyrosinase activity can be attributed solely to increased enzyme synthesis. Other studies by Fuller *et al.* (1987) provided evidence that melanogenesis absolutely requires both continued transcription and translation. However, in contrast

to the above results, the increase in tyrosinase mRNA which they detected was insufficient to account for the large increase in enzyme activity.

Valverde *et al.* (1992) attempted to reconcile these apparent contradictions with their discovery of tyrosinase isoenzymes with different catalytic properties. They proposed that the isoenzyme preferentially induced by melanotropic agents displays a larger ratio of tyrosine hydroxylase to dopa oxidase activity, and would therefore primarily affect the first, rate-limiting step of the melanogenic pathway.

These tyrosinase-related proteins (TRPs) are structurally related to tyrosinase, showing 45% sequence homology with conserved copper-binding sites. Together with tyrosinase, they constitute the "tyrosinase gene family" and the expression of their protein products is increased by α-MSH stimulation (Abdel-Malek *et al.*, 1995). TRP-1 has been shown to have dihydroxyindole carboxylic (DHICA) oxidase activity and may therefore have an enzymatic role in the eumelanin pathway (Jiménez-Cervantes *et al.*, 1994). It is present in both human epidermis (Tobin *et al.*, 1994) and cultured melanocytes (Abdel-Malek *et al.*, 1993). Orlow *et al.* (1993) found TRP-1 to be associated with pre-melanosomes unlike tyrosinase which is primarily found in mature melanosomes. This raises the possibility of TRP-1 having a melanosomal development role. TRP-2 is detectable in human melanocytes *in vivo* (Tobin *et al.*, 1994) and, in mice, has been shown to act as a dopachrome tautomerase, an enzyme involved in eumelanogenesis (Tsukamoto *et al.*, 1992).

1.4.2.1.2. Melanin production

There are two main types of mammalian melanin produced which share the same biosynthetic pathway: eumelanin, which gives rise to brown-black coloration, and phaeomelanin, which produces yellow-red coloration (Prota, 1980). As discussed above, tyrosinase acts on its L-tyrosine substrate, converting it first to dopa and then to dopaquinone. At low tyrosinase activity, the levels of dopa are low and the default pathway is the synthesis of cysteinyl-dopa which is incorporated into melanin to give phaeomelanin. On excess production of dopa, as results after maximal stimulation by MSH, dopa is converted to dopachrome which gives black eumelanin when incorporated into melanin.

The relative amounts of eumelanin and phaeomelanin are controlled primarily by two loci in mammals: *extension* and *agouti* (Jackson, 1993).

Extension

It has been shown that the murine *extension* locus encodes the melanocortin-1 receptor, or MC1-R (section 1.6.). The locus increases brown / black pigment when dominant *(E)*, and blocks eumelanin synthesis, thereby extending the range of red / yellow pigment, when recessive *(e)*.

The absence of functional MC1-R in the recessive yellow mouse demonstrates its dispensability for normal melanocyte growth and development. However, MSH receptor activity is absolutely required for most eumelanin pigmentation of hair (Robbins *et al.*, 1993). Eumelanin synthesis in dermal melanocytes is less dependent on MSH receptor stimulation than it is in hair follicular melanocytes since eumelanin

is still found in the skin of homozygous recessive *(e/e)* animals (Hauschka *et al.*, 1968). Several dominant mutant murine alleles have been isolated. The tobacco allele, E^{tob}, results from a serine-to-leucine change at position 69 in the first intracellular loop of the receptor. The expressed receptor exhibits a slightly elevated basal activity and is a greater stimulant of adenylate cyclase as compared to the wild-type. The mutant sombre alleles, E^{So} and $E^{So\text{-}3J}$, in contrast, create constitutively active receptors which are a result of leucine-to-proline changes at position 98 and glutamic acid-to-lysine at position 92, respectively (Robbins *et al.*, 1993). High concentrations of α-MSH were found to have no additional stimulatory effect, although the α-MSH analogue, [Nle^4,DPhe^7]-α-MSH, further activated these sombre mutants to maximal level (Cone *et al.*, 1996).

Agouti

Cloning and characterisation of the *agouti* locus have found the murine gene to encode for a 131 amino acid polypeptide with a central lysine-rich domain, a C-terminal tail containing ten cysteine residues capable of forming five disulphide bonds and a signal sequence (Bultman *et al.*, 1992). This latter property suggests a paracrine role for agouti protein. *In vitro* site-directed mutagenesis studies have established the importance of the signal peptide and the C-terminal cysteine residues for full biological activity. However, at least a portion of the lysine-rich basic domain appears to be dispensable for normal function (Perry *et al.*, 1996).

Protein database scans have indicated that agouti is a novel protein with no strong identity or sequence homology to other known families. However, its overall structure is similar to several short venomous peptide toxins which disrupt the

function of cellular receptors and ion channels in a similar manner to the mechanism proposed for agouti protein in coat-colour determination (Olivera *et al.*, 1994).

Agouti functions to regulate the differential production of melanin pigments by melanocytes. In animal hair follicles, it opposes the α-MSH-induced synthesis of eumelanin resulting in a band of yellow phaeomelanin (Jackson, 1993).

Recent research showed the competitive inhibition of both agonist binding and activation at the murine melanoma MC1-R over a range of agouti protein and MSH concentrations (Lu *et al.*, 1994; Blanchard *et al.*, 1995). This supports the view that agouti acts to inhibit melanocortin binding and action at the receptor level. However, this action appears to be specific to certain melanocortin receptor subtypes as antagonism also occurs at the MC4 receptor but not the MC3 or MC5 receptors (section 1.6) (Lu *et al.*, 1994). There is also evidence that agouti protein may increase intracellular Ca^{2+} concentrations, perhaps by the binding to, and stimulation of, Ca^{2+} channels, (Zemel *et al.*, 1995) - an observation supported by Hunt and Thody's finding (1995) that agouti antagonises the effect of verapamil on melanogenesis. Hunt and Thody (1995) also demonstrated the inhibitory effect of agouti protein on basal melanogenesis together with an absence of inhibition of α-MSH-induced melanogenesis except at high agouti protein concentrations. Siegrist *et al.* (1996) observed an anti-proliferative effect by agouti protein on B16 murine melanoma cells *in vitro*, with concomitant MC1-R down-regulation. They hypothesised that down-regulation of the MC1-R produces lower levels of intracellular second messengers such as cAMP which are necessary for normal cell growth and function.

Taken together, these data suggest that the antagonism hypothesis is an oversimplification and support a multi-functional role for agouti protein in the

regulation of melanogenesis, perhaps via a specific agouti receptor as proposed by Conklin and Bourne (1993) and Yen *et al.* (1994).

Dominant mutations at this locus in the mouse lead to phenotypic changes, including obesity, hyperinsulinaemia and a predominantly yellow coat colour (Wolff *et al.*, 1986; Wolff, 1987; Klebig *et al.*, 1994; Yen *et al.*, 1994). Agouti has been found to antagonise the MC4 receptor which is largely expressed in the hypothalamus (Lu *et al.*, 1994). This is an area recognised to be important in the regulation of feeding behaviour, and has led to the hypothesis of aberrant ectopic agouti expression producing obesity as a result of pathogenic antagonism of one or more melanocortin receptors.

As no agouti pigmentation phenotype is known in man, it was for a long time uncertain as to whether humans expressed the agouti protein. Kwon *et al.* (1994) resolved the debate with their cloning and characterisation of the human homologue. It was found to be 85% identical to the mouse gene, encoding a 132 amino acid protein. The group mapped it to a region of chromosome 20, close to a locus which has been implicated in the development of non-insulin-dependent diabetes.

Human agouti mRNA has been identified in testis, ovary and heart, and at lower levels in adipose tissue, liver and foreskin (Willard *et al.*, 1995; Wilson *et al.*, 1995). This discovery together with demonstrated inhibition of melanogenesis by agouti protein in human melanocytes (Hunt and Thody, 1995) provides further evidence of a possible correlation with disease states in man similar to those seen in mice as described above.

1.4.2.1.3. UV radiation

The physiological response to ultraviolet radiation includes an increase in melanocyte number, melanin synthesis, and the transfer of pigment granules to surrounding keratinocytes (Goldsmith, 1991).

Exposure of Cloudman melanoma cells in culture to UVB was found to increase MSH binding capacity and cellular responsiveness to MSH (Bolognia *et al.*, 1989), leading to the proposal that the effects of UV radiation on melanogenesis may be mediated through the MSH receptor system. Support for this hypothesis came from a demonstration that exposure to UVB radiation stimulates the production of mRNA for both POMC and the melanocortin-1 receptor in the murine melanoma cells and keratinocytes (Chakraborty *et al.*, 1995). The superoxide anion, $O_2^{\cdot-}$, was found to be a preferable substrate to molecular oxygen for tyrosinase (Wood and Schallreuter, 1991) thereby providing melanocytes with a specific anti-oxidant mechanism. Cytotoxicity induced by the superoxide anion was found to be lower on melanocortin stimulation of a murine melanoma cell line expressing high tyrosinase levels. This protective effect correlated with tyrosinase, rather than melanin biosynthesis (Valverde *et al.*, 1996). These findings suggest that it is not melanin production *per se* that provides protection against UV-induced damage, rather the utilisation of superoxide by tyrosinase to produce melanin.

1.4.2.2. CNS actions

1.4.2.2.1. Behavioural effects

Ferrari (1958) first demonstrated the behavioural changes induced by intracisternal injection of MSH peptides into mammals and early data have been reviewed in detail by de Wied and Jolles (1982), and O'Donohue and Dorsa (1982).

The manifestations included excessive grooming, a habit characteristic of rodents exposed to novel or conflicting environmental stimuli. The minimum sequence necessary to induce this phenomenon was found to be ACTH(4-7) (Gispen *et al.*, 1975), and was blocked by opiate (Gispen and Wiegant, 1976), muscarinic (Ferrari *et al.*, 1963), and dopaminergic antagonists (Wiegant *et al.*, 1977), indicating the involvement of multiple neurotransmitter systems.

Other effects include heightened sexual arousal (Everard *et al.*, 1977; Thody *et al.*, 1979), and improved avoidance learning together with retention of avoidance-induced behaviour in hypophysectomised rats, (de Wied, 1964, 1965, 1966).

1.4.2.2.2. Peripheral nerve regeneration

Exogenous administration of melanotropic peptides, including the α-MSH(4-9) analogue, [Met$(O_2)^4$,DLys^8,Phe^9]α-MSH, (Org2766), has a trophic action on nerves, an effect which is most apparent during development and nerve regeneration, i.e. in instances of nerve plasticity. It has been proposed that this phenomenon is an amplification of the stimulatory action of endogenous melanocortins (Plantinga *et al.*, 1995). Indeed, melanocortin immunoreactivity has been demonstrated in degenerating, but not intact, nerves (Edwards *et al.*, 1984), further suggesting that local production by traumatised nerves helps mediate neurite outgrowth.

Schwann cells are known to play a significant role in facilitating regeneration and a melanocortin receptor has been isolated from such cells (Dyer *et al.*, 1993). Although originally proposed to be of the MC1-R subtype, further work apparently contradicts this hypothesis as the Org2766 pentapeptide melanocortin sequence was found to be needed for full binding capacity, (Dyer *et al.*, 1995). An explanation could be the expression of multiple melanocortin receptor subtypes on the Schwann cell surface. These results are supported by the observation of Tatro *et al.* (1994) that Org2766 showed no ability to compete with [Nle^4,DPhe^7]α-MSH for binding throughout the CNS, implying the existence of further melanocortin receptors to mediate the effects of this peptide.

1.4.2.2.3. Anti-inflammatory effects

Cannon *et al.* (1986) found that α-MSH directly interferes with the inflammatory action of interleukin-1 (IL-1) on target cells. They postulated that IL-1 and α-MSH are involved in a negative feedback loop whereby stimulated mononuclear cells induce IL-1 to increase pituitary peptide release, which in turn suppresses the production and cellular actions of IL-1. α-MSH appears to have no effect in the absence of IL-1, suggesting that it acts as an endogenous antagonist. However, its superpotent analogue, [Nle^4,DPhe^7]α-MSH, does not effectively block IL-1 action on thymocytes implying that α-MSH action may not be mediated by the receptors cloned to date (section 1.6.).

The C-terminal tripeptide, α-MSH(11-13), exhibits antipyretic and anti-inflammatory action but has lower potency than the parent peptide (Deeter *et al.*,

1988; Richards and Lipton, 1984). However, Hiltz *et al.* (1991) found that alterations of amino acid chirality within the tripeptide can markedly alter potency. D-isomer substitution at position 13, and di-substitution to give [DLys^{11}, DVal^{13}]α-MSH(11-13) confers four-fold greater potency than that exhibited by the L-tripeptide. [DLys^{11}] substitution into the tripeptide results in approximate equipotency with α-MSH(11-13) whereas [DPro^{12}]α-MSH has no significant anti-inflammatory activity. This supports the concept of α-MSH as a natural modulator of the host response and suggests that the anti-inflammatory sequence lies within the carboxy-terminal fragments.

Ceriani *et al.* (1994) found that peripheral inflammation induced by a number of cytokines viz. IL-1β, IL-8, platelet activating factor (PAF), and leukotriene-B4 (LTB4) was inhibited by central administration of both α-MSH and α-MSH(11-13). Spinal transection of these mice completely abolished this effect, indicating the need for intact descending pathways for the anti-inflammatory influence of the central peptide. These findings contradict current theory that mediation and modulation of inflammation is controlled solely by local events and substances produced by peripheral cells and tissues.

Interestingly, intraperitoneal injection of α-MSH(11-13) into spinal transected mice had a strong anti-inflammatory effect, suggesting that the tripeptide can also act directly as an anti-inflammatory in the periphery without induction of central anti-inflammatory signals. The parent peptide produced a small and delayed anti-inflammatory effect, perhaps indicating metabolism of the injected α-MSH and subsequent action of the more active tripeptide (Macaluso *et al.*, 1994).

α-MSH has been identified in the synovial fluid of rheumatoid arthritic patients, suggesting local production (Catania *et al.*, 1994). Star *et al.* (1995) showed the inhibition of the inflammatory mediator nitric oxide (NO) by α-MSH in cultured murine macrophages via inhibition of NO synthase II mRNA and protein production. They also detected low level MC1-R expression on cultured macrophages and found α-MSH to be released by macrophages in response to cytokine treatment. These data suggest that α-MSH is an autocrine factor in macrophages which modulates inflammation by counteracting the effects of pro-inflammatory cytokines. Human neutrophils have also been shown to express MC1 receptors, but unlike macrophages, do not produce melanocortins. α-MSH was found to reduce neutrophil migration, this effect being attributed to alterations in signal transduction induced by cAMP (Catania *et al.*, 1996).

The combined evidence therefore shows that α-MSH has both central and peripheral sites of action and its wide spectrum of activity suggests it inhibits an agent or event common to multiple forms of inflammation.

1.5. Structure - Activity Relationships of the Melanocortins

Early investigations were carried out by measuring and comparing the pigment-dispersing properties of the naturally occurring melanotropic peptides, their analogues, and fragments thereof on reptilian skin. Extrapolation of these results to the various melanocortin receptor subtypes which have since been cloned must be undertaken with caution, although useful insights can be gained from such work.

These data have been extensively reviewed by Eberle (1988), and the following points summarise the general conclusions drawn.

1.5.1. N-terminal Sequence

Acetylation of the N-terminal has been shown to have variable effects depending on the assay used. For example, α-MSH shows almost ten-fold greater potency as compared to desacetyl-α-MSH in Rana melanophores but approximately equivalent activity in Xenopus melanocytes (Eberle *et al.*, 1984). If the size or lipophilicity of this functional group is increased, peptide activity is greatly reduced in these systems (Eberle, 1988). Acetylation decreases N-terminal hydrophilicity, which may increase receptor affinity or protect the peptide from degradation.

The N-terminal tetrapeptide, Ac-Ser-Tyr-Ser-Met-OH, is biologically inactive but when covalently linked to α-MSH(5-13), activity is increased by 50 to 100 fold (Eberle, 1988). Decreased hydrophilicity of residues 1-3, or decreased lipophilicity of [Met^4], results in lower potency. However, replacement of [Met^4] by the isosteric norleucine produces increased activity (Sawyer *et al.*, 1980) as discussed in section 1.5.4. Introduction of an iodine atom at [Tyr^2] slightly decreases potency in several assays whereas insertion of two atoms greatly reduces activity in all assay systems studied (Eberle and Hübscher, 1979).

These data suggest that the primary role of the N-terminal residues is to form a hydrophobic / hydrophilic contact with the receptor and has led to its description as a "peptide potentiator".

1.5.2. Central Region

These residues are known to be critical for full activity of the melanotropic peptides (Eberle, 1988) and would therefore be expected to be particularly sensitive to alteration. The retro-inverse analogue of the α-MSH(5-9) sequence is inactive, suggesting that the peptide backbone as well as the spatial arrangement of the side chains is important for receptor binding and stimulation (Chung and Li, 1967).

Yajima *et al.* (1965, 1966, 1967) investigated in detail the effect of a change in configuration of these core residues and found that substitution of the D-stereoisomer at positions [Phe^7]+[Trp^9] and [Phe^7] alone produced ten-fold greater activity than that seen with the all L-analogue. Single substitution to give [DTrp^9]α-MSH or di-substitution to give [DHis^6,DPhe^7]α-MSH and [DPhe^7,DArg^8]α-MSH gives similar activity to α-MSH, with all other diastereoisomeric substitutions being detrimental.

Other alterations at positions 7 and 8 greatly reduce melanotropic potency, except for replacement of [Arg^8] by norleucine which produces a full agonist (Al-Obeidi *et al.*, 1990), suggesting that [Phe^7] and [Arg^8] play a key role in eliciting the response after hormone-receptor interaction.

[Glu^5] appears to be the most dispensable residue in this sequence although the attachment of large groups to the side chain reduces affinity (Eberle, 1988).

1.5.3. C-terminal Sequence

[Gly^{10}] was described as having a spacer function as substitution with alanine was found to have minimal effect and the addition of one or two further amino acids only moderately affected activity (Medzihradszky, 1976). Omission of this residue,

however, decreases pigment-dispersion in the frog skin assay to 1% of the parent peptide (Medzihradszky 1976; Medzihradszky *et al.*, 1979).

The C-terminal tripeptide, Lys^{11}-Pro^{12}-Val^{13}, is generally regarded to be more important for biological activity than the N-terminal tripeptide. It exhibits weak but distinct activity in the Rana and Anolis assays, resulting in the claim of Eberle and Schwyzer (1975) that it contains a "secondary message sequence". However, other studies show that the tripeptide does not significantly increase the activity of certain α-MSH fragments (Hruby *et al.*, 1987) which, together with data from Sawyer *et al.* (1990), dispute its importance. Loss of the basic side chain of [Lys^{11}] or an increase in lipophilicity decreases activation whereas its D-stereoisomer analogue retains some activity. [DPro^{12}] substitution abolishes activity and [Val^{13}] alterations were found to have minimal effect on potency provided that the side chain remains lipophilic (Eberle, 1988).

ACTH has approximately 1% of the activity of α-MSH in the classical frog skin assay and it is thought that the extension of the C-terminal as found in ACTH hinders contact between the active site of the hormone and its receptor. However, ACTH and α-MSH have been found to have similar activity in human melanocytes and melanoma cells, (Chhajlani and Wikberg, 1992; Gantz *et al.*, 1993a). This raises the possibility of a gradual evolution of the human MSH receptor into an MSH / ACTH receptor.

1.5.4. [Nle^4,DPhe^7]α-MSH: A Superpotent Melanocortin Agonist

Radioiodination of the [Tyr^2] residue of α-MSH for binding assay purposes is difficult as concomitant oxidation of [Met^4] produces a hundred-fold loss of activity (Siegrist *et al.*, 1992). This can be overcome by the use of the analogue [Nle^4]α-MSH in which the sulphur atom of methionine has been replaced by a methylene group. This analogue has been shown to be more potent than α-MSH at stimulating adenylate cyclase activity (Medzihradszky, 1976), as well as being resistant to inactivation by chloramine-T, the oxidant used in peptide iodination for assay purposes.

It has long been recognised that heat-alkali treatment of α-MSH results in its prolonged biological activity (Lee and Buettner-Janusch, 1963). Analysis of the treated peptide revealed partial racemisation, most notably at the [Met^4] and [Phe^7] positions (Sawyer *et al.*, 1980). Heat-alkali treated [Nle^4]α-MSH was also found to exhibit this prolongation despite position 4 being no longer prone to significant racemisation. This suggested that [DPhe^7] is responsible for the observed effect and was confirmed by the chemical synthesis and biological analysis of [Nle^4,DPhe^7]α-MSH (Hadley *et al.*, 1981). The high potency and post-iodination stability of [^{125}I-Tyr^2, Nle^4,DPhe^7]α-MSH as compared to α-MSH has led to its routine use as the standard for melanotropic peptide assays.

The observed prolongation of action may be due to slow dissociation kinetics from the receptor resulting from favourable conformational properties of the diastereoisomer for "irreversible" peptide-receptor interaction (Haskell-Luevano *et al.*, 1996). [Nle^4,DPhe^7]α-MSH was also found to be resistant to degradation by

serum enzymes, suggesting that enzymatic stability is partly responsible for enhanced peptide action *in vivo* (Hruby *et al.*, 1987).

1.5.5. Cyclic Peptides

Potent agonists with rigid structures can provide valuable information regarding the spatial organisation of receptor sites on which they act.

The MSH peptides are linear and therefore extremely flexible. They would be expected to have a random conformation in solution with the preferred conformation only being induced by contact of the hormone with cell surface lipids and receptor proteins, thus ensuring both kinetically and thermodynamically optimal hormone-receptor interaction.

Restriction of this conformational flexibility is a prerequisite for studying the receptor-specific conformations of the peptide. This is carried out in practice by cyclisation of suitable linear derivatives. Specific topological features can be deduced from such compounds as their conformational properties in solution are likely to be very similar to those at the receptor.

It has been suggested that α-MSH analogues adopt a β-turn in the active tetrapeptide, His-Phe-Arg-Trp, and molecular modelling work has shown that it is indeed possible for such a turn to exist. However, the lowest energy conformers were found to lack this structure (Chan *et al.*, 1995). Several approaches have sought to stabilise this postulated reverse turn, including the synthesis of monocyclic α-MSH derivatives. One such analogue, cyclic[Cys^4,Cys^{10}]α-MSH, was described as "superpotent" in reptilian bioassays (Sawyer *et al.*, 1982), but was later shown to have a slightly lower binding affinity than the natural ligand in the B16 murine

melanoma cell line (Sahm *et al.*, 1996). It showed a significantly higher binding affinity than its linear counterpart although the activities of the linear and cyclic analogues were similar. This was proposed to be a consequence of the reduction of the disulphide bridge under the activity conditions used (Sahm *et al.*, 1996). Haskell-Luevano *et al.* (1995b) synthesised bicyclic derivatives with the aim of further limiting the number of available conformations around this "message" sequence. However, the further constraints introduced, resulted in these analogues being less potent than their monocyclic parents, although appropriate modifications may lead to antagonists.

1.5.6. Antagonists

Receptor-specific and potent antagonists would be valuable tools to aid understanding of MSH interaction with its receptors and to help determine physiological roles. This is especially so in the brain where melanocortin receptor expression is complex and associated with numerous CNS functions. Melanocortin receptor antagonist development has been slow as there appears to be little distinction between binding and trigger elements. This suggests that those residues responsible for strong binding are also responsible for receptor activation. Early research resulted in peptides that exhibited low potencies or mixed action, i.e. the display of agonist properties at high concentration and weak antagonistic or potentiating properties at low concentrations.

Al-Obeidi *et al.* (1990), reported the linear α-MSH(4-10) analogue Ac-Nle-Asp-Trp-DPhe-Nle-Trp-Lys-NH_2 to be an antagonist in the frog skin assay but an agonist in the lizard skin assay. Jayawickreme *et al.* (1994) employed a multi-use

peptide library, enabling large-scale screening of potential antagonists of which the most potent was found to be Met-Pro-DPhe-Arg-DTrp-Phe-Lys-Pro-Val-NH_2. This compound competitively inhibited [^{125}I-Tyr^2,Nle^4,DPhe^7]α-MSH binding from each cloned melanocortin receptor subtype, albeit with different potencies (Chhajlani, 1996). Larger combinatorial libraries identified a shorter peptide with antagonistic properties. DTrp-Arg-Leu-NH_2 antagonised the MC1 receptor but exhibited a higher IC_{50} value, within the micromolar range, than that determined for the fuller length peptide cited above (Quillan *et al.*, 1995). Adan *et al.* (1994b) investigated the antagonist properties of various linear ACTH(4-10) analogues on the rat MC3, human MC4 and ovine MC5 receptors with modifications in the (6-10) positions. The paraiodophenylalanine-substituted analogue, [Phe-I^7]ACTH(4-10), was one of the most potent compounds tested and it antagonised all three receptors, perhaps through steric hindrance by the introduced iodine atom. Further substitution at position 7 with bulky aromatic amino acids resulted in the first reported potent and selective MC receptor antagonists. For example, substitution with [D-2'-naphthylalanine^7] to give the cyclic lactam peptide Ac-Nle^4-c[Asp^{5}DNal(2)^7,Lys^{10}]α-MSH(4-10) produced a potent antagonist for the MC4 receptor, a less potent antagonist at the MC3 receptor and a full agonist at the MC1 and MC5 receptors (Hruby *et al.*, 1995).

These data intriguingly point to different structural requirements for antagonist activity at different pigmentary receptors in different species and at different melanocortin receptors in the same species.

1.5.7. Further Melanocortin Receptor Characterisation Tools

The physiology of the different melanocortin receptor subtypes can also be probed using specific antisera. To date, only two antipeptide antibodies have been prepared, both against the human MC1 receptor, which specifically immunostained MC1 receptor expressing cells, including the cells of malignant melanoma tumours (Xia *et al.*, 1995a). Composites have been synthesised consisting of multiple copies of [Nle^4,DPhe^7]α-MSH and a fluorophore on a biologically inert macromolecule. The multivalency produced stronger binding and the fluorophore increased detection sensitivity and was used to demonstrate the presence of specific melanotropin receptors on various human melanoma cell lines (Sharma *et al.*, 1994).

Both these types of melanotropin-receptor-expressing-cell-surface markers may represent potential tools for identification, localisation and chemotherapy of melanoma.

1.6. The Melanocortin Receptor Family

Comparison of the melanocortin receptor sequences with those of other receptors has defined them as a subgroup within the G-protein-coupled receptor superfamily. G-protein-coupled receptors are characterised by being organised into seven putative hydrophobic transmembrane domains, each region consisting of 20-25 amino acids. They share considerable sequence homology, particularly in these transmembrane regions which are thought to form the ligand binding pocket (Lameh *et al.*, 1990). It has not been possible to identify consensus amino acid sequences that confer G-protein specificity, thus G-protein interactions cannot be predicted from the primary amino acid sequence. Studies with other G-protein-coupled receptors have

shown the third cytoplasmic loop, 3i, to be important in the signalling cascade (Lefkowitz and Caron, 1988), although the precise mechanism remains unclear. Agonist-bound receptors interact with heterotrimeric G-proteins located on the cytoplasmic side of the cell membrane with subsequent stimulation of second messenger systems.

The melanocortin receptors are the smallest subgroup of G-protein-coupled receptors identified to date, having short amino-terminal extracellular and carboxy-terminal intracellular domains as well as a short second extracellular loop (Mountjoy *et al.*, 1992). These receptors also lack several amino acid residues common to most G-protein-coupled receptors (Probst *et al.*, 1992) including proline residues in the fourth and fifth transmembrane domains, which are thought to introduce a bend in the α-helical structure and to participate in the formation of the binding pocket (Applebury and Hargrave, 1986), and one or both cysteine residues thought to form a disulphide bond between the first and second intracellular loops (Dixon *et al.*, 1987; Karnik *et al.*, 1988).

To date, five melanocortin receptors have been cloned which share between 39% and 61% amino acid homology. The MC3, MC4 and MC5 receptors appear to be more closely related to each other (55-61%) than to the MC1 and MC2 receptors (43-46%).

1.6.1. Melanocortin-1 Receptor

Cloning of the melanocortin receptors began with the isolation by Chhajlani and Wikberg (1992) of a human gene whose product is the "classic MSH receptor",

but is now more commonly referred to by the recognised nomenclature as the melanocortin-1 receptor, or MC1-R. The gene encodes for a 317 amino acid protein with a molecular weight of 34.8 kDa which is considerably lower than the value of 45 kDa reported from photoaffinity labelling studies (Gerst *et al.*, 1988; Solca *et al.*, 1989) and suggests that the receptor is normally glycosylated.

Mountjoy *et al.* (1992) concurrently isolated both the human (hMC1) and murine (mMC1) receptors and found 76% sequence homology between them. These independently determined sequences for the human receptor differed by two amino acids although later work by Gantz *et al.* (1993a) produced a sequence identical to that reported by Mountjoy *et al.* (1992).

Functional MC1-R is expressed on human melanocytes (Donatien *et al.*, 1992), most cultured and *in vivo* murine melanoma cell lines (Tatro *et al.*, 1990) and some human melanoma cell lines (Ghanem *et al.*, 1988; Legros *et al.*, 1981; Siegrist *et al.*, 1989). Low level expression has more recently been detected on neutrophil and macrophage cell surfaces (section 1.4.2.2.3.) and in the periaqueductal grey matter of the brain (Xia *et al.*, 1995b), suggesting mediation by this receptor of some of the physiological actions of the melanocortins in this region.

As described previously, the murine MC1-R gene maps to a single locus at the distal tip of chromosome 8 and is identical with the pigmentation locus, *extension* (Robbins *et al.*, 1993). The localisation of the human MC1-R gene to chromosome 16q24 was determined by Gantz *et al.* (1994b) and Magenis *et al.* (1994).

High levels of MC1-R mRNA were found in bovine testis (Vanetti *et al.*, 1994), and its product shows 80% sequence homology with hMC1-R. This receptor may be involved in spermatogenesis although no transcripts for melanocortin

receptors have been detected in human testis, suggesting a possible species difference.

Chhajlani and Wikberg (1992) found α-MSH and ACTH to have equivalent binding affinities on this receptor. These data are consistent with the observation of Gantz *et al.* (1993a) of equal potency and efficacy as measured by cAMP production. However, these results are at variance with those of Mountjoy *et al.* (1992) who found ACTH to have lower potency and efficacy than α-MSH on the murine receptor. It is therefore possible that the ability to differentiate between α-MSH and ACTH is a property unique to the murine melanocortin receptors. β-MSH had a ten-fold lower potency than α-MSH whereas γ-MSH and the truncated peptides ACTH(4-10) and ACTH(1-10) were unable to elicit a full cAMP response even at maximal concentrations.

These data illustrate the importance of the amino- and carboxy- terminal residues for full biological activity and specificity at this receptor subtype.

1.6.2. Melanocortin-2 Receptor

This receptor is recognised as the adrenocorticotropic hormone (ACTH) receptor, or MC2-R and has been localised to the adrenal cortex and adipocytes (Oelofsen and Ramachandran, 1983). Mountjoy *et al.* (1992) isolated the human gene and found 39% sequence homology to the human MC1 receptor. On the basis of this low homology there has been some disagreement as to whether it should be included in the melanocortin receptor nomenclature (Chhajlani *et al.*, 1993).

Cammas *et al.* (1995) cloned the murine homologue which exhibits 84% DNA sequence homology and 89% peptide homology to its human counterpart. This group reported ready expression of the murine MC2 receptor in HeLa cells whereas difficulties in the expression of the human homologue have been reported by a number of laboratories.

Despite their close structural relationship to ACTH, α-MSH and other melanocortins were found to have no significant stimulatory action (Cammas *et al.* 1995, Schiöth *et al.*, 1996a) on this receptor subtype. This indicates that the "core" tetrapeptide His-Phe-Arg-Trp, is less important for binding to the MC2-R than has been reported for other melanocortin receptors. It further suggests that binding to, and stimulation of the MC2 receptor is mediated by separate epitopes. Binding studies performed on transfected cells confirmed the loss of agonist activity with ACTH analogues containing fewer than the first 17 residues and found an antagonist role for ACTH(11-24) (Kapas *et al.*, 1996).

This receptor maps to a conserved syntenic region of chromosome 18 in the mouse and human (Gantz *et al.*, 1993c; Magenis *et al.*, 1994). Although it does not map near any previously characterised phenotypic deviant, the identification of an ACTH receptor gene mutation in an individual with ACTH resistance identifies this region as a site of familial ACTH resistance (Weber *et al.*, 1993).

1.6.3. Melanocortin-3 Receptor

Gantz *et al.* (1993a) characterised the 361 amino acid human homologue of the third member of the melanocortin receptor family, which has a molecular weight of 35 kDa after de-glycosylation as determined by photoaffinity labelling (Sahm *et al.*,

1994). Surprisingly, this receptor has been shown to couple to both cAMP and inositol phosphate / Ca^{2+}-mediated signalling systems with the latter exhibiting an unexpected biphasic effect. Both ACTH and α-MSH exhibited a stimulatory effect on inositol phospholipid turnover at low concentrations but a dose-dependent inhibitory effect at higher doses. The 3i portion of the MC3 receptor appears to be responsible for this biphasic response as a chimeric H2-histamine receptor substituted with the 3i region of hMC3-R conferred this biphasic property on the normally monophasic wildtype H2 receptor (Konda *et al.*, 1994).

Northern blot hybridisation showed receptor expression in the CNS to be largely localised to the cortex, hypothalamus, hippocampus and thalamus. This distribution corresponds quite well with the distribution of γ-MSH immunoreactivity (Kawai *et al.*, 1984). It was also found to be highly expressed in the placenta. As α-MSH levels are known to rise markedly in the maternal circulation during late pregnancy (Clark *et al.*, 1978), it is possible that the MC3 plays a role in these changes.

Ligand specificities were found to be quite different from the human MC1 receptor with [Nle^4,$DPhe^7$]α-MSH, α-MSH, β-MSH, γ-MSH, and ACTH exhibiting equipotency on the hMC3-R with respect to cAMP production. The truncated peptides ACTH(1-10) and ACTH(4-10) demonstrated full efficacy but their observed lower potency was attributed to their smaller size (Gantz *et al.*, 1993a). This suggests that the common core sequence of these melanotropic peptides forms the specific recognition site.

The rat and murine homologues were cloned by Roselli-Rehfuss *et al.* (1993) and Desarnaud *et al.* (1994), respectively, and consist of 323 amino acids, the latter

showing 88% identity with the human gene. Both groups reported binding and cAMP data that correlate well with the above results for the human homologue. This receptor therefore, was cited as the first identified subtype to which γ-MSH binds with significant affinity although specificity is lacking. Sahm *et al.* (1994) also determined comparable affinities for α-MSH and γ_1-MSH on the rat MC3-R but found [Nle^4,DPhe^7]α-MSH to have approximately 100-fold higher affinity which is at variance with the above reports. Alanine substitution within the α-MSH peptide determined the favourable presence of tyrosine at position 2 for binding to the rat MC3 receptor (Sahm *et al.*, 1994).

This receptor maps to an area of conserved synteny between mouse chromosome 2 and human chromosome 20 (Gantz *et al.*, 1993c; Magenis *et al.*, 1994). This site overlaps with the location reported for the condition known as benign familial human neonatal epilepsy (Leppert *et al.*, 1989), and in the mouse an epilepsy susceptibility locus has been mapped near the MC3 receptor locus. These data promote the MC3 receptor gene as a candidate gene for epilepsy.

1.6.4. Melanocortin-4 Receptor

Gantz *et al.* (1993b) subsequently cloned the human MC4 receptor. The intronless gene encodes a protein of 333 amino acids and was localised to chromosome 18. As with the MC3 receptor, it is expressed in the CNS, predominantly in the hypothalamus, but has a more widespread distribution throughout each major division of the brain (Mountjoy *et al.*, 1994).

In agreement with their data for the MC1 and MC3 receptors, Gantz *et al.* (1993b) found α-MSH and ACTH to have equipotency as measured by cAMP

production. γ-MSH, ACTH(4-10) and ACTH(1-10) did not elicit a full response on this receptor whereas β-MSH exhibited equipotency with α-MSH and ACTH. This latter observation is in contrast to data for the MC1-R. This implies that a portion of the β-MSH molecule at the C-terminal extension can determine selectivity between these two receptors. The group hypothesised that [Pro^{12}] of ACTH, which is also present in α-MSH and β-MSH but not γ-MSH, is critical for binding as a full agonist to the human MC4 receptor (chapter 5). The presence of MC4 mRNA in regions of the brain associated with learning and memory appears to produce a pharmacological basis for the CNS effects described above. However, neither the MC4-R nor the MC3-R respond well to Org2766 or ACTH(4-10), peptides that are recognised to be more active than native melanocortins in the retention of learned behaviour (de Wied and Jolles, 1982) and neural regeneration (Biijlsma *et al.*, 1981; Strand *et al.*, 1980). This suggests that the behavioural and regenerative effects of the melanocortins are mediated by further brain melanocortin receptors.

1.6.5. Melanocortin-5 Receptor

Various species homologues of the MC5 receptor have been isolated: the human MC5 (Chhajlani *et al.*, 1993; Fathi *et al.*, 1995), the mouse MC5 (Gantz *et al.*, 1994a; Labbé *et al.*, 1994; Fathi *et al.*, 1995), the rat MC5 (Griffon *et al.*, 1994), and the ovine MC5 (Barrett *et al.*, 1994).

The human MC5 receptor gene encodes for a 325 amino acid protein and together with its murine homologue has been found to have a wide distribution, being expressed in skeletal muscle, lung, spleen, brain (Gantz *et al.*, 1994a; Labbé *et al.*, 1994), and in adipocytes (Boston and Cone, 1996). The potency order on the

human receptor was found to be identical to that reported for the human MC1-R, with α-MSH exhibiting equipotency with ACTH. However, the overall affinities for the melanotropic peptides were determined to be several-fold lower (Chhajlani *et al.*, 1993). Despite these similarities, the receptor shows greatest homology (53%) to the MC3 receptor described by Gantz *et al.* (1993a).

Once again, α-MSH was found to be significantly more potent than ACTH in the stimulation of cAMP production on the murine MC5 receptor (Gantz *et al.*, 1994a; Labbé *et al.*, 1994). These conflicting human versus murine data lend further weight to the hypothesis that the ability to differentiate between α-MSH and ACTH is a property unique to murine melanocortin receptors. The fragment ACTH(4-10) which is common to all melanocortins was found to have no significant biological activity. However, the truncated peptides containing an amino-terminal, namely ACTH(1-10), or carboxy-terminal, namely ACTH(4-13), extension exhibited full efficacy albeit with diminished potency relative to α-MSH in stimulating cAMP production. These data imply that the heptapeptide core may act as an important spacer between the two termini with the specific sequences playing a less important role in the binding of the melanocortins to the murine MC5-R (Gantz *et al.*, 1994a).

The overall lower affinities seen for the melanotropic peptides on the MC5-R suggest the existence of an, as yet undiscovered, high affinity endogenous ligand.

1.7. Clinical Perspective

Melanoma is notoriously difficult to treat and MSH coupled with an anti-cancer agent represents a potential chemotherapeutic approach. This theory exploits the higher MC1 mRNA receptor expression in melanoma cells as compared with

normal melanocytes and other cells (Ghanem *et al.*, 1988), and relies on conjugate entry into the melanoma cells by receptor-mediated endocytosis (Varga *et al.*, 1977). Tatro *et al.* (1992) and Morandini *et al.* (1994) have demonstrated peptide- and cell-type specific uptake via the MC1 receptor with cytotoxic diphtheria toxin and melphalan coupled to α-MSH, or fragments thereof, respectively. However, this concept has major limitations as not all human melanoma cells express detectable numbers of the MC1 receptor (Libert *et al.*, 1989) and not all of those that do were found to respond to [Nle^4,DPhe^7]α-MSH (Jiang *et al.*, 1995). In addition, the correlation between *in vivo* and *in vitro* data appears somewhat weak (Süli-Vargha *et al.*, 1990).

Similarly, Bard *et al.* (1990) have investigated the potential use of a chelating derivative of α-MSH with radioisotope attachment in malignant melanoma. However, they found that the high non-specific uptake observed would preclude the therapeutic targeting of their compounds although use as an imaging agent might be possible.

Two compounds are currently in trials as potential tanning agents. The superpotent α-MSH analogue [Nle^4,DPhe^7]α-MSH (section 1.5.4.), also known as Melanotan-I, has been shown to induce tanning in the absence of sunlight in normal males, albeit with minor side effects. A cyclic lactam analogue, Ac-Nle^4-c[Asp^5-His^6-DPhe^7-Arg^8-Trp^9-Lys^{10}]-NH_2, or Melanotan-II, was found to increase human skin pigmentation at cumulative doses much lower than with Melanotan-I, although side effects were also more prominent (Dorr *et al.*, 1996). Further studies with these peptides are currently taking place.

1.8. Aims and Objectives

The melanocortins are a peptide family to which a diverse range of functions have been attributed. It is most probable that these various effects are associated with specific melanocortin receptor subtypes. Subtype-specific agonists and antagonists might therefore be exploited therapeutically. However, a prerequisite for such development is a detailed understanding of the mechanisms by which the melanocortins interact with their receptors to produce these responses.

Previous research has established the importance of the tryptophan-9 residue of α-MSH for high affinity binding to the melanocortin receptors, yet a detailed knowledge of the necessary features of this tryptophan moiety is lacking. Part of this work therefore, involved testing substituted α-MSH analogues to aid further understanding of the physicochemical requirements at this position.

The MC1 and MC4 receptor subtypes are particularly intriguing given their similar ligand binding profiles and that the importance of the melanocortin C-terminal for subtype selectivity has been postulated (section 1.6.4.). This hypothesis was investigated and the role of the C-terminal more fully defined by determining the effect of α-MSH analogues on the binding to and stimulation of the human MC1 and MC4 receptors. Use of human receptor homologues is more clinically relevant, given the proposed existence of a species difference (section 1.6.) and also enabled a fuller study of this supposition.

Further insight into hormone-receptor interaction can also be gained from a study into receptor residues involved in formation of the ligand-binding pocket and G-protein stimulation. A model for melanocortin interaction with the MC1 receptor has been proposed in this laboratory and the work presented here comprised an

attempt to investigate this hypothesis. Use of site-directed mutagenesis techniques to produce point mutations at postulated key receptor residues coupled with biological testing of these altered receptors would enable determination of the validity of this model.

CHAPTER 2: MATERIALS and METHODS

2.1. Cell Culture

2.1.1. Materials

2.1.1.1. Water

Water for the preparation of all cell culture media and solutions was freshly double glass distilled using a bi-distillation Fistreem still fitted with a Fistreem pre-deioniser (Fisons Ltd., Loughborough, Northants.).

2.1.1.2. Growth medium and additives

All solutions detailed below were routinely obtained from Gibco Life Technologies Ltd., Paisley, Scotland.

10x RPMI 1640 (without L-glutamine and sodium bicarbonate).

100x MEM non-essential amino acids

L-glutamine 200 mM

Penicillin (10,000 IU/ ml) and streptomycin (10,000 mg/ml)

Foetal bovine serum (FBS)

Batches of foetal bovine serum were tested prior to routine use to ensure support of cell growth. All cells lines were cultured in 1x RPMI 1640 medium supplemented with 10% FBS, 2 mM L-glutamine, 100 IU/ml penicillin and 100 IU/ml streptomycin, 1x MEM non-essential amino acids and 0.2% w/v sodium bicarbonate. pH was adjusted to 7.4 by the addition of an appropriate volume of 1N sodium hydroxide. The medium was stored at 4°C and used within two weeks.

2.1.1.3. Further solutions

Solutions of 7.5% w/v sodium bicarbonate, 1N sodium hydroxide and 0.02% w/v EDTA in PBS were prepared in freshly de-ionised double distilled water. Phosphate buffered saline (PBS) tablets deficient in magnesium and calcium (Oxoid Ltd., Basingstoke, Hants.) were each dissolved in 100 ml de-ionised double distilled water to a pH of 7.3.

The above solutions were sterilised by autoclaving for 15 minutes at 15 lbs/sq. inch (121°C) on a liquid cycle in a Swingclave Type SFT-LAB oven (British Steriliser Co. Ltd.).

2.1.1.4. Laboratory apparatus

All aseptic techniques were performed in a laminar flow cabinet (MDH Ltd.) with vertical recirculation. Cells were maintained at 37°C in a LEEC PF2 anhydric incubator (Laboratory and Engineering Company). An inverted microscope, WILD M40 (Wild Heerbrugg Ltd.) was used for monitoring cell growth and determining cell numbers together with a standard double grid haemocytometer (Fisons Ltd.).

2.1.1.5. Disposables

Sterile tissue culture flasks were obtained from Falcon (Fahrenheit Labs., Bristol) polypropylene ampoules for cell freezing from Corning, (Fahrenheit Labs.) 96- and 24- well culture plates were supplied by Nunc, Roskilde, Denmark.

2.1.1.6. Glassware

Used glassware was soaked in a 2% v/v solution of RBS 25 (Fisons) for 30 minutes with rinsing in three changes of single distilled water. Items were subsequently soaked in double distilled water for approximately two hours, dried in a hot air oven (Gallenkamp) capped with aluminium foil and oven sterilised (Gallenkamp) by dry heat at 160°C for 1 hour.

2.1.2. Methodology

2.1.2.1. Mammalian cell lines

The SV40 transformed monkey kidney cell line COS7, and the human kidney embryonic (HEK) 293 cell line were obtained from the European Collection of Animal Cell Cultures (ECACC), Porton Down, Salisbury.

HEK 293 cells transfected with the hMC1 and hMC4 receptor genes ligated into the vector pcDNA1 Neo were donated by R.D. Cone, Vollum Institute, Portland, Oregon and a B16 murine melanoma cell line was supplied by L.R. Kelland, Institute of Cancer Research, Sutton.

2.1.2.2. Cell receipt, recovery and storage

All cell lines were obtained as frozen samples. Cryotube contents were rapidly defrosted by brief incubation in a 37°C water bath, diluted with 5 ml pre-warmed medium and centrifuged for 10 minutes at 200 *g* in a Jouan B3.11 bench-top centrifuge. The cell pellet was resuspended and transferred to a tissue culture flask containing pre-warmed, fresh medium.

Further cell stocks were prepared for storage by detachment (section 2.1.2.3.) pelleting and resuspension in fresh medium containing 10% v/v DMSO (Aldrich, spectrophotometric grade) as a cryoprotectant. Cells underwent gradual freezing to -70°C in a Union Carbide BF6 biological freezer unit plug inserted into a Union Carbide LR33 liquid nitrogen freezer and were then transferred to a Union Carbide LR-40 liquid nitrogen freezer for storage at approximately -148°C.

2.1.2.3. Cell line maintenance and subculture

Cells were grown as monolayers in 175 cm^2 tissue culture flasks and examined daily for possible microbial contamination. The time taken to reach monolayer coverage varied between cell lines but all were subcultured on reaching 70-80% confluency. The medium was replaced between passages if necessary, as denoted by the yellow colour formed by the phenol red indicator within the RPMI 1640 medium. This ensured an adequate nutrient supply and optimum pH for cell growth. Subculturing entailed washing the monolayer twice with PBS followed by a 10 minute incubation at 37°C with 2 ml 0.02% w/v EDTA / PBS. Due to the particularly adherent nature of the COS7 cells, a trypsin (0.05% w/v) / EDTA (0.02% w/v) solution in modified Puck's saline A (Gibco BRL) was used as an alternative to the above for monolayer removal. Detached cells were diluted with medium and the resulting cell suspension centrifuged at 200 *g* for 10 minutes. The pellet was resuspended in 10 ml fresh medium, a sample counted (section 2.1.2.4.) and sterile 175 cm^2 flasks inoculated with approximately 2 x 10^6 cells.

2.1.2.4. Determination of cell density

A 0.1% w/v trypan blue (Sigma, Poole, Dorset) solution in PBS was used according to the manufacturer's directions for the determination of cell density. After several minutes to allow dye uptake, a sample of the stained suspension was loaded onto a grid haemocytometer and viewed under an inverted microscope. Viable cells exclude the dye whereas non-viable cells stain a uniform dark blue.

2.1.2.5. Re-selection of 293 transfectants using geneticin (G418)

pcDNA1 Neo carries the gene for geneticin resistance which can be used as a selection marker for cells transfected with this plasmid.

MTT assay for determination of cell number

Assays were based on a modified MTT assay as described by Mosmann (1983) and Arnould *et al.* (1990). Cells were seeded into 96-well plates at the desired density. Medium was removed when appropriate by inversion, and cells washed twice with serum-free RPMI 1640. A 200 µl volume of 1 mg/ml MTT formazan (Sigma) in complete medium was added to each well and the plate incubated at 37°C for 3 hours. The MTT solution was carefully removed from the plate by gentle inversion and the remaining formazan blue crystals solubilised with 200 µl DMSO. The plate was gently agitated on an orbital mixer for 5 minutes to allow complete solubilisation and optical density measured on a Titretek plate reader at 540 nm with a reference wavelength of 690 nm.

MTT assay calibration

A calibration curve was constructed to establish compliance with the Beer-Lambert Law over the employed cell density range. 293 cells were seeded in a 96-well plate at various densities to a maximum of 5 x 10^4 cells/well and allowed to adhere overnight. An MTT assay was subsequently performed and analysed as described above.

MTT viability assay for optimisation of G418 treatment of cells

293 cells were seeded at a density of 5 x 10^3 cells per well in a 96-well plate and incubated overnight in full medium. Fresh incubation medium containing 0-2 mg/ml geneticin was added to the cells with culturing under standard conditions for 5 days. The plate was analysed by an MTT assay to determine cell survival.

From the resulting data (chapter 4) a final concentration of 0.8 mg/ml geneticin was added to the culture medium for two passages to re-select for the 293 cells stably transfected with the pcDNA1 Neo plasmid.

2.2. hMC1-R Expression in COS7 Cells

2.2.1. Plasmid Vectors and Bacterial Strains

Control expression studies were performed using the mammalian expression vector pRSV*lacZ*, obtained from D. Ogllvie, Zeneca Pharmaceuticals, Cheshire and electroporated into *E. coli* XL1-Blue.

pcDNA1 Neo and *E. coli* MC1061 which expresses the P3 plasmid as required for successful bacterial transformation with this vector were obtained from R&D Systems Europe Ltd., Abingdon, Oxon. pcDNA1 Neo containing the human MC1

receptor gene (pcDNA1 Neo / hMC1-R), was donated by R.D. Cone, Vollum Institute, Portland, Oregon.

2.2.2. *Preparation of Electrocompetent* E. coli *MC1061 Cells*

An overnight culture of *E. coli* MC1061 was diluted 1:100 and grown to an OD_{600} of 0.5-1.0 in 500 ml LB medium in a shaking incubator at 37°C. After chilling on ice the cells were centrifuged at 4000x *g* for 15 minutes at 4°C. The ionic strength of the suspension was gradually reduced by washing the cells sequentially in (i) 500 ml ice-cold sterile water (ii) 250 ml ice-cold sterile water (iii) 10 ml sterile ice-cold 10% v/v glycerol with final resuspension in 1 ml 10% v/v glycerol. The electrocompetent ice-cold cell suspension was dispensed as 40 µl aliquots in sterile microfuge tubes, snap-frozen in cardice / methanol and stored at -70°C.

2.2.3. *Transformation of* E. coli *MC1061 / P3 Cells by Electroporation*

The chosen method was based on that described by Dower *et al.* (1988). Electrocompetent *E. coli* MC1061 cells were thawed slowly on ice and 2 µg chilled pcDNA1 Neo / hMC1-R added to each aliquot. The cell suspension was pipetted into a sterile pre-chilled 0.2 cm electroporation cuvette (Bio-Rad Laboratories Ltd., Herts.). The cuvette was placed into the pre-chilled cuvette holder of a Gene Pulser and Pulse Controller (Bio-Rad) set to a capacitance of 25 µF and a resistance of 200 Ω. The cells were subjected to a single 2.5 kV pulse resulting in a time constant for the capacitor discharge of 5 ms. Cell recovery took place in 1 ml SOC medium at 37°C for one hour with shaking. Transformed cells were selected for by plating onto

LB agar containing ampicillin (30 μg/ml) and tetracycline (7.5 μg/ml) with overnight incubation at 37°C.

In a control transformation, antibiotic resistance was confirmed as plasmid-mediated by electroporating cells in the absence of recombinant DNA.

2.2.4. Small-scale Plasmid Preparations (Minipreps)

Plasmid isolation to confirm successful transformation took place using an alkali lysis method based on the procedure described by Birnboim and Doly (1979) as modified by Sambrook *et al.* (1979).

Several random colonies were picked from the plate with a sterile wire and grown overnight in 5 ml LB broth containing ampicillin (30 μg/ml) and tetracycline (7.5 μg/ml). 1 ml of each of these overnight suspensions were centrifuged at 10,000 *g* for one minute. The supernatants were removed and 100 μl of Solution I (50 mM glucose / 25 mM Tris / 10 mM EDTA) added to each tube by vigorous vortexing. A 200 μl volume of freshly prepared Solution II (0.2N NaOH / 1% SDS from 10N NaOH and 20% SDS stocks, respectively) was added with subsequent mixing by gentle inversion followed by a 10 minute incubation on ice. A 150 μl volume of ice-cold Solution III (0.5M potassium acetate / 0.12% glacial acetic acid / 0.28% water) was added to each tube followed by gentle vortexing and a further incubation on ice for 5 minutes. The tubes were centrifuged for 5 minutes at 10,000 *g* with removal of the supernatants to further sterile eppendorfs. The supernatants were extracted with an equal volume of phenol : chloroform and chloroform : isoamyl alcohol. Eppendorf contents were vortexed, re-centrifuged at 10,000 *g* for

2 minutes and the upper aqueous layers removed to clean tubes. Plasmid DNA was precipitated by the addition of two volumes 96% v/v ethanol with gentle mixing and chilling for 5 minutes on ice before centrifuging at 10,000 *g* for 5 minutes. The supernatant was discarded and the remaining pellet washed with 1 ml 70% v/v ethanol. This was carefully decanted with any residual alcohol being evaporated under vacuum in a Speedvac SVC 100 at medium drying temperature. The resultant dried plasmid was resuspended in 50 µl TE buffer containing RNAase 20 µg/ml and the presence of pcDNA1 Neo / hMC1-R confirmed by linearisation and gel electrophoresis.

2.2.5. Plasmid Digestion

DNA digestion was performed using restriction enzymes and buffers (NEB Ltd., Hitchin, Herts.) according to the manufacturer's directions. Incubation took place at 37°C for approximately 60 minutes to allow complete digestion.

2.2.6. Agarose Gel Electrophoresis

Agarose gels were cast and set in Bio-Rad DNA sub-cells. Ultrapure (Gibco BRL) agarose, electrophoresis grade was dissolved in 0.5x TBE buffer at 100°C and when cooled to approximately 60°C, ethidium bromide was added to a final concentration of 0.5 µg/ml. After pouring and positioning of the gel comb the gel was allowed to set at room temperature for approximately 30 minutes before being submerged in 0.5x TBE buffer in the gel tank. DNA samples were mixed with 0.2 volumes of 5x DNA loading buffer and gently pipetted into the wells along with a λDNA / Hind III marker (Promega, Southampton). Electrophoresis was carried out

for approximately one hour at 100 V until the tracking dye neared the end of the gel. The resulting DNA bands were visualised on a UV light box.

The remaining primary culture of the successful transformants was centrifuged at 10,000 *g* for 1 minute and the cells resuspended in 1 ml LB broth containing 10% v/v glycerol and stored at -70°C.

2.2.7. Large-scale Plasmid Isolation, Purification and Quantification

Large scale plasmid isolation for eukaryotic transfection employed a Plasmid Maxi Kit (Qiagen Ltd., Dorking, Surrey) the buffer composite of which is detailed in Appendix B.

A sterile loopful of transformed bacterial stock was used to prepare a primary culture and subsequently transferred to 500 ml of antibiotic-supplemented LB broth for a secondary overnight culture. The bacterial suspension was transferred to four 50 ml tubes and centrifuged at 2000 *g* for 15 minutes at 4°C in a Chillspin bench-top centrifuge. This step was repeated for the remainder of the culture. Each pellet was resuspended in 2.5 ml buffer P1 and the contents pooled in an ultra-centrifuge tube. 10 ml buffer P2 was added and the tube contents mixed by gentle inversion. After four minutes, 10 ml buffer P3 was added to the cell lysate. The tube was incubated on ice for 30 minutes then centrifuged at 70,000 *g* at 4°C for 60 minutes in a Beckman Ti45 rotor. The supernatant was removed promptly and applied to an anion exchange purification column pre-equilibrated with 10 ml buffer QBT. Column washing took place with 30 ml buffer QC followed by plasmid elution using 15 ml buffer QF. Plasmid DNA was precipitated by the addition of 10.5 ml isopropanol, gentle mixing of tube contents and centrifugation at 4°C for 45 minutes

at 70,000 g. The resultant DNA pellet was washed with 15 ml ice-cold 70% v/v ethanol and re-pelleted by centrifugation. The isolated plasmid DNA was stored in TE buffer (pH 8.0) at -20°C.

Determination of sample purity and quantification

Triplicate samples of plasmid DNA solution were diluted in TE buffer for optical density (OD) measurement using a Milton Roy Spectronic 601 spectrophotometer. A measure of purity is given by the ratio of absorbance at 260 nm and 280 nm with contaminating proteins and phenol absorbing at 280 nm. A value of 1.8 or greater is considered acceptably pure for transfection purposes and all samples met this standard.

An OD of 1.0 at 260 nm corresponds to approximately 50 μg/ml for double-stranded DNA.

2.2.8. Transfection of COS7 Cells by Electroporation

Transient transfection of the COS7 cells was performed using electroporation protocols based on procedures described by Neumann *et al.* (1982) and Wong and Neumann (1982). The procedure was modified by the use of lower voltage and higher capacitance settings as described by Chu *et al.* (1987). For these mammalian transfections the Bio-Rad Gene Pulser apparatus was connected to a Bio Rad Capacitance Extender and 0.4 cm electroporation cuvettes used (Bio-Rad).

Semi-confluent layers of COS7 cells were pelleted by centrifugation for 10 minutes at 200 *g*. Cells were washed in 5 ml ice-cold PBS and re-pelleted. This washing process was repeated with pellet resuspension in 0.5 ml PBS to give an

approximate cell concentration of 5-10 x 10^6 cells/ml and transferred to pre-chilled 0.4 cm electroporation cuvettes. A 20 μg sample of supercoiled pcDNA1 Neo / hMC1-R was added to each cuvette and after a 5 minute incubation on ice, electroporation took place at the optimal transfection settings of 300 V and 250 μF as determined below. The cuvettes were subsequently incubated on ice for 10 minutes before transferral to tissue culture flasks containing fresh medium.

Although electroporation is applicable to most cell types, critical parameters vary and must be determined for each cell line used.

Parameter optimisation

2.2.8.1. FITC-dextran uptake during electroporation

Optimisation of electroporation settings was performed with measurement of cellular uptake of FITC-labelled dextran (Sigma, average MW 71,200) in a protocol based on that described by Andreason and Evans (1989) and Graziadei (1991).

COS7 cells were prepared for electroporation as described above to a lower concentration of 2 x 10^6 cells/ml. To each 500 μl aliquot was added 50 μl FITC-dextran 10 mg/ml with incubation of the cuvettes on ice for 5 minutes. Electroporation was performed over 100-400 V at capacitance values of 125 and 250 μF. A non-electroporated control of COS7 cells and FITC-dextran was left on ice for the entirety of the assay for determination of non-electroporation-associated cell death. After a further 5 minute incubation on ice, cells were seeded into 100 mm tissue culture dishes and incubated at 37°C in 5% CO_2 / 95% air for four hours. Cells were removed by trypsinisation and together with non-adherent and dead cells were

washed and resuspended in 50 µl PBS for fluorescence measurement by FACS analysis. Cell death was quantified by labelling cells with 100 ng/ml propidium iodide and measuring the fluorescence of the same population of cells in a protocol based on that described by Sasaki *et al.* (1987).

2.2.8.2. In situ cytochemical staining for β-galactosidase activity

A qualitative determination of electroporation efficiency and an approximation of the post-transfection interval required for maximum expression was made using the plasmid pRSV*lacZ*. This vector encodes the *E. coli lacZ* gene for β-galactosidase under the control of the Rous sarcoma virus long terminal repeat sequence. Expression efficiency was determined by histochemical staining using 5-bromo-4-chloro-3-indolyl-β-D-galactopyranoside (X-gal) based on the method described by MacGregor *et al.* (1991).

Transfected cells were seeded onto 100 mm culture dishes (Nunc) and incubated at 37°C with fresh culture medium. At post-transfection time intervals of 24, 48 and 72 hours the growth medium was aspirated from the adherent cell monolayers. Cells were washed twice with PBS and overlaid with fixative solution (1% glutaraldehyde, 1 mM magnesium chloride, 100 mM sodium phosphate) with incubation for 5 minutes at 4°C. Removal of the fixative solution was followed by two further PBS washes. A 1:10 dilution of X-gal 2% w/v in DMF was made with 3.3 mM potassium ferrocyanide, 3.3 mM potassium ferricyanide, 1 mM magnesium chloride, 150 mM sodium chloride and this staining solution incubated with the cells for a minimum of four hours in a humidified atmosphere at 37°C.

After staining the cells were washed three times with PBS and examined under a light microscope. Cells expressing the *lacZ* gene hydrolyse the chromogenic substrate X-gal to the insoluble dye bromochloroindole. A positive reaction is seen as a blue colour against an unstained background.

2.3. Peptide Synthesis

Peptides were prepared in house by Dr. G.W.J. Olivier and Dr. U.G. Sahm using solid-phase peptide synthesis methods based on the Fmoc strategy (Atherton and Sheppard, 1989) and is therefore not described in detail.

Peptide purification involved semi-preparative HPLC with a gradient elution of 0.1% TFA in water and 0.1% TFA in 70% acetonitrile / 30% water at a flow rate of 3 ml / minute. UV spectrophotometry at 217 nm was used to monitor the eluate. Fraction collection took place every 30 seconds and subjected to analytical scale HPLC. Appropriate peptide fractions were then pooled and freeze-dried. Confirmation of peptide purity was executed using FAB-MS provided by Swansea University Mass Spectrometry Service: α-MSH M+H calculated 1664.8, found 1664; [Nle^4,DPhe^7]α-MSH M+H calculated 1646.8, found 1647; [Nle^4,DPhe^7,Phe^9]α-MSH M+H calculated 1607.8, found 1608; [Nle^4,DPhe^7,Tyr^9]α-MSH M+H calculated 1623.8, found 1624; [Nle^4,DPhe^7,Thr^9]α-MSH M+H calculated 1564.8, found 1565; [Nle^4,DPhe^7,Ala^9]α-MSH M+H calculated 1531.8, found 1532; [Asp^{10}]α-MSH M+H calculated 1722.8, found 1723; [Phe^{10}]α-MSH M+H calculated 1754.8, found 1755, [Phe^{12}]α-MSH M+H calculated 1714.8, found 1715; [Asp^{10},Phe^{12}]α-MSH M+H calculated 1772.8, found 1772; [Ala^{11},Ala^{12}]α-MSH M+H calculated 1581.7, found

1582; [Ala^{11},Ala^{13}]α-MSH M+H calculated 1579.7, found 1581; [Ala^{11},Ala^{12},Ala^{13}]α-MSH M+H calculated 1553.7, found 1554.

2.4. Radioiodination of [Nle^4,DPhe^7]α-MSH

Radioactive iodine was coupled at the [Tyr^2] position of [Nle^4,DPhe^7]α-MSH by the oxidative chloramine-T method described by Eberle and Hübscher (1979).

2.4.1. Column Chromatographic Solutions

* 1% v/v TFA (Aldrich, analytical grade).

* 50%, 60% and 80% v/v methanol + 1% v/v TFA.

0.25M sodium phosphate buffer, pH 7.4 (freshly prepared from stock solutions).

* Stored at 4°C for a maximum of 3 months.

2.4.2. Iodination Reaction Reagents

0.25% w/v BSA in 0.05M sodium phosphate buffer, pH 7.4. *

1% w/v Polypep (Sigma) in 0.05M sodium phosphate buffer, pH 7.4. *

0.1% w/v chloramine-T (BDH Chemical Ltd.) dissolved in distilled water immediately prior to use.

* prepared on day of use.

2.4.3. Pre-conditioning of Purification Columns

A C18 reverse phase column packed with Spherisorb ODS (Anachem) was pre-conditioned by washing according to the following protocol:

3 x 1 ml 1% v/v TFA.

3 x 1 ml 80% v/v methanol / 1% v/v TFA.

1 x 1 ml 1% w/v Polypep solution.

3 x 1 ml 80% v/v methanol / 1% v/v TFA.

3 x 1 ml 1% v/v TFA.

2.4.4. Peptide Iodination

Ten µl $Na^{125}I$ (nominally 37 MBq of activity) was added to 1.5 µg [Nle^4,$DPhe^7$]α-MSH diluted to 20 µl in 0.25M sodium phosphate buffer, pH 7.4. Reactive oxidation was initiated with the addition of 10 µl 0.1% w/v chloramine-T solution. After 30 seconds the reaction was quenched with 0.6 ml 0.25% w/v BSA. The reaction mixture was applied to the pre-conditioned ODS column followed by two washes with phosphate buffer to remove the unreacted $Na^{125}I$. The iodinated ligand was eluted by washing the column with 4 x 1 ml 50% v/v methanol / 1% v/v TFA followed by 2 x 1 ml 60% v/v methanol / 1% v/v TFA.

The eluate was retained for further purification by reverse-phase HPLC.

2.4.5. [^{125}I-Tyr^2,Nle^4,$DPhe^7$]α-MSH Purification

Further purification of the eluate was essential to separate the mono- from the di-iodinated product. An exponential gradient of 0.1% TFA in water and 0.1% TFA in 70% acetonitrile / 30% water was used and fractions collected at one minute intervals from 25 to 40 minutes after injection. The desired mono-iodinated product eluted between 35 and 36 minutes after injection with elution of the di-iodinated peptide approximately three minutes later. Radioactivity of the collected fractions

was quantified on a LKB 1277 Gammamaster gamma counter (Wallac, Milton Keynes, UK). A trace for the elution profile is shown in Figure 2.1.

The fractions associated with the mono-iodinated peptide peak were pooled and the collective activity measured in counts per minute (cpm). Apparatus efficiency was determined by regular standardisation with a sample of $Na^{129}I$ of known activity and estimated accuracy of ± 3% (Wallac) and found to be constant at 70%. The concentration of [^{125}I-Tyr^2,Nle^4,DPhe^7]α-MSH was determined as outlined below.

2.4.6. Calculation of Radiotracer Concentration

By definition, 1 atom of ^{125}I associates with 1 mole [Nle^4,DPhe^7]α-MSH to give 1 mole [^{125}I-Tyr^2,Nle^4,DPhe^7]α-MSH.

Carrier-free $Na^{125}I$ has a specific activity of 80.5×10^{15} Bq/atom (Amersham)

$\therefore$ Activity of 1 mole [^{125}I-Tyr^2,Nle^4,DPhe^7]α-MSH = 80.5×10^{15} Bq

1 Bq = 1 decay per second, or 60 decays per minute and the efficiency of the gamma counter = 70%

$\therefore$ 1 mole [^{125}I-Tyr^2,Nle^4,DPhe^7]α-MSH would register $(80.5 \times 10^{15}) \times 60 \times 0.7$ cpm

= 3.38×10^{18} cpm on the LKB 1277 Gammamaster gamma counter.

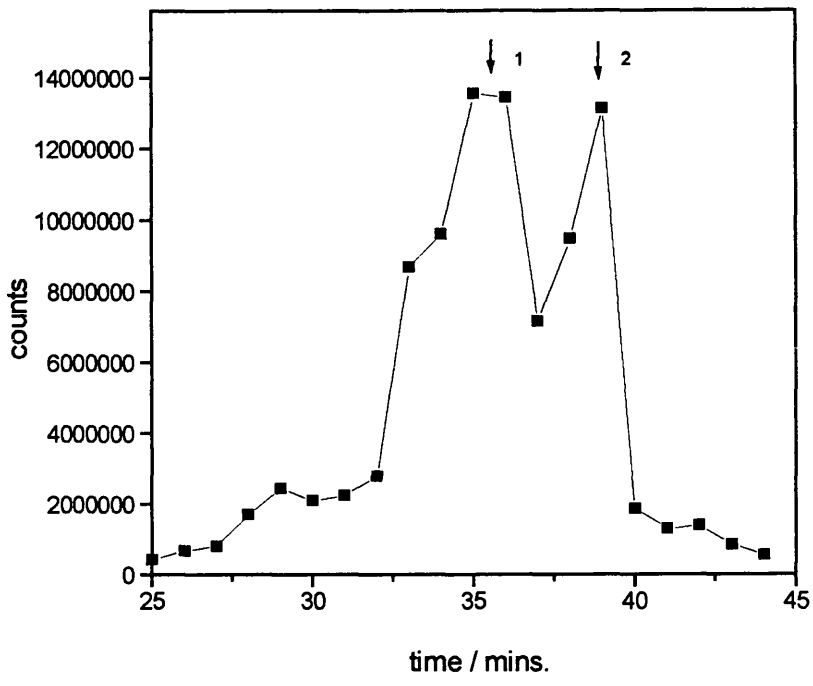

Figure 2.1. Elution profile of: (1) mono-iodinated and (2) di-iodinated [Nle^4,DPhe^7]α-MSH from HPLC purification as measured on the LKB 1277 Wallac Gammamaster gamma counter.

2.5. Radioligand Binding Assays

The method used was adapted from Siegrist *et al.* (1988) as described by Sahm (1994) and followed the general protocol detailed below.

Due to the detachment of COS7 and 293 cells from culture plates during incubation at 4°C, 96-well filter plates were routinely used. Cells were detached and seeded at a density of 2 x 10^5 cells / well. After a 4 hour incubation at 37°C to allow the cells to settle, the medium was filtered using a vacuum-manifold and the cells washed twice with 150 µl PBS. Appropriate dilutions of [^{125}I-Tyr^2,Nle^4,DPhe^7]α-MSH and competing ligands were made in a serum-free RPMI 1640 binding buffer containing 25 mM HEPES and 0.2% w/v BSA and 100 µl aliquots added to each well. Each time / concentration point was assayed in quadruplicate.

After sufficient incubation at 4°C for equilibrium binding (section 2.5.1.), cells were washed twice with PBS, filters transferred to LP4 tubes using the Multiscreen Assay System (Millipore) and activity measured on the LKB 1277 Gammamaster gamma counter.

2.5.1. Determination of Equilibrium Binding Time

Seeded cells were stimulated with approximately 0.2 nM [^{125}I-Tyr^2,Nle^4,DPhe^7] α-MSH in binding buffer and non-specific binding was determined concurrently by the addition of 1000x of unlabelled [Nle^4,DPhe^7]α-MSH. The equilibration time for radioligand binding at 0-4°C to COS7 and 293 cells was determined by measuring cell-associated radioactivity at appropriate time intervals.

2.5.2. *Determination of Time of Maximum Expression in COS7 Cells*

The time-course of receptor expression in the transfected COS7 cells was investigated by measuring cell-associated radioactivity from 24 to 144 hours post-electroporation. At each post-electroporation time-point cells were detached from culture flasks, seeded and incubated at 4°C with radioligand, nominally 0.2 nM, and excess unlabelled peptide as described above.

The results from these assays (chapter 3) led to the routine use of a 72 hour post-transfection interval with a 16 hour peptide stimulation time.

2.5.3. *Binding Isotherm of [^{125}I-Tyr^2,Nle^4,DPhe^7]α-MSH*

An isotherm was generated using a range of radioligand concentrations. Non-specific binding was determined using a 1000-fold excess of cold ligand. Specific binding was calculated by subtraction.

Binding isotherm analysis

Receptor numbers and dissociation constants were determined using *MINSQ* non-linear least squares regression analysis employing the Langmuir Isotherm equation:

$$[HR] = \frac{n\,K_a\,[H]}{1 + K_a[H]} = \frac{n[H]}{K_d + [H]}$$

where [H] = concentration of free hormone

[HR] = concentration of hormone-receptor complex

n = total receptor number

K_a = association constant of ligand- receptor complex

$K_d = 1 / K_a$ = dissociation constant of ligand-receptor complex

The linearising plot of [HR] / [H] against [HR] produces the Scatchard plot with a gradient approximating to $-K_a$ and x-axis extrapolation giving an estimation of n (Scatchard, 1949).

2.5.4. Competition Binding Assays

Serial dilutions of each peptide were made in binding buffer containing a fixed concentration of [^{125}I-Tyr^2,Nle^4,DPhe^7]α-MSH, nominally 0.2 nM. Displacement of radioligand by each concentration of competing ligand was monitored by measurement of cell-associated radioactivity as described above.

Analysis of competition binding data

MINSQ non-linear least squares regression analysis was used to calculate dissociation constants from the competition binding data employing the following equation:

$$cpm_{(test)} = cpm_{(min)} + \frac{(cpm_{(max)} - cpm_{(min)}) \times [R]}{[R] + K_{dr} \times \frac{[I]}{K_i}}$$

where $cpm_{(test)}$ = cpm associated with a given competitor concentration

$cpm_{(max)}$ = cpm associated with maximum radioligand binding (no competitor)

$cpm_{(min)}$ = cpm associated with minimum radioligand binding (excess competitor)

[R] = concentration of radiotracer

[I] = concentration of competitor

K_{dr} = dissociation constant of radiotracer

K_i = dissociation constant of competitor

2.6. cAMP Quantification

Functional coupling of the melanocortin receptors was analysed by quantifying cAMP produced by peptide stimulation. The method used was based on the procedure detailed by Salomon (1991).

2.6.1. Pre-prepared Solutions

20x BSA (Sigma) 2 mg/ml, stored at -20°C.

20x IBMX (Sigma) 10 mM dissolved in water in a boiling water bath and stored at -20°C for a maximum of three months.

10x PCA (BDH Chemicals, Poole, England) 25% v/v stored in the dark

1000x cAMP (Sigma) 0.1M neutralised with Tris-Cl to pH 7.5

2.6.2. *[^{3}H]-cAMP Production*

Cells were seeded into 24-well plates at a density of 5 x 10^5 cells / well and incubated overnight at 37°C in a humidified atmosphere of 5% CO_2 / 95% air. Cells were subsequently incubated with pre-warmed culture medium containing 2.5 μCi/ml [8-^{3}H]-adenine (Amersham International Plc., Bucks.). The radioactive medium was aspirated after a pre-determined incubation period (section 2.6.3.2.) and the cells washed with 0.5 ml pre-warmed PBS. Serial dilutions of test peptides were made in pre-warmed serum-free culture medium supplemented with 0.1 mg/ml BSA and 0.5 mM IBMX. Cells were stimulated with 0.5 ml samples of this medium for a fixed time (section 2.6.3.1.) at 37°C. Each concentration was assayed in quadruplicate. The medium was aspirated and 1 ml ice-cold 2.5% v/v PCA containing 0.1 mM cAMP added to each well. After a 30 minute incubation on ice with occasional agitation for efficient [^{3}H]-cAMP extraction, 0.8 ml cell-free PCA extract was transferred to clean tubes and neutralised with 80 μl 4.2N KOH. The tubes were vortexed and the potassium perchlorate precipitate allowed to settle. If necessary, samples were stored at 4°C overnight or at -20°C for longer periods.

2.6.3. *Chromatographic Separation of [^{3}H]-cAMP*

Distilled water was added to each tube to a final volume of 1.3 ml. The tubes were vortexed and the crystals allowed to resettle. A 0.1 ml sample was removed for determination of total [^{3}H]-adenine uptake and the remaining solution subjected to double-column chromatography as described by Johnson and Salomon (1991).

2.6.3.1. Column apparatus and reagents

Two sets of 17 ml polypropylene separation columns (Mitchell Plastics Inc.) with plastic filter discs were mounted over each other in a tiered rack set which in turn was suspended over 4 ml collection tubes.

Dowex 50 AG50W-X8 resin (Bio-Rad) was washed sequentially with approximately 6 volumes each of 0.1N NaOH, water, 1N HCl and water before initial use and poured into the first set of columns in an approximately 2:1 slurry. When the flow rates decreased the columns were regenerated by repeating the above. Approximately 0.6 g neutral alumina activity grade 1, type WN-3 (Sigma) was poured dry into the lower column set.

2.6.3.2. Column washing procedure

Before each use the Dowex 50 columns were washed with 3 x 10 ml distilled water and the alumina columns with 8 ml 100 mM Tris-Cl, pH 7.4.

The neutralised PCA extract solutions were decanted onto Dowex 50 columns, leaving the perchlorate crystals undisturbed. Each column was then washed with 3 ml water and the eluate discarded. The Dowex 50 columns were then placed directly above the alumina columns and washed with 8 ml water. The slightly acidic eluate from the Dowex 50 resin caused retention of [^{3}H]-cAMP on the alumina. After elution from the alumina, the columns were placed over collection tubes and [^{3}H]-cAMP eluted with 4 ml 100 mM Tris-Cl, pH 7.4. A 0.5 ml sample of each eluate was added to 4 ml Optiphase scintillation cocktail (Wallac) with vigorous vortexing. Radioactivity of the scintillation vial contents was quantified on a LKB Wallac 1215 RackBeta liquid scintillation counter.

The Dowex 50 columns were regenerated after each use with 5 ml 1N HCl and the alumina columns with 8 ml Tris-Cl, pH 7.4.

2.6.3.3. Quench curve

A 10 µl volume of [8-^{3}H]-cAMP of known activity (Amersham) was diluted to 500 µl in PBS and mixed with Optiphase scintillant in each of 10 scintillation vials. 0-2000 µl of chloroform was added to each vial with subsequent analysis on the scintillation counter. Figure 2.2. shows the quench curve generated by calculation of efficiencies and channel ratios. The counting efficiency of an unknown sample is read from the quench curve using its R value and used to calculate dpm associated with sample cpm. Quench curve generation and storage together with dpm determination was performed automatically.

2.6.4. Assay optimisation

A B16 murine melanoma cell line which natively expresses the MC1 receptor was used for initial assay optimisation negating the need for expensive and time-intensive plasmid preparation.

2.6.4.1. Determination of optimum stimulation time

After pre-incubation with [^{3}H]-adenine, cells were stimulated with 5 nM [Nle^4,DPhe^7]α-MSH. [^{3}H]-cAMP quantification proceeded according to the above protocol at various stimulation times from 10-120 minutes.

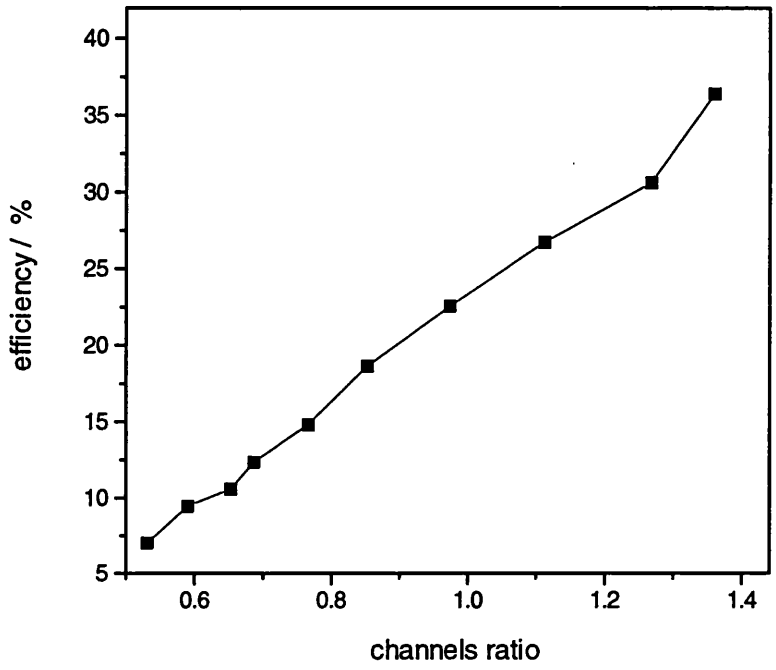

Figure 2.2. Standard quench curve for [^{3}H]-cAMP on the LKB Wallac 1215 RackBeta liquid scintillation counter showing the relationship between counting efficiency and channel ratios, R.

2.6.4.2. Determination of maximum [^{3}H]-adenine-uptake time

Cells were incubated with [^{3}H]-adenine for 30 to 180 minutes and subsequently stimulated with 5 nM [Nle^4,DPhe^7]α-MSH. After PCA extraction 0.1 ml samples were taken and counted to give a measure of total [^{3}H]-adenine uptake.

Calculation of EC_{50} values

MINSQ non-linear least squares regression analysis was used to calculate EC_{50} values for the tested peptides employing the following equation:

$$dpm_{(test)} = dpm_{(max)} + \frac{(dpm_{(min)} - dpm_{(max)})}{1 + \frac{[C]}{EC_{50}}}$$

where: dpm(test) = dpm associated with a given peptide concentration

dpm(max) = dpm associated with maximum stimulation

dpm(min) = background dpm (no stimulant)

[C] = peptide concentration

EC_{50} = peptide concentration required to produce half maximal stimulation

2.7. Statistical Analysis

Data analysis was performed using *MINITAB 9.1.* Significant differences were determined using a one-way analysis of variance following Fisher's multiple comparison procedure at the 99% confidence interval.

2.8. Site-directed Mutagenesis of the hMC1-R

2.8.1. Nucleotide Sequence Analysis

Analysis of the human MC1 receptor gene sequence (accession number x65634) as submitted by Cone *et al.* (1992) to the Genbank, and restriction enzyme choice was determined using the GCG (University of Wisconsin Genetics Computer Group) package at the SERC Seqnet computing facility at Daresbury, UK. Genbank database searching was performed using the FASTA software.

2.8.2. Ligation of the hMC1-R Gene into pBluescript (SK+)

The hMC1-R gene was excised from pcDNA1 Neo / hMC1-R for insertion into the bacterial vector, pBluescript (SK+) (Stratagene). Digestion took place (section 2.2.5.) using the restriction enzymes *Bam*H1 and *Xba*1 (NEB). pBluescript was similarly restricted in a separate reaction mixture. The digested samples were analysed by gel electrophoresis (section 2.2.6.) with excision of appropriate bands and purification by DNA adsorption to a silica matrix using the Geneclean II DNA purification system (Bio-101, La Jolla, CA, USA). Four and a half volumes of 6M NaI and 0.5 volumes of Geneclean-TBE modifier were added to each gel slice with incubation at 50°C until the agarose melted. To this DNA mixture was added 5 µl of Geneclean glassmilk suspension with a 5 minute incubation on ice to allow DNA adsorption onto the glass beads. Glassmilk beads were pelleted at 10,000 *g* for 5 seconds and washed 3 times with Geneclean 'NEW' wash. DNA was eluted from the beads into water at 50°C for 5 minutes.

The restricted products were ligated with a 5-fold excess of insert DNA over vector using T4 DNA ligase (NEB) in accordance with the manufacturer's

instructions. The ligation mixture was incubated at 16°C overnight and purified following the Geneclean protocol using three volumes of NaI and 5 µl Glassmilk. The ligated product was transformed into the host cells by electroporation.

2.8.3. E.coli *XL1-Blue Transformation with pBluescript (SK+) / hMC1-R*

Electrocompetent *E. coli* XL1-Blue (Stratagene) were prepared and electroporated with pBluescript / hMC1-R (sections 2.2.2., 2.2.3.). Transformed cells were selected for by spreading onto LB-agar plates supplemented with 100 µg/ml ampicillin and 12.5 µg/ml tetracycline and coated with 40 µl X-gal (Melford Laboratories) 20 mg/ml in DMF and 4 µl 0.84M IPTG. After incubation at 37°C for approximately 18 hours, cells containing recircularised pBluescript plasmids appeared blue whereas recombinants grew as white colonies. Several white colonies were picked with a sterile wire and grown overnight in antibiotic- supplemented LB broth. Plasmid DNA was recovered using the miniprep procedure (section 2.2.4.) and presence of the hMC1-R gene confirmed by restriction endonuclease digestion and gel electrophoresis.

2.8.4. Recognition Peptide Synthesis and Purification

A recognition peptide for attachment to the N-terminal of the hMC1-R was synthesised based on the octapeptide sequence engineered by Hopp *et al.* (1988). Primer design incorporated *Eco*R1 and *Bam*H1 restriction sites for ligation with pBluescript / hMC1-R.

Synthesis of the complementary single stranded oligonucleotides DNA took place in-house (School of Biochemistry, University of Bath) with DNA elution from

the resin using ammonia solution (Aldrich). The eluates were incubated at 55°C overnight and subsequently dried under medium heat in a Speedvac SVC 100 for ammonia evaporation. The pellets were resuspended in water.

2.8.5. Concentration of DNA by Ethanol Precipitation

DNA was precipitated from aqueous solution by the addition of 3M sodium acetate pH 5.2, to a final concentration of 0.3M followed by two volumes of 96% ethanol at -20°C. The solution was vortexed thoroughly and precipitated at -70°C for 15 minutes. The DNA pellet was recovered by centrifugation at 10,000 *g* at 4°C for 30 minutes using a Jouan A14 centrifuge. The supernatant was aspirated and the pellet washed with 70% ethanol at 4°C. The DNA was subsequently dried at 37°C for 10 minutes and resuspended in TE buffer.

The concentration of DNA was quantified and purity determined by optical density measurement (section 2.2.7.). For single stranded DNA an OD_{260} of 1.0 corresponds to approximately 40 µg/ml DNA.

2.8.6. Primer Annealing, Restriction and Purification

Approximately 20 µg of each oligonucleotide were mixed together and ethanol precipitated as described above. The resulting pellet was resuspended in water, heated at 70°C for 10 minutes for strand annealing and subsequently cooled to room temperature. Approximately 5 µg of this annealed mixture was restricted with *Bam*H1 and *EcoR*1 (section 2.2.5.). An equal volume of phenol : chloroform was added to the digestion mixture with thorough vortexing. The mixture was centrifuged

for 10 minutes at 10,000 *g* at 4°C. The supernatant was removed and underwent ethanol precipitation as detailed above.

2.8.7. Ligation of the Recognition Peptide with pBluescript (SK+) / hMC1-R

pBluescript / hMC1-R was digested with *Bam*H1 and *Eco*R1 and run on an 0.8% w/v agarose gel. The desired band was excised from the gel and purified using Geneclean. The digested vector was ligated with the annealed and restricted oligonucleotide using T4 DNA ligase. The ligation mixture was purified, used to transform *E. coli* XL1-Blue and resultant colonies "mini-prepped" (sections 2.8.2., 2.8.3., 2.2.4.). Prepared plasmid was re-restricted with *Bam*H1 and *Eco*R1 and analysed for successful ligation by polyacrylamide gel electrophoresis.

2.8.8. Non-denaturing Polyacrylamide Gel Electrophoresis

Non-denaturing polyacryamide gel electrophoresis was performed using a Bio-Rad Miniprotean cell as described by Sambrook *et al.* (1989). The glass plates were thoroughly cleaned to remove all traces of grease and assembled with 0.4 mm spacers between them. To 20 ml of a 30% w/v acrylamide solution was added 140 µl of 10% w/v ammonium persulphate solution and 7 µl TEMED to catalyse polymerisation. A sharktooth comb (Bio-Rad) was inserted and the gel allowed to set for 60 minutes at room temperature. The comb was gently removed and the gel surface washed with 1x TBE.

To determine ligation success, the modified vector was digested with *Bam*H1 and *Eco*R1 and gently pipetted into the wells together with a pBR322 / *Hae*III marker (Sigma). The gel was run for approximately 90 minutes at 50 V and

subsequently stained by submerging in 1x TBE containing 0.5 μg/ml ethidium bromide for approximately 40 minutes with viewing on a UV light box.

2.8.9. Mutagenesis of the hMC1-R

Mutagenesis of the human MC1 receptor was to be performed according to manufacturer's directions using the Clontech Transformer Site-Directed Mutagenesis kit (Cambridge Bioscience).

CHAPTER 3: RESULTS and DISCUSSION (Part I)

Binding affinity of α-MSH derivatives to COS7 / hMC1-R cells

The tetrapeptide His-Phe-Arg-Trp which is invariant between the isolated MSH peptides has been denoted as the smallest active fragment of α-MSH (Otsuka and Inouye, 1964). It was later described as the 'classical' active site of α-MSH and is therefore sensitive to structural change (Eberle, 1988). However, whilst the presence of the tryptophan-9 residue of α-MSH is important for full activity, this residue has been shown to be more amenable to certain structural changes. Despite this finding, no systematic study into the role of tryptophan at this position has been carried out.

The aim of this work was to determine the essential features of the tryptophan moiety for high affinity binding to the human MC1 receptor. To this end modified peptides were synthesised, the choice of substituents being made on the basis of the physicochemical properties of the particular amino acid residues. Optimisation of electroporation parameters for the COS7 cell line took place and using these data the human MC1 receptor was transiently and regularly expressed in these cells. Binding and cAMP assays were optimised and subsequently employed to correlate binding affinity with functional activity of the peptide analogues under analysis.

The COS7 cell line is frequently used for transient, high-level receptor expression. It is derived from an African green monkey kidney cell line CV-1, by transformation with an origin-defective simian virus, SV40, integrated into the chromosomal DNA, hence the acronym COS, (*C*V-1 *o*rigin, *S*V40) (Gluzman, 1981).

COS cells express high levels of the SV40 large tumour (T) antigen which is required to initiate viral DNA replication at the origin of SV40. Three T-antigen positive cell lines were isolated and developed of which two, designated COS1 and COS7, are in common use. Transfection of these cells with any plasmid containing an SV40 origin of replication such as pcDNA1 Neo, enables the T-antigen to initiate runaway replication of the plasmid. This produces high expression levels of any gene of interest ligated into the vector. However, the excessive stress placed on the cells by the replicating plasmid and the ensuing high levels of protein production result in plasmid loss. This loss typically occurs within a week of electroporation, hence the transient nature of gene expression and the need for repeated transfection.

The human MC1 receptor sequence was obtained using PCR with human melanoma as a template and degenerate oligonucleotides from transmembrane domains III and VI as primers. Screening of a human genomic DNA library and hybridisation took place at high stringency. An approximately 1 kb *Hin*dIII and *Xba*I fragment including the human MC1 receptor gene was ligated into the polylinker sequence of the mammalian expression vector, pcDNA1 Neo (Figure 3.1.) (Mountjoy *et al.*, 1992).

3.1. Optimisation of hMC1-R Expression in COS7 Cells

Electroporation is generally recognised to produce high efficiency transfection of a wide range of mammalian cells. Subjecting the cells to a high-voltage electric field results in the temporary disruption of the cell membrane and pore formation with subsequent passage by electrophoresis of biological molecules into the cell nucleus (Winterbourne *et al.*, 1988). Membrane reclosure after electroporation is a

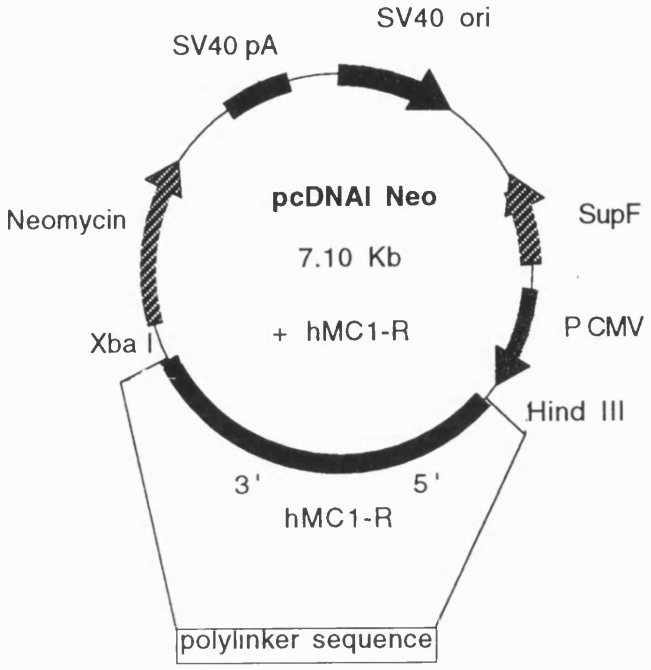

Figure 3.1. Schematic representation of the expression vector pcDNA1 Neo depicting salient features for replication and selection in mammalian cells together with the site of ligation of the human MC1 receptor.

natural decay process and a short post-transfection incubation on ice has been found to increase the electroporation efficiency of certain cell lines (Potter, 1988). Although linearised DNA has been found to promote the integration into chromosomal DNA necessary for stable transfection, supercoiled DNA is preferable

for transient expression (Potter, 1988). This is possibly a result of reduced degradation of the supercoiled form.

Optimal transfection parameters vary between cell lines and should, therefore, be determined for each system used to ensure maximal expression.

3.1.1. Electroporation Parameter Optimisation Using FACS

Fluorochrome-conjugated dextrans such as FITC-dextran are high molecular weight molecules that cannot passively enter cells and are not associated with the external cellular surface (Graziadei *et al.*, 1991). These characteristics along with their cellular non-toxicity (Oliver *et al.*, 1984), make these compounds suitable molecular markers for quantification of cellular uptake.

FITC-labelled dextran was used in conjunction with FACS analysis (section 2.2.8.1.) to optimise uptake into COS7 cells during the electroporation process. Measurements were made over a voltage range of 100 to 400 V at capacitance settings of 125 μF and 250 μF and the data are given in appendix D. Cellular uptake of FITC-dextran was quantified by FACS analysis of cell fluorescence. Cell death was quantified by staining with the nucleic acid interchelator, propidium iodide. Entry of propidium iodide in isotonic solution into cells is prevented by the cell membrane and laser-excited fluorescence is seen only within the nuclei of dead cells (Krishnan, 1975).

Figure 3.2a. illustrates the general trend of the greater uptake of FITC-dextran with increasing voltage as evidenced by increased fluorescence. This increase is more marked at the higher capacitance setting of 250 μF and at lower voltages, with

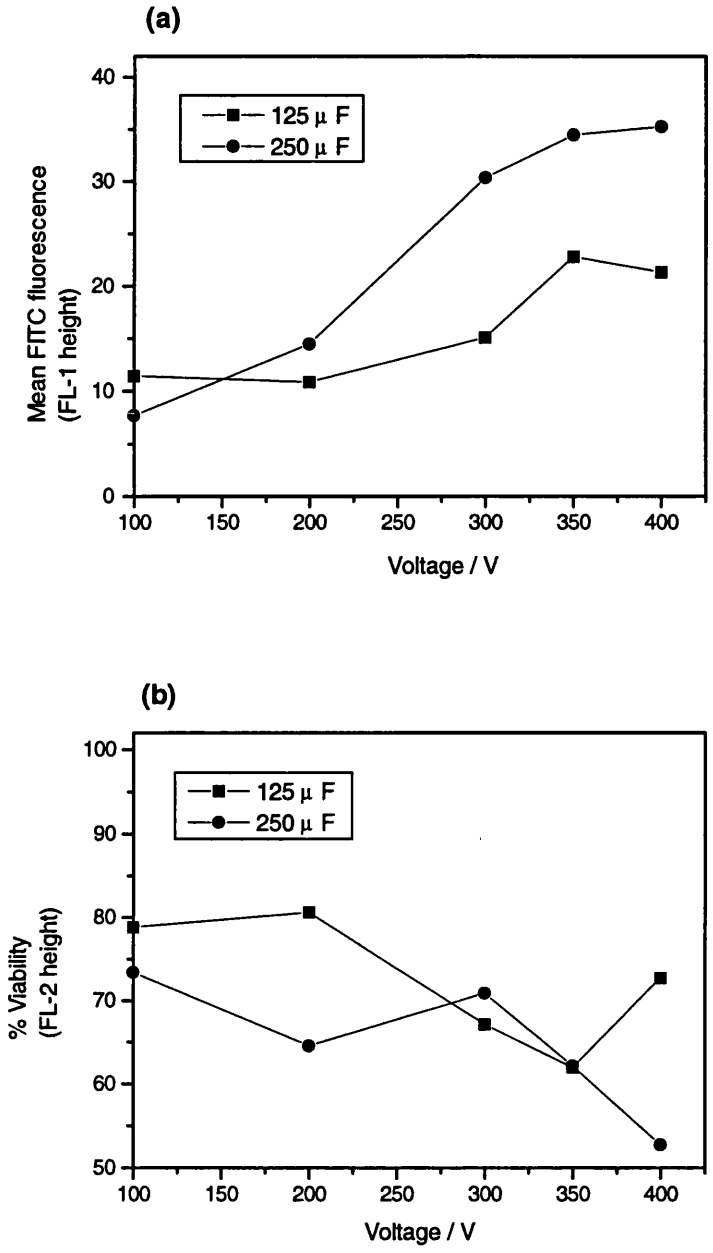

Figure 3.2. FACS analysis of COS7 cells electroporated with FITC-labelled dextran at capacitance settings of 125 and 250 μF. **(a)** Fluorescence intensity as a function of electroporation voltage; **(b)** Cell viability as a function of electroporation voltage, determined by the proportion of non-viable cells taking up 100 ng/ml propidium iodide.

values above 300 V apparently producing negligible further increases in uptake. The higher uptake observed for the 250 μF capacitance value at voltages of 300 V or more, is also associated with a rapid decrease in cell viability (Figure 3.2b.). Selection of electroporation parameters therefore involves a compromise between the greater cell death obtained at higher voltage and capacitance values and the correspondingly greater uptake of FITC-dextran by the remaining viable cells.

On the basis of these data electroporation settings of 250 μF and 300 V were used routinely for the transient transfection of COS7 cells.

3.1.2. X-gal Staining of COS7 Cells

The above work illustrates the uptake by electroporated COS7 cells of high molecular weight but non-nucleic acid material. A qualitative determination of plasmid uptake efficiency and the time required for maximum gene expression was made using the 7.8 kb reporter vector pRSV*lacZ* (section 2.2.8.2.). The *E. coli lacZ* gene encodes the glycoside hydrolase, β-D-galactosidase (β-gal) under the control of the Rous sarcoma virus long terminal repeat. 5-bromo-4-chloro-3-indolyl-β-D-galactoside (X-gal) acts as a substrate for this enzyme, being broken down to give galactose and soluble indoxyl molecules. The potassium ferrocyanide and ferricyanide within the staining solution together act as an oxidation catalyst converting the soluble indoxyl to insoluble indigo, thus enhancing localisation of the stain (MacGregor *et al.*, 1991).

Electroporation was performed using the predetermined parameters of 250 μF and 300 V. Results are shown in Figure 3.3. for the cell staining of control COS7 samples electroporated in the absence of plasmid and COS7 cells transfected with

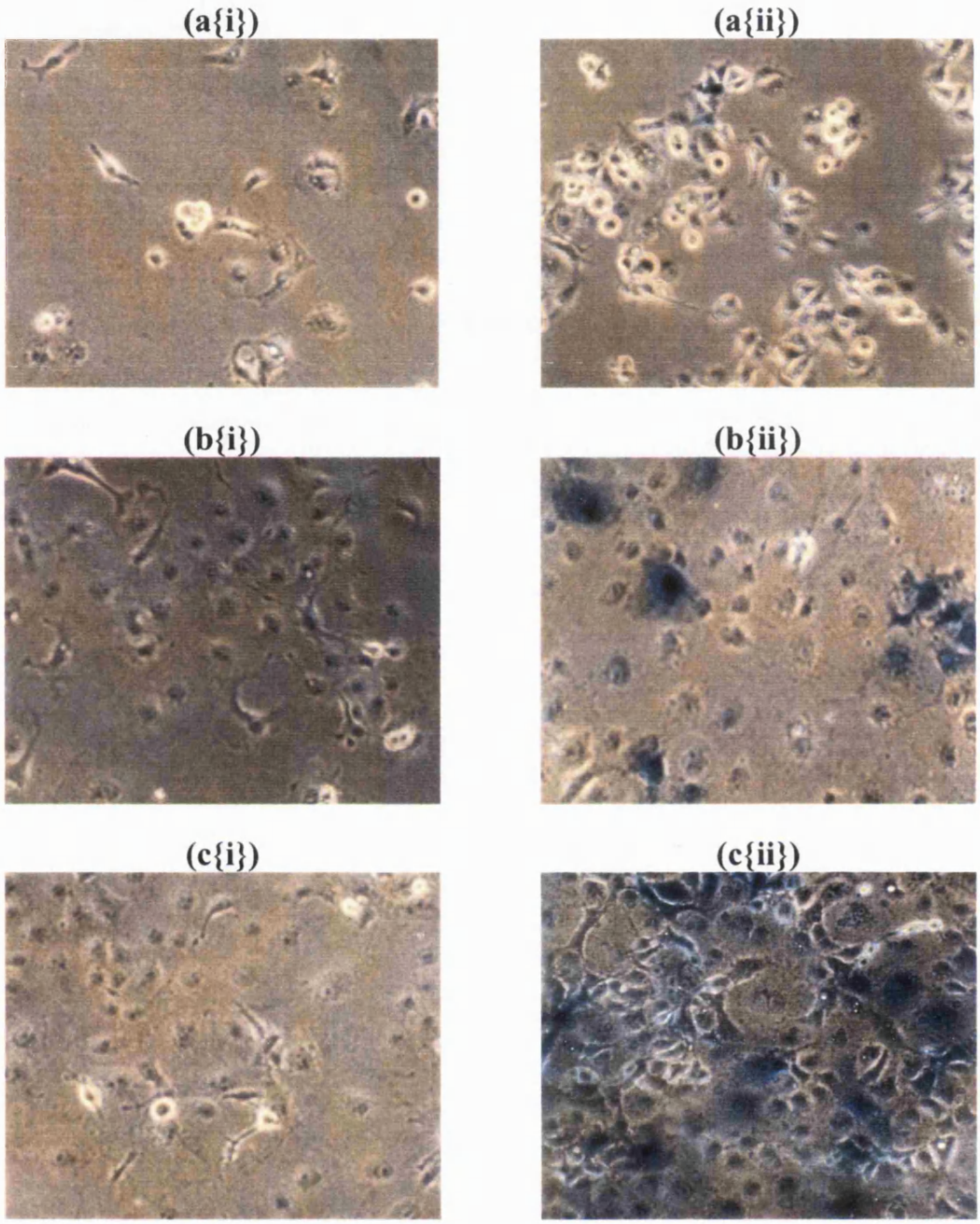

Figure 3.3. COS7 cells fixed and treated with X-gal solution after electroporation. {i} electroporation in the absence of plasmid (control); {ii} electroporation with 20 μg pRSV*lacZ*. Post-transfection interval: (a) 24 hours; (b) 48 hours; (c) 72 hours.

20 μg of pRSV*lacZ*, at post-electroporation time points of 24, 48 and 72 hours. No staining in the control cell samples was observed over the studied time period (Figure 3.3a{i}, b{i}, c{i}), indicating the absence of an endogenous β-gal response. This validates the assumption that the staining depicted in Figure 3.3a{ii}, b{ii} and c{ii} is due solely to *lacZ* expression as a consequence of pRSV*lacZ* uptake via the electroporation process. Expression, determined by the number of blue / green stained cells, was minimal after 24 hours but significantly greater at both the 48 and 72 hour time points. Maximum expression equated with approximately 60 to 80% staining.

From these data it is clear that electroporation is an efficient method for introducing recombinant DNA into COS7 cells and suggests that a post- transfection interval of 48 to 72 hours would be required for maximum gene expression.

3.1.3. Optimum Post-Electroporation Interval for MC1-R Expression

A time-course experiment was performed (section 2.5.2.) to confirm the optimum interval before assaying the electroporated COS7 cells. A time lag, such as that required for *lacZ* expression (section 3.1.2.) would be expected to be necessary to enable plasmid replication and the associated protein synthesis to occur. The results are presented graphically in Figure 3.4. Total radioligand binding i.e. both specific and non-specific, was determined by incubating cells with radioligand alone. Addition of 1000-fold excess unlabelled [Nle^4,$DPhe^7$]α-MSH displaces radioligand from the expressed receptors and the resulting radioactivity is due solely to non-specific binding to the cell surface and filter plate. Specific receptor binding of [^{125}I-Tyr^2,Nle^4,$DPhe^7$]α-MSH is calculated by subtraction of these values. Figure 3.4.

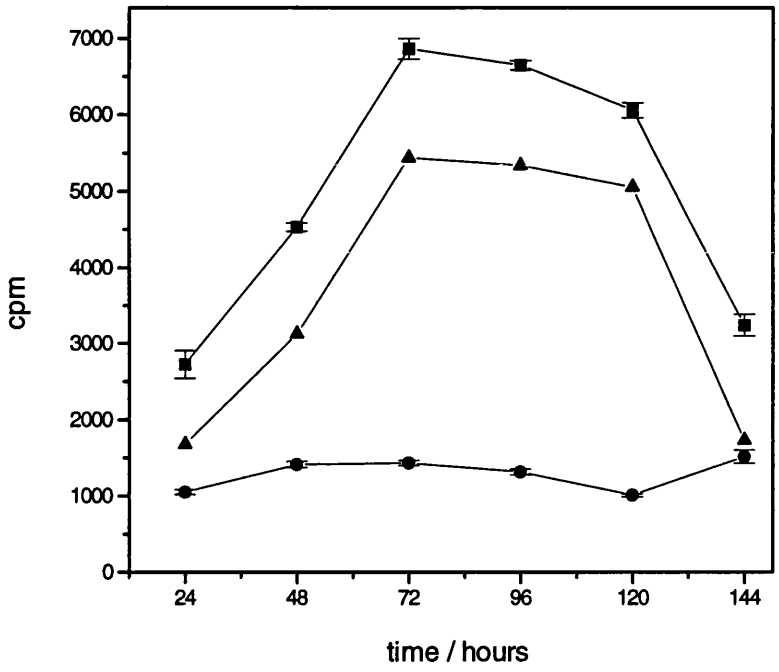

Figure 3.4. Binding at 0-4°C of [^{125}I-Tyr^2,Nle^4,DPhe^7]α-MSH to the human MC1 receptor transiently expressed in COS7 cells, as a function of post-electroporation incubation time at 37°C.

(■) total binding of 0.28 nM [^{125}I-Tyr^2,Nle^4,DPhe^7]α-MSH; (●) non-specific binding in the additional presence of 1000x excess non-iodinated [Nle^4,DPhe^7]α-MSH; (▲) specific binding calculated by subtraction.

shows an approximately linear increase in specific binding, hence hMC1 receptor expression, between 24 and 72 hours post-transfection with a plateau being reached before a rapid loss of expression after five days.

From these data, a 72 hour incubation at 37°C post-electroporation was allowed before execution of binding assays.

3.2. Optimisation of Binding Assay Parameters

3.2.1. Confirmation of an Absence of Endogenous Receptors

The suitability of the COS7 cell line for heterologous expression of the human MC1 receptor is dependent upon an absence of endogenous melanocortin receptor expression. A comparison of ligand binding was made (section 2.5.3.) between COS7 cells electroporated with the hMC1-R and non-transfected wild-type COS7 cells. Figure 3.5. clearly shows that whereas specific binding to the electroporated COS7 cells rises exponentially with increasing concentrations of [^{125}I-Tyr^2,Nle^4,DPhe^7]α-MSH until receptor saturation is reached, total binding to wild-type cells is virtually indistinguishable from non-specific binding. Specific binding as determined by subtraction is therefore negligible. These observations are at variance with those reported by Weber *et al.* (1993) who discovered a small response of COS7 cells to melanocortin stimulation as determined by cAMP measurement and proposed the existence of an endogenous melanocortin receptor. However, the negligible specific binding determined in this study confirms the suitability of COS7 cells for hMC1 receptor expression.

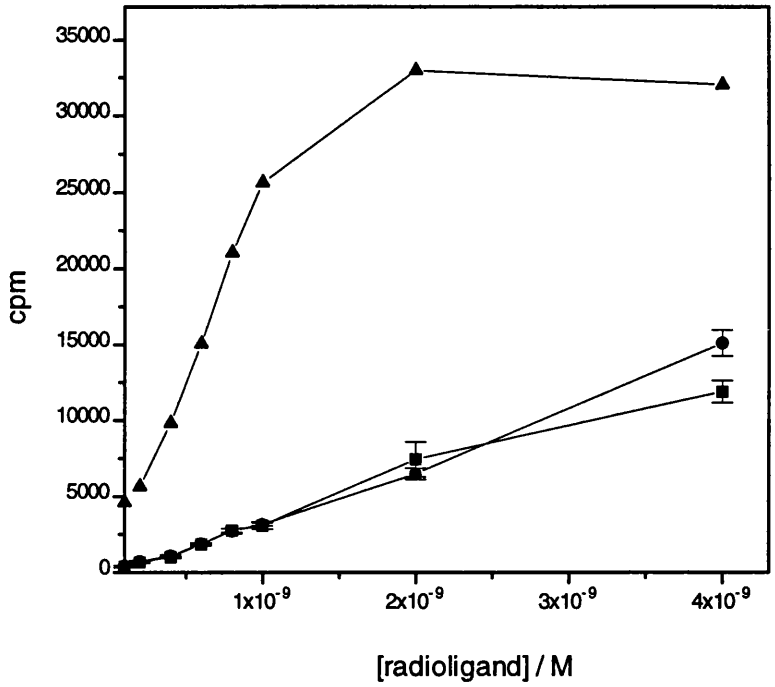

Figure 3.5. Comparison of binding at 0-4°C of [^{125}I-Tyr^2,Nle^4,DPhe^7]α-MSH to the hMC1-R transiently expressed in COS7 cells with binding to wild-type COS7 cells.

(■) total binding of [^{125}I-Tyr^2,Nle^4,DPhe^7]α-MSH to wild-type COS7 cells; (●) non-specific binding to wild-type COS7 cells, in the additional presence of 1000x excess non-iodinated [Nle^4,DPhe^7]α-MSH.

(▲) specific binding to COS7 cells electroporated with the hMC1-R.

3.2.2. Determination of Equilibrium Binding Time

Under equilibrium binding conditions the rates of formation and breakdown of the hormone-receptor complex are equal. Determination of the time required for equilibrium binding of [^{125}I-Tyr^2,Nle^4,DPhe^7]α-MSH to the MC1 receptor was performed as described in section 2.5.1. Equilibrium binding is attained after approximately 12 hours at 0-4°C with negligible decrease of this maximum over the studied 24 hour period (Figure 3.6.). Non-specific binding appears to be time-independent, remaining approximately constant throughout the time period of the assay.

The presence of a competing ligand invariably slows the approach to binding equilibrium by reducing the free receptor concentration. This diminishes the effective association rate constant of the radioligand. Determination of the time required for equilibrium binding in the presence of unlabelled ligand is therefore imperative. Binding assays are routinely performed at 0-4°C in this laboratory as association at higher temperatures has been found to be more rapid but does not reach steady state (Eberle, 1988). This is largely due to the equally rapid and significant hormone-receptor internalisation that has been shown to occur at these temperatures (Adams, 1993).

These data together with practical time considerations led to the use of a 16 hour incubation period at 0-4°C for the electroporated cells with the melanocortin analogues in all subsequent assays.

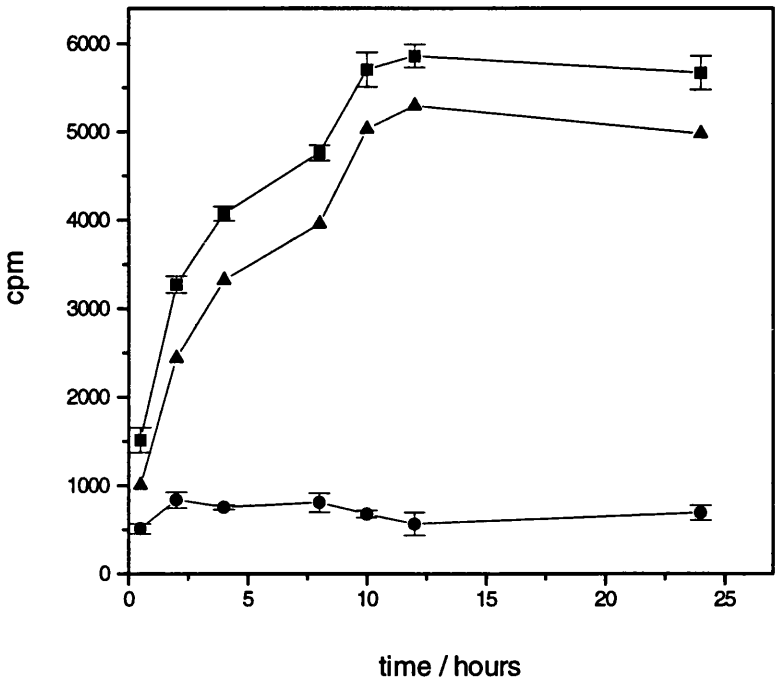

Figure 3.6. Binding at 0-4°C of [^{125}I-Tyr^2,Nle^4,DPhe^7]α-MSH to the hMC1-R transiently expressed in COS7 cells, as a function of incubation time.

(■) total binding in the presence of 0.23 nM [^{125}I-Tyr^2,Nle^4,DPhe^7]α-MSH; (●) non-specific binding in the additional presence of 1000x excess non-iodinated [Nle^4,DPhe^7]α-MSH; (▲) specific binding calculated by subtraction.

3.3. Binding Isotherm of [^{125}I-Tyr^2,Nle^4,DPhe^7]α-MSH

The dissociation constant, K_d, for the binding of [^{125}I-Tyr^2,Nle^4,DPhe^7]α-MSH to the human MC1 receptor transiently expressed in COS7 cells was determined from four replicate binding assays (section 2.5.3.). A representative isotherm is shown in Figure 3.7. Non-specific binding shows an approximately linear dependence on radioligand concentration and is non-saturable over the working concentration range. The form of the specific binding curve is described by the Langmuir Isotherm (section 2.5.3.). At low concentrations, formation of the hormone-receptor complex, as determined by cpm measurement, shows a linear dependence on radioligand concentration. As the tracer concentration increases, the gradient decreases until a plateau is reached indicating saturation of receptor binding. An average K_d of 0.56 ± 0.07 nM was calculated using *MINSQ* non-linear least squares regression. This is comparable to the value of 0.48 nM obtained in our laboratory for the murine MC1 receptor (Sahm, 1994). The receptor population also determined by *MINSQ* analysis was within the range of 25,000 to 60,000 per cell, which is significantly greater than the range of 5000 to 25,000 per cell obtained with B16 murine melanoma cells (Sahm, 1994). This high expression is indicative of efficient electroporation and is in accordance with expected values for high copy number plasmids containing an SV40 origin of replication. The inter-assay difference in receptor number is not unexpected given the variation of growth characteristics, transfectability and protein expression properties of COS cells over time. Scatchard analysis yielded a linear plot (Figure 3.8.) thus confirming the presence of a homogeneous receptor population.

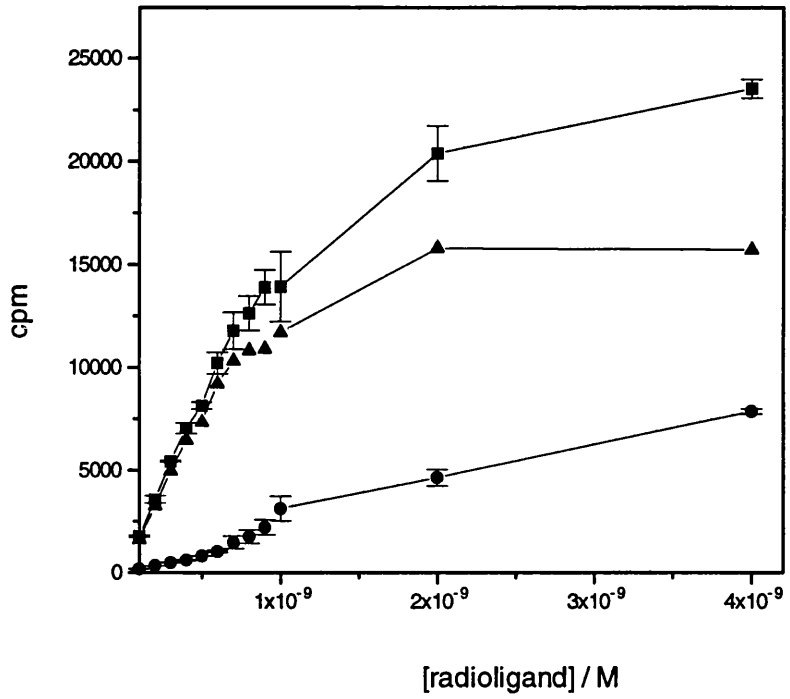

Figure 3.7. Isotherm for the binding at 0-4°C of [^{125}I-Tyr^2,Nle^4,DPhe^7]α-MSH to the hMC1-R transiently expressed in COS7 cells.

(■) total binding of [^{125}I-Tyr^2,Nle^4,DPhe^7]α-MSH; (●) non-specific binding in the additional presence of 1000x excess non-iodinated [Nle^4,DPhe^7]α-MSH; (▲) specific binding calculated by subtraction.

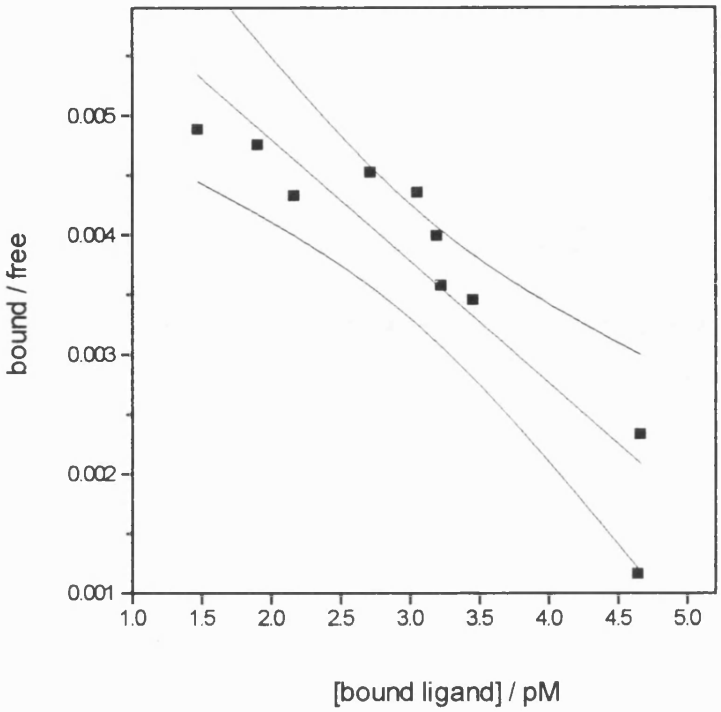

Figure 3.8. Scatchard plot for the confirmation of a homogeneous melanocortin receptor population in COS7 cells transiently transfected with the hMC1-R.

(Curves show 95% confidence interval.)

Non-specific binding to the filter plates was high in the absence, but significantly lower in the presence of cells. This binding to the empty wells could not be reduced by the addition of excess unlabelled [Nle^4,DPhe^7]α-MSH, thus confirming its non-specific nature.

3.4. Binding of [Nle^4,DPhe^7]α-MSH Analogues Substituted at Position 9

The peptide standard used for all competition binding assays was the "superpotent" α-MSH analogue, [Nle^4,DPhe^7]α-MSH (section 1.5.4.). [DPhe^7]α-MSH analogues have been shown to exhibit higher receptor binding affinities than their [LPhe^7]α-MSH counterparts (Peng *et al.*, 1996). Given the predicted sensitivity of position 9 to structural alteration (see below) and to render as measurable any detrimental effect on binding affinity, substituted peptides were synthesised as [Nle^4,DPhe^7]α-MSH, rather than α-MSH, derivatives.

Binding experiments were performed as described in section 2.5.4. The results obtained conformed to the sigmoidal plot expected for such assays with standard deviations associated with the replicates of generally less than 10% (Figure 3.9.). Displacement of [^{125}I-Tyr^2,Nle^4,DPhe^7]α-MSH by the substituted peptides resulted in the binding curve being shifted to the right, a phenomenon indicative of competition by lower affinity analogues. Each peptide with the exception of [Nle^4,DPhe^7,Ala^9]α-MSH, was capable of complete inhibition of radioligand binding. [Nle^4,DPhe^7,Ala^9]α-MSH, however, was unable to displace fully [^{125}I-Tyr^2,Nle^4,DPhe^7]α-MSH from the MC1 receptor at 0.1 mM, the highest working concentration, as dictated by peptide availability.

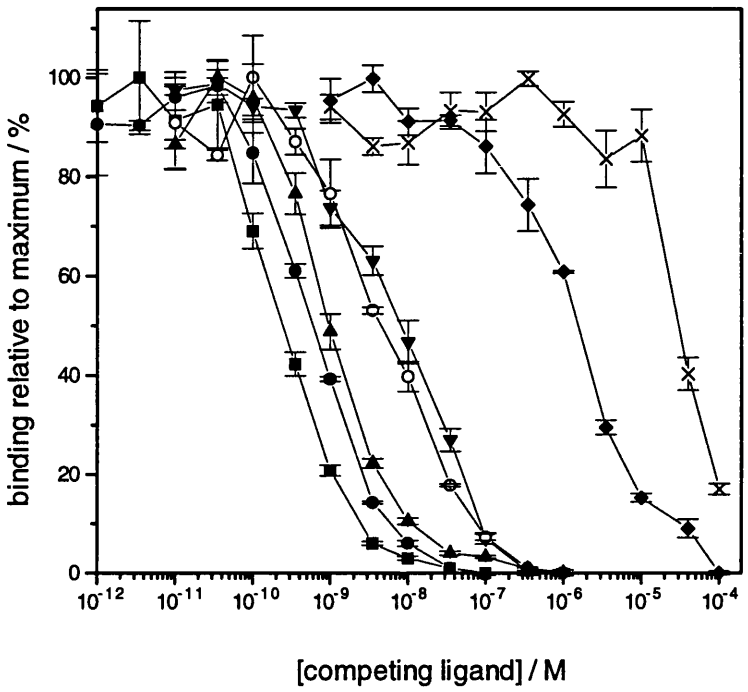

Figure 3.9. Competitive binding at 0-4°C of 0.20 nM [^{125}I-Tyr^2,Nle^4,DPhe^7]α-MSH and position 9-substituted analogues to the hMC1-R transiently expressed in COS7 cells.

(■) [Nle^4,DPhe^7]α-MSH;

(O) α-MSH;

(●) [Nle^4,DPhe^7,DTrp^9]α-MSH;

(▲) [Nle^4,DPhe^7,Phe^9]α-MSH;

(▼) [Nle^4,DPhe^7,Tyr^9]α-MSH;

(◆) [Nle^4,DPhe^7,Thr^9]α-MSH;

(×) [Nle^4,DPhe^{7}Ala^9]α-MSH.

Ligand affinities are routinely cited as the reciprocal of their association constants, the notation for which throughout this work is K_i, i.e. the dissociation constant as determined by inhibition of radioligand binding. Absolute dissociation constants for these substituted analogues were determined by *MINSQ* analysis and are given in Table 3.1 together with K_i values relative to [Nle^4,DPhe^7]α-MSH. Statistical analysis of the binding data (section 2.7.) is given in appendix E.

[Nle^4,DPhe^7]α-MSH exhibited a dissociation constant of 0.68 nM which is 10-fold lower than the value of 6.6 nM assigned to α-MSH (Table 3.1.). A diastereoisomeric change at position 9 of [Nle^4,DPhe^7]α-MSH to D-tryptophan produced an insignificant difference in affinity to the L-tryptophan analogue. This indicates a lack of preference for specific stereochemistry at this position. Substitution with phenylalanine to give [Nle^4,DPhe^7,Phe^9]α-MSH retains the aromatic ring and non-polarity at position 9 but considerably increases hydrophobicity as measured on the Kyte and Doolittle (1982) and Engelman *et al.* (1986) hydropathy scales (appendix A). However, this peptide exhibited no significant reduction in affinity as compared to [Nle^4,DPhe^7]α-MSH which shows the dispensability of the pyrrole moiety. [Nle^4,DPhe^7,Tyr^9]α-MSH exhibited a significantly reduced binding affinity of 16-fold and 6-fold as compared to [Nle^4,DPhe^7]α-MSH and [Nle^4,DPhe^7,Phe^9]α-MSH, respectively. Tyrosine-9 substitution retains aromaticity but the hydroxyl group increases hydrophilicity. and suggests that the significant difference in affinity between [Nle^4,DPhe^7,Phe^9]α-MSH and [Nle^4,DPhe^7,Tyr^9]α-MSH is a consequence of reduced hydrophobicity at this

Peptide	K_i / M (± standard deviation).	Binding relative to [Nle^4,DPhe^7]α-MSH
α-MSH	6.59×10^{-9} ($\pm 7.50 \times 10^{-10}$) n = 3	0.10
[Nle^4,DPhe^7]α-MSH	6.82×10^{-10} ($\pm 1.43 \times 10^{-10}$) n = 3	1
[Nle^4,DPhe^7,DTrp^9]α-MSH	1.51×10^{-9} ($\pm 2.25 \times 10^{-10}$) n = 3	0.45
[Nle^4,DPhe^7,Phe^9]α-MSH	1.82×10^{-9} ($\pm 2.82 \times 10^{-10}$) n = 3	0.37
[Nle^4,DPhe^7,Tyr^9]α-MSH	1.14×10^{-8} ($\pm 2.90 \times 10^{-9}$) n = 3	0.060
[Nle^4,DPhe^7,Thr^9]α-MSH	2.42×10^{-6} ($\pm 1.19 \times 10^{-6}$) n = 4	0.00028
[Nle^4,DPhe^7,Ala^9]α-MSH	2.59×10^{-5} ($\pm 7.77 \times 10^{-6}$) n = 4	0.000026

Table 3.1. Dissociation constants (± standard deviation) and relative values compared to [Nle^4,DPhe^7]α-MSH for peptide analogues as determined by displacement binding at 0-4°C of [^{125}I-Tyr^2,Nle^4,DPhe^7]α-MSH from the hMC1-R transiently expressed in COS7 cells. (n = number of replicate experiments)

position. The linear amino acid substitutions to give [Nle^4,DPhe^7,Thr^9]α-MSH and [Nle^4,DPhe^7,Ala^9]α-MSH resulted in the greatest detrimental effect on binding, with these analogues exhibiting a greater than 3500 and 35000-fold reduction in affinity, respectively. Threonine is a linear amino acid with a polar side-chain and a hydrophobicity comparable to that of tryptophan (appendix A). Alanine has a higher or comparable hydrophobicity to tryptophan according to the Kyte and Doolittle (1982) and Engelman *et al.* (1986) hydropathy scales, respectively. [Nle^4,DPhe^7,Ala^9]α-MSH exhibits the lowest affinity of the tested peptides, with a significantly higher dissociation constant than [Nle^4,DPhe^7,Thr^9]α-MSH. This suggests that the small alanine side-chain alters peptide backbone conformation producing a further detrimental effect on binding to the MC1-R. The greatly reduced binding affinity observed with these two analogues as compared to [Nle^4,DPhe^7]α-MSH stresses the importance of aromaticity at position 9.

Many structure-activity studies have been carried out with melanocortin analogues over the years although the majority of this work was performed prior to receptor subtype cloning and employed amphibian melanin-dispersion assays. Since the isolation and characterisation of the melanocortin-1 receptor, however, further studies on various mammalian homologues have been reported. The murine receptor has been the most widely studied as a consequence of its high levels of endogenous expression although significant data have now been reported for the human homologue.

The affinities obtained for [Nle^4,DPhe^7]α-MSH and α-MSH on the human MC1 receptor in this study were approximately 3-fold higher than those determined

for the murine analogue in this laboratory (Sahm, 1994) under similar assay conditions. However, the two peptides show similar relative values on the receptor homologues with [Nle^4,DPhe^7]α-MSH exhibiting a 10-fold higher potency than α-MSH. Replacement of methionine-4 of α-MSH with the isosteric norleucine has been found to be possible with no loss of affinity or activity. The term "superpotency" was coined for the behaviour of its derivative [Nle^4,DPhe^7]α-MSH as compared to α-MSH (Sawyer *et al.*, 1980; Siegrist *et al.*, 1988). [DPhe^7] substitution was subsequently found to confer "superpotency" on further linear and some cyclic α-MSH derivatives (Cody *et al.*, 1985) and to exhibit higher receptor binding affinities than their [LPhe^7]α-MSH counterparts (Peng *et al.*, 1996). All other tested alterations at position 7 produced a reduction of pigment-dispersing activity (Eberle, 1988). More recently, substitution with alanine-7 was found to decrease binding affinity to 0.2% of that exhibited by α-MSH for the murine MC1 receptor (Sahm, 1994).

Yajima *et al.* (1966, 1967) were the first to investigate the effect of stereoisomeric substitutions within the core sequence of α-MSH. They reported a greater activity for the pentapeptide His-DPhe-Arg-Trp-Gly as compared to its all L-analogue in the frog skin assay and determined that additional D-stereoisomer substitution was only possible at the tryptophan-9 residue of α-MSH without loss of potency. This is in agreement with later findings by Sawyer *et al.* (1980). Sugg *et al.* (1986) attempted to correlate biological data with side-chain topology of the central residues. They investigated the effect of D-tryptophan substitution within the fragment [Nle^4]α-MSH(4-11) and reported a 10-fold higher potency than its parent

analogue and equipotency with [Nle^4,DPhe^7]α-MSH(4-11) in the lizard skin bioassay and 30-fold higher potency than [Nle^4]α-MSH(4-11) in the frog skin assay. The anisotropic properties of these central residues were utilised in NMR studies to elucidate solution topology and the possible preferred and adopted conformations recognised by the receptor. Consistent with their biological data, the resonances of the [Trp^9] indole protons were found to be less sensitive to stereochemical change than other D-substitutions within the central core. However, the backbone conformation of these analogues was found to be preserved and the enhanced melanotropic potency of these fragments attributed to the chiral topological arrangement of the side chains in the core sequence. These data on the stereochemistry at this position are in broad agreement with the results reported here for the full length peptide [Nle^4,DPhe^7,DTrp^9]α-MSH. However, the variation in data obtained from the different biological assays performed by Sugg *et al.* (1986) illustrate the apparent disparity between different amphibian models. This emphasises the caution required when attempting to compare data obtained from uncloned receptors in different assay systems.

Van Nispen *et al.* (1977) investigated the effect of replacement of tryptophan-9 with pentamethylphenylalanine (Pmp) and phenylalanine in α-MSH. Substitution to give [Pmp^9]α-MSH reduced biological activity in the lizard skin assay to half of that observed for α-MSH but it exhibited 4 to 5-fold higher activity than [Phe^9]α-MSH. These results were attributed to the comparable charge-donor properties between tryptophan and pentamethylphenylalanine with the correspondingly poorer donor properties of phenylalanine. This hypothesis would suggest that substitution of tryptophan with leucine would result in even lower activity than the phenylalanine

derivative and, indeed, Eberle and Schwyzer (1979) found [Leu^9]α-MSH to have approximately half the affinity of [Phe^9]α-MSH in the lizard skin assay.

Sugg *et al.* (1986) reported different effects of leucine-9 substitution in different assay systems and with different parent fragments. In the lizard skin assay, the fragment [Nle^4]α-MSH(4-11) was found to be equipotent with the full length α-MSH. Substitution of leucine-9 into [Nle^4]α-MSH(4-11) produced a 1500-fold decrease in potency whereas substitution into the [DPhe^7] analogue to give [Nle^4,DPhe^7,Leu^9]α-MSH(4-11) further halved activity to approximately 0.03% of the parent fragment. However, in the frog skin assay, the fragment [Nle^4]α-MSH(4-11) was weak as compared to α-MSH. In this system [Nle^4,Leu^9]α-MSH(4-11) was approximately equipotent with [Nle^4]α-MSH(4-11) whereas [Nle^4,DPhe^7,Leu^9]α-MSH(4-11) had 400-fold lower potency than [Nle^4,DPhe^7]α-MSH(4-11). These data further highlight that any conclusions drawn from structure-activity investigations should be restricted to the species used. The results are unusual as leucine-9 substitution into the [DPhe^7] analogue had a greater detrimental effect than substitution into [Nle^4]α-MSH. The higher potency normally conferred to [DPhe^7] analogues might be expected to mask some of the affinity loss observed with further amino acid substitution within the peptide.

Topographical modifications were investigated by Haskell-Luevano *et al.* (1995a) who theorised that the introduction of a methyl group at the β-carbon of tryptophan-9 would restrict freedom of rotation. This would decrease the number of possible side-chain conformations whereas peptide cyclisation still permits a large degree of flexibility of amino acid side chains. They synthesised Ac-[Nle^4]-

c[Asp^5,His^6,DPhe^7,Arg^8,β-Me-Trp^9,Lys^{10}]-NH_2, a cyclic α-MSH analogue with incorporation of a methyl group at the *pro-S* or *pro-R* position of the β-carbon of tryptophan-9 limiting topography to four possible conformations. The potency order of these isomers was found to be *2S,3S* > *2R,3R,* > *2R,3S,* >> *2S,3R* as determined by receptor binding and stimulation of cAMP. As the only notable difference between these analogues is side chain orientation, the variation in potency between the conformers suggests a more defined role for the indole moiety than determined in this work. However, as the cyclic nature of the analogue already alters peptide backbone conformation, extrapolation to the linear analogues investigated here may not be valid.

In summary, the data obtained from this investigation show that aromaticity appears to be the most critical property of the tryptophan-9 residue of α-MSH for conferring high affinity binding to the human MC1 receptor. According to a model proposed in this laboratory for the interaction of melanocortins with the MC1 receptor, [Trp^9] would interact with Phe(45), perhaps via stacking interactions (chapter 6). Loss of aromaticity at position 9 would disrupt this interaction thereby destabilising the ligand binding pocket for the His-Phe-Arg-Trp pharmacophore. Hydrophobicity of tryptophan-9 is also important for high ligand affinity whereas there appears to be a lower requirement for a pyrrole moiety and specific stereochemistry.

3.5. Quantification of Functional Activity by [^{3}H]-cAMP Measurement

The cAMP assay employed for this work is detailed in section 2.6. Its applicability was determined using the murine melanoma cell line B16, which natively expresses the MC-1 receptor thus bypassing the time-intensive plasmid isolation and electroporation process. This cell line was used thereafter as a positive control when optimising assay conditions for the COS7 and 293 cells. The 293 cell line is a human epithelial kidney cell line which is commonly used for stable receptor expression (chapters 4 and 5).

3.5.1. Determination of Optimum Stimulation Time

Quoted values for melanocortin peptide stimulation times for [^{3}H]-cAMP production range from 10 minutes (Fathi *et al.*, 1995) to 120 minutes (Desarnaud *et al.*, 1994), these differences presumably reflecting a dependence on cell type. Figure 3.10. illustrates the dependence of [^{3}H]-cAMP production on the time of incubation at 37°C with [Nle^4,DPhe^7]α-MSH for the cell lines used throughout this work. Both the B16 cell line and stably transfected 293 cells achieve maximum [^{3}H]-cAMP production after an approximately 45 minute incubation with the stimulant peptide and exhibit a gradual decrease thereafter. However, in comparison, the transiently transfected COS7 cells exhibit negligible production with levels not significantly different from those obtained with their untransfected counterpart. This indicates an apparent lack of functional coupling.

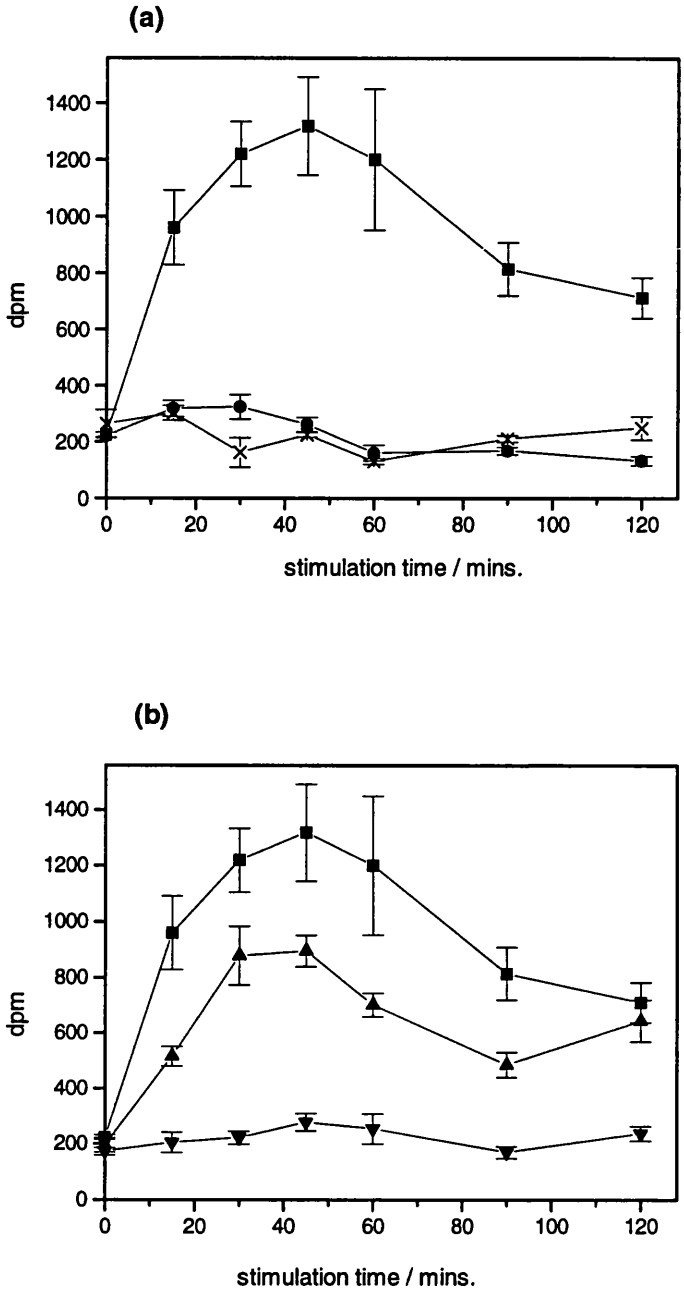

Figure 3.10. Effect of incubation time at 37°C with 5 nM [Nle^4,DPhe^7]α-MSH on [^{3}H]-cAMP production in: (■) B16 cells natively expressing the mMC1-R; (a)(●) COS7 cells transiently expressed with the hMC1-R; (x) untransfected COS7 cells; (b)(▲) 293 cells stably transfected with the hMC1-R; (▼) untransfected 293 cells.

3.5.2. Determination of Maximum [^{3}H]-Adenine Uptake Time

The time required for saturation of [^{3}H]-adenine uptake might also be expected to vary between cell lines. Figure 3.11. illustrates that incubating the cells with [^{3}H]-adenine at 37°C produces an approximately linear increase in uptake until saturation is reached. An incubation period of about 120 minutes is required for saturation of the three cell lines. The B16 and COS7 cells exhibit comparable uptake levels whereas 293 cells appear to have a lower saturation threshold.

3.5.3. Possible Explanations for Absence of Functional Activity in COS7 Cells

Functional expression can be demonstrated and quantified by measurement of different parameters depending on both the end-product of hormone-receptor stimulation and the cell type being used for expression. For example, functional activity in the B16 cell line which natively expresses the murine MC1 receptor can be assessed by measurement of cAMP generation, tyrosinase stimulation or melanin synthesis. These different assays would be expected to give comparable relative activity measurements and, indeed, allowing for inter-assay variation, this has been shown to be the case for tyrosinase and melanin production (Sahm, 1994). However, artificial expression of the melanocortin receptors in the COS7 cell system would not be expected to result in melanin production as these cells lack the necessary synthetic machinery. Possible parameters for activity measurement are therefore more limited and functional expression in transfected cells is commonly determined by cAMP generation. The absence of detectable [^{3}H]-cAMP production after melanocortin peptide stimulation in the transfected COS7 cells (section 3.5.1.)

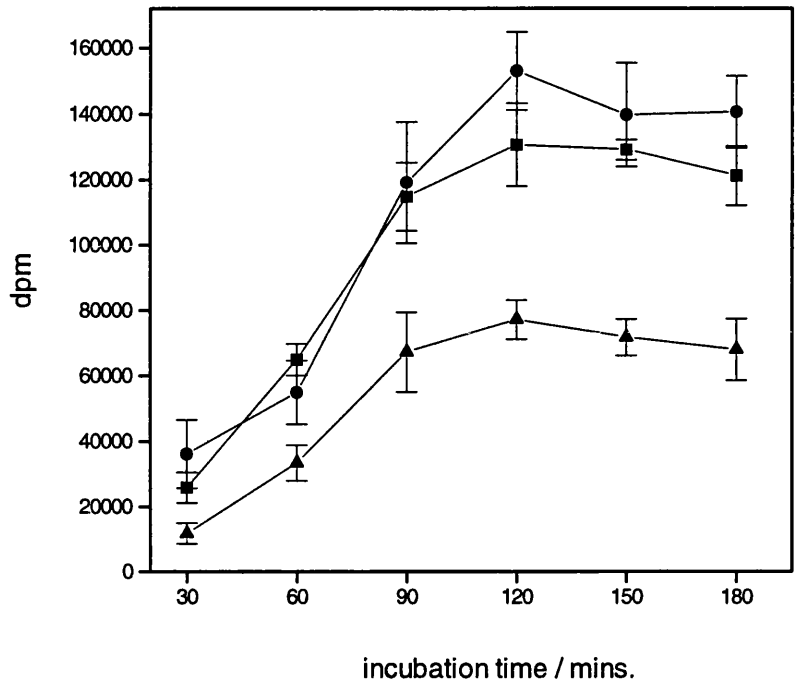

Figure 3.11. Effect of time of incubation of [^{3}H]-adenine at 37°C on [^{3}H]-cAMP production in: (■) B16 cells natively expressing the mMC1-R; (●) COS7 cells transiently expressing the hMC1-R; (▲) 293 cells stably expressing the hMC1-R.

indicates either some procedural error or a true absence of functional receptor activity.

The comparatively high [^{3}H]-adenine uptake (Figure 3.11.) achieved in COS7 cells eliminates inadequate substrate levels as the source of the problem. Concurrent binding assays were performed on every batch of transfected cells used for cAMP studies to confirm receptor presence. The high levels of specific ligand binding routinely obtained confirmed the reproducibility of electroporation.

A comparison of [^{3}H]-cAMP production in the closely related COS7 and COS1 cell lines was undertaken (Figure 3.12.). There appears to be no significant difference between them, a predictable result given the similar origin of both cell lines (Gluzman, 1981). A further explanation for the apparent lack of functional activity might be the rapid efflux of cAMP from the cells after production, and this possibility was investigated by comparison of intracellular and extracellular [^{3}H]-cAMP levels. The latter was measured by retaining the medium after peptide stimulation whilst performing nucleotide extraction from the adhered cells as per normal (section 2.6.2.). Both samples were subsequently subjected to double-column chromatography. However, Figure 3.13. indicates a comparable intracellular and extracellular [^{3}H]-cAMP level which is no higher than the background tritium level of the alumina columns.

The complex cellular processes involved in successful receptor stimulation raise numerous possible explanations for the absence of functional activity. Although COS7 cells are able to carry out some post-translational modifications they may not process the protein in an identical manner to the cell that normally produces it. The

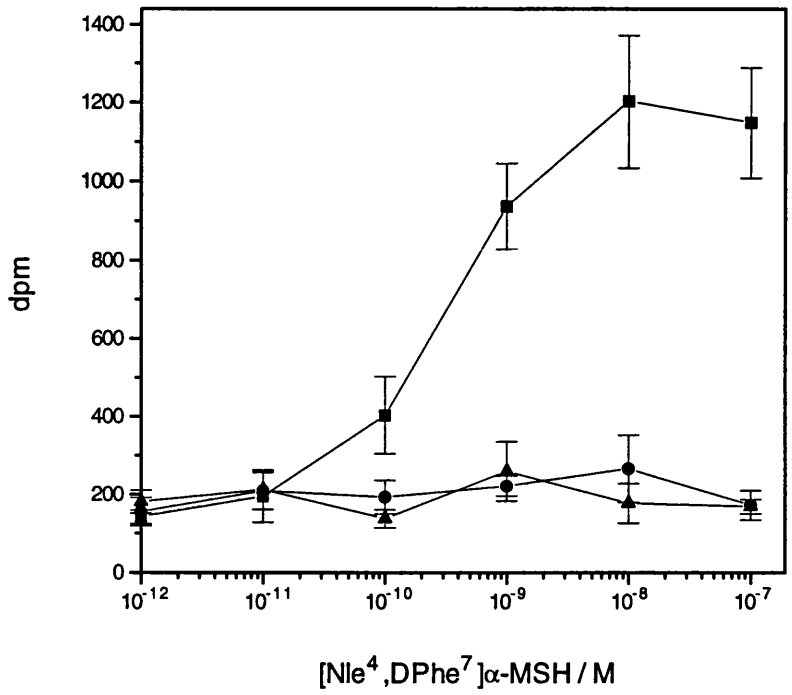

Figure 3.12. [^{3}H]-cAMP production as a result of incubation with various concentrations of [Nle^4,DPhe^7]α-MSH at 37°C for 45 minutes.

(■) B16 cells expressing the native mMC1-R; (●) COS7 cells transiently expressing the hMC1-R; (▲) COS1 cells transiently expressing the hMC1-R.

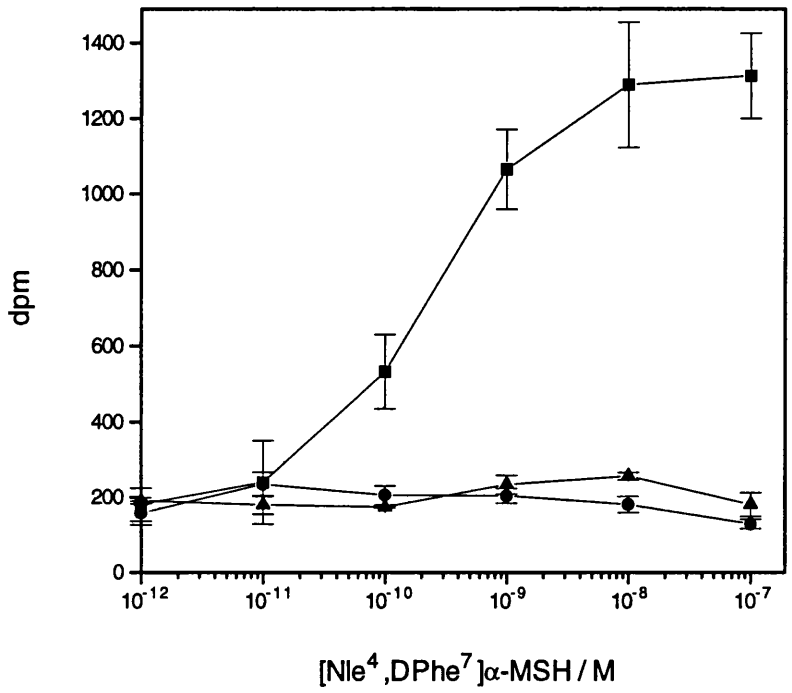

Figure 3.13. [^{3}H]-cAMP production as a result of incubation with various concentrations of [Nle^4,DPhe^7]α-MSH at 37°C for 45 minutes.

(■) B16 cells natively expressing the mMC1-R, (intracellular levels); (●) COS7 / hMC1-R, (intracellular levels); (▲) COS7 / hMC1-R cells, (extracellular levels).

human MC1 receptor is known to be glycosylated at residues Asn(15) and Asn(29) (Mountjoy *et al.*, 1992). Given the large receptor expression achieved via electroporation, an overburdening of the COS7 cell glycosylation machinery might occur, resulting in the expression of non-functional receptors. However, this is unlikely to be a valid explanation as the role of glycosylation, whilst uncertain, is generally believed not to be associated with agonist binding. Indeed, removal of the two glycosylated asparagine residues of the β_2-adrenoceptor has been shown to have little effect on agonist or antagonist binding or coupling of the receptor to adenylate cyclase (O'Dowd *et al.*, 1989).

G-proteins are heterotrimeric, being composed of α, β and γ subunits. Each is encoded by multiple distinct genes, thereby producing a diverse range of subunit chains. cAMP generation follows receptor-linked activation of the heterotrimeric protein, G_s and interaction of the free $G_s\alpha$-chain with adenylate cyclase. The β and γ chains form a tight complex anchoring G_s to the cytoplasmic face of the plasma membrane (Alberts *et al.*, 1994). Six distinct mammalian adenylate cyclase isoenzymes with unique tissue distributions have been isolated each of which differs in their activation requirements. For example, G-protein $\beta\gamma$ dimers are important regulators of some adenylate cyclase subtypes (Watson and Arkinstall, 1994). One isoenzyme, designated adenylate cyclase type III is detectable in 293 kidney cells but is insensitive to G-protein $\beta\gamma$, (Glatt and Snyder, 1993). Transfection of other receptors, such as the 5-HT_{1A} receptor, into different cell lines produced a cell-type dependent differential signal transduction by the same receptor (Banerjee *et al.*, 1993). This phenomenon may be a consequence of stimulation of different $G_s\alpha$

subtypes. These data outline the diversity of the G-proteins and suggest that one of the many necessary components for successful expression of the human MC1 receptor may be absent from the COS cell system.

Despite the above discussion, apparently successful quantification of cAMP generation via melanocortin receptor stimulation has been reported in both COS1 (Gantz *et al.*, 1993b; Fathi *et al.*, 1995) and COS7 (Barrett *et al.*, 1994; Weber *et al.*, 1993) cells. None of these publications however, cite data for MC1 receptor stimulation. Other studies suggest that expression difficulties in COS cells have been encountered by other groups. For example, Desarnaud *et al.* (1994) quote binding data for the mMC3-R in COS7 cells but expression data in stably transfected CHO cells. No functional expression data are included with the COS7 results reported by Chhajlani and Wikberg (1992) for hMC1-R and Chhajlani *et al.* (1993) for the hMC5 and mMC5 receptor binding. All of the studies cited above employed expensive, commercially available radioimmunoassay kits, and it is possible that the assay method adopted here is insufficiently sensitive to detect the relatively small quantities of cAMP produced in the COS7 cells. However, this does not explain the success of this method for the 293 cell line, which exhibits both a lower transfected receptor population (chapter 4) and a lower uptake of [^{3}H]-adenine.

It is evident from the above discussion that there is no unequivocal explanation for the absence of functional activity in the COS7 cells. The importance of correlating binding and activity data for the peptides under investigation and the timely availability of 293 cells stably transfected with the melanocortin peptides led to use of the latter for all further assays.

CHAPTER 4: RESULTS and DISCUSSION (Part II)

Binding affinity and biological activity of α-MSH derivatives in 293/hMC1-R cells

This chapter describes binding affinity and functional activity assays undertaken with α-MSH derivatives in HEK 293 cells stably transfected with the human MC1 receptor. The natural ligands α-MSH and desacetyl-α-MSH were compared to investigate the possibility of an endogenous role of the latter. Various α-MSH analogues were synthesised to investigate the importance of the C-terminal residues. Emphasis was placed on possible explanations for the different ligand binding and activation profiles obtained with the human MC1 and MC4 receptors (chapter 5) with a view to determining the specific structural requirements in this region for these receptor subtypes.

4.1. Re-selection Using Geneticin

HEK 293 cells were obtained with the hMC1-R sequence ligated into the vector pcDNA1 Neo, as described in the previous chapter. Stable transfectants were isolated by polyclonal selection using the antibiotic geneticin (G418), the gene for whose resistance is encoded by this plasmid. Despite the so-termed 'stable' nature of the expressed hMC1-R within the 293 cells, receptor expression was found to decrease significantly with repeated subculturing. This suggests a slower growth rate of the transfected cells with their subsequent loss from the cell population. The rapid decrease in receptor expression is probably a consequence of the polyclonal selection

procedure which is more convenient but less discriminating than monoclonal isolation of transfectants.

To maximise receptor expression hence assay sensitivity, regular re-selection of stable transfectants was performed using geneticin. The optimum geneticin concentration was determined using an MTT viability assay (section 2.1.2.5.). Figure 4.1a. shows a linear relationship between cell density and absorbance of the MTT-formazan-treated cells in accordance with the Beer-Lambert Law. This confirms the suitability of the assay over this cell density range. Figure 4.1b. illustrates that inclusion of geneticin to a final concentration of 0.8 μg/ml in cell culture medium for five days prior to MTT-formazan treatment reduces absorbance to approximately background levels. This indicates an almost complete loss of cell viability. It may therefore be presumed that similar treatment of transfected 293 cells will result in a surviving population, the majority of which will express the geneticin resistance gene and hence the hMC1 receptor.

293 / hMC1-R cells were used for a maximum of five passages after which the mixed population was grown in culture medium supplemented with 0.8 μg/ml geneticin for a further two passages enabling re-selection of transfectants.

4.2. Optimisation of Binding Assay Conditions

4.2.1. Confirmation of an Absence of Endogenous Receptors

Figure 4.2. depicts the [Nle^4,DPhe^7]α-MSH binding profiles obtained from 293 cells transfected with the human MC1 receptor compared with wild-type 293 cells. The latter exhibited comparable levels of total and non-specific binding with specific binding, as determined by subtraction, being negligible. This lack of specific binding

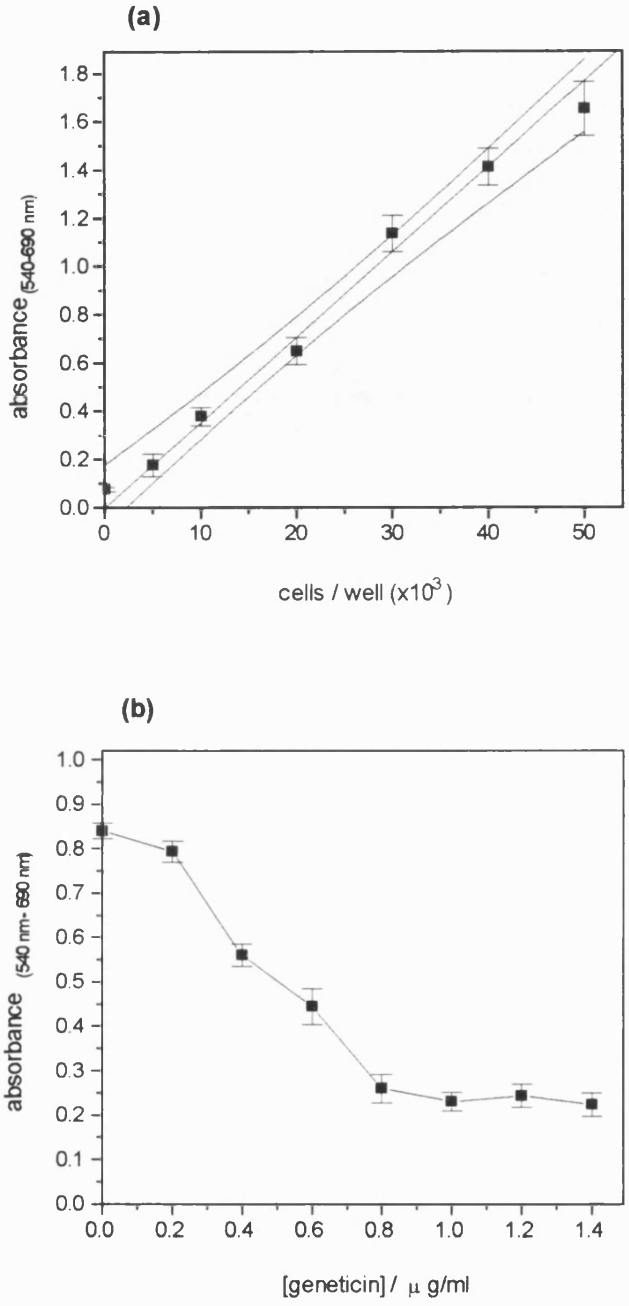

Figure 4.1. **(a)** The absorbance of 293 cells treated with MTT-formazan / DMSO as a function of cell number (curves show 95% confidence interval); **(b)** The absorbance of 5 x 10^3 293 cells incubated with geneticin for 5 days prior to treatment with MTT-formazan / DMSO.

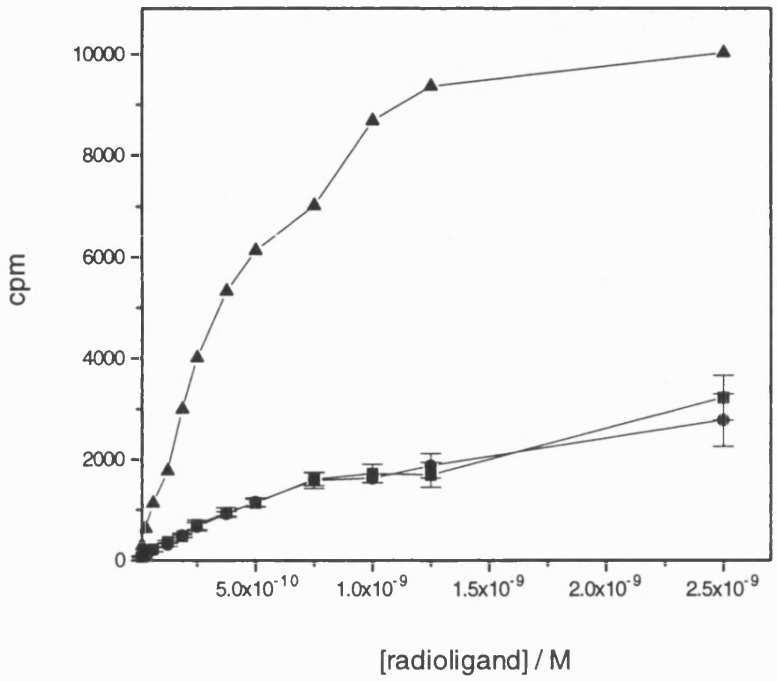

Figure 4.2. Comparison of binding at 0-4°C of [^{125}I-Tyr^{2},Nle^{4},DPhe^{7}]α-MSH to the hMC1-R stably expressed in 293 cells with binding to wild-type 293 cells.

(■) total binding of [^{125}I-Tyr^{2},Nle^{4},DPhe^{7}]α-MSH to wild-type 293 cells; (●) non-specific binding to wild-type 293 cells, in the additional presence of 1000x excess non-iodinated [Nle^{4},DPhe^{7}]α-MSH; (▲) specific binding to 293 / hMC1-R cells.

confirms the absence of endogenous melanocortin receptors in wild-type 293 cells. It may therefore be assumed that any specific binding achieved in transfected 293 cells must be a consequence of the hMC1-R gene introduced by transfection.

4.2.2. Determination of Equilibrium Binding Time

The time required for equilibrium binding at 0-4°C of [^{125}I-Tyr^2,Nle^4,DPhe^7]α-MSH to the human MC1 receptor was determined for a fixed concentration of radioligand (section 2.5.1.). Additional determinations were made in the presence of 0.5 nM, 5 nM, 50 nM and 1000-fold excess [Nle^4,DPhe^7]α-MSH to ensure equilibrium is reached over a suitable concentration range.

Figure 4.3. shows that cell-associated radioactivity reaches a plateau within 24 hours for all studied concentrations, indicating attainment of equilibrium. This is longer than the equilibrium binding time required for COS7 cells and may be a consequence of the lower receptor concentration in the 293 cells which, according to the Law of Mass Action, would reduce the hormone and receptor association rate. No appreciable hormone-receptor dissociation, as denoted by a decrease in cell-associated radioactivity, is observed over the 30 hour assay incubation thus confirming the stability of the different assay components over this time period.

4.3. Binding Isotherm of [^{125}I-Tyr^2,Nle^4,DPhe^7]α-MSH to the 293 / hMC1-R

The dissociation constant, K_d, for [^{125}I-Tyr^2,Nle^4,DPhe^7]α-MSH binding to the human MC1 receptor stably expressed in 293 cells was determined from four replicate assays (section 2.5.3.) and assigned a value of 0.67 ± 0.08 nM using *MINSQ* non-linear least squares analysis. The receptor population, also determined

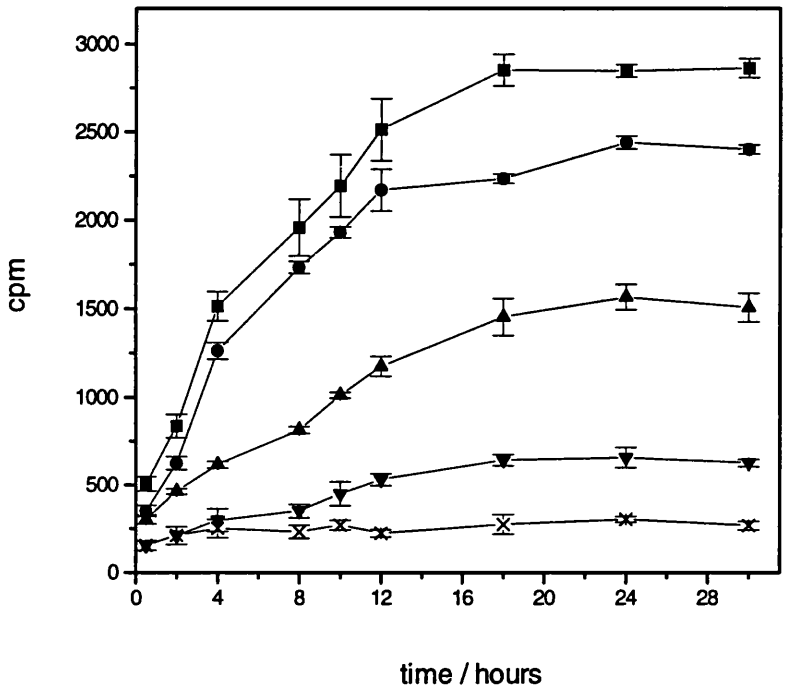

Figure 4.3. Binding at 0-4°C of 0.22 nM [^{125}I-Tyr^2,Nle^4,DPhe^7]α-MSH to the hMC1-R stably expressed in 293 cells, as a function of peptide incubation time.

(■) 0.22 nM [^{125}I-Tyr^2,Nle^4,DPhe^7]α-MSH alone, and in the additional presence of: (●) 0.5 nM [Nle^4,DPhe^7]α-MSH; (▲) 5 nM [Nle^4,DPhe^7]α-MSH; (▼) 50 nM [Nle^4,DPhe^7]α-MSH; (×) 0.22 μM [Nle^4,DPhe^7]α-MSH (non-specific binding)

by *MINSQ* analysis, was within the range of 3000 and 14000 per cell. Experimental data (Figure 4.4.) show a linear rise of non-specific binding with increasing radioligand concentration indicating its non-saturation over this concentration range. Specific binding shows an approximately linear rise with increasing radioligand concentration to 1 nM after which a plateau is reached representing full receptor occupancy.

The calculated dissociation constant is predictably very similar to the figure of 0.56 nM obtained for the transiently expressed human MC1 receptor described in the previous chapter. The receptor population per cell is lower than that measured in the transiently transfected COS7 cells; an expected observation given the more stringent requirements for successful stable expression. Scatchard analysis (Figure 4.5.) confirmed the presence of a homogeneous receptor population as would be expected given the proven absence of endogenous expression.

4.4. Binding and Activity of α-MSH Analogues

Dissociation constants were determined by *MINSQ* analysis (section 2.5.4.). Standard deviations between replicates were consistently less than 10% for binding assays and 20% for activity assays. Means and standard deviations were determined for each peptide from three or more experiments. Absolute values are shown in Table 4.1. and relative values as compared to α-MSH given in Table 4.2. Examples of experimental data are presented in Figure 4.6.,4.8.,4.9. A measure of intrinsic efficacy of each peptide was determined by its ratio of relative activity to relative affinity (Table 4.2.). The results are discussed separately for each group of peptides.

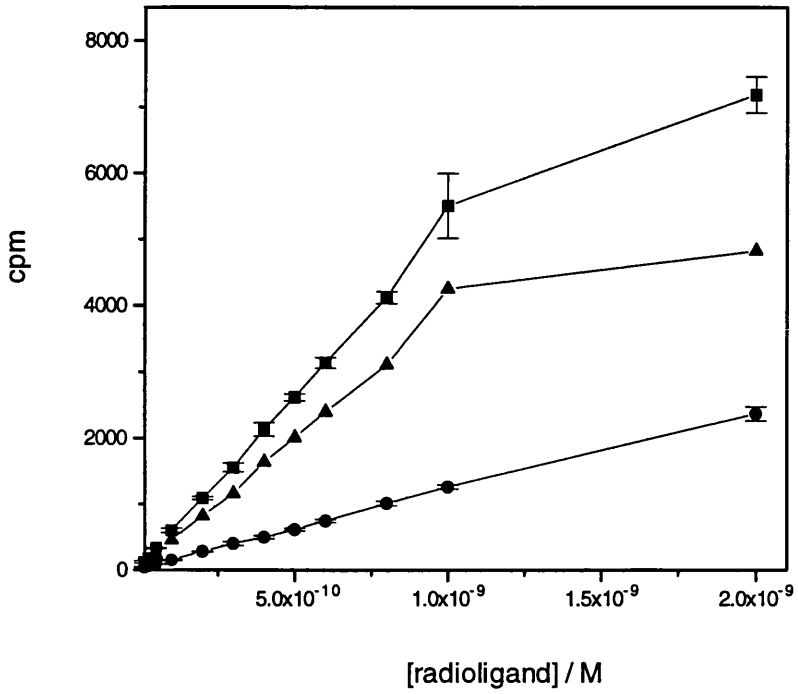

Figure 4.4. Isotherm for the binding at 0-4°C of [^{125}I-Tyr^2,Nle^4,DPhe^7]α-MSH to the hMC1-R stably expressed in 293 cells.

(■) total binding of [^{125}I-Tyr^2,Nle^4,DPhe^7]α-MSH; (●) non-specific binding in the additional presence of 1000x excess non-iodinated [Nle^4,DPhe^7]α-MSH; (▲) specific binding calculated by subtraction.

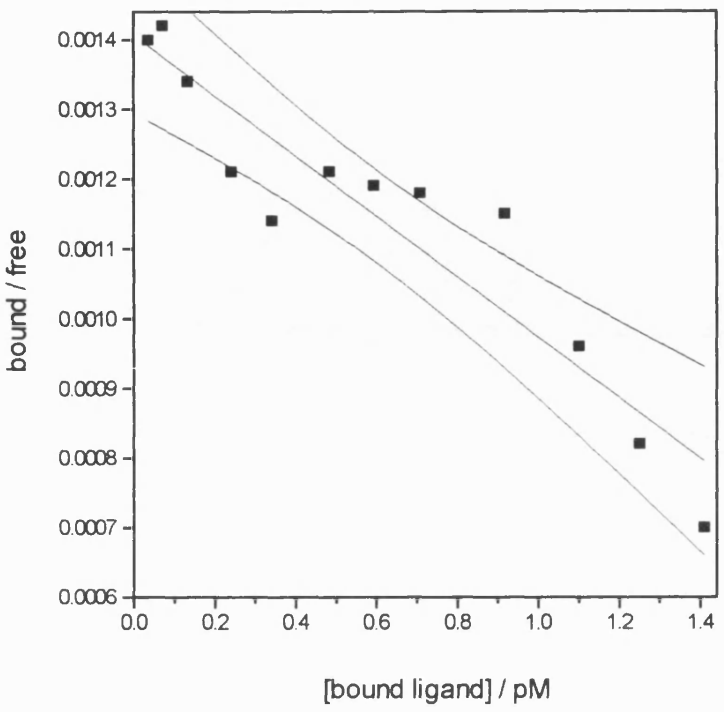

Figure 4.5. Scatchard plot for the confirmation of a homogeneous melanocortin receptor population in 293 cells stably transfected with the hMC1-R.

(Curves show 95% confidence interval)

Peptide	K_i / M (± standard deviation)	EC_{50} / M (± standard deviation)
[Nle^4,DPhe^7]α-MSH	5.74×10^{-9} ($\pm 1.20 \times 10^{-9}$) n = 9	3.64×10^{-10} ($\pm 1.79 \times 10^{-10}$) n = 5
α-MSH	3.02×10^{-8} ($\pm 3.49 \times 10^{-9}$) n = 4	3.19×10^{-9} ($\pm 5.29 \times 10^{-10}$) n = 3
desacetyl-α-MSH	8.03×10^{-9} ($\pm 3.38 \times 10^{-10}$) n = 3	3.87×10^{-9} ($\pm 5.91 \times 10^{-10}$) n = 3
[Asp^{10}]α-MSH	7.86×10^{-8} ($\pm 2.35 \times 10^{-8}$) n = 3	4.32×10^{-9} ($\pm 1.03 \times 10^{-9}$) n = 3
[Phe^{10}]α-MSH	2.76×10^{-8} ($\pm 9.54 \times 10^{-9}$) n = 5	3.38×10^{-9} ($\pm 5.80 \times 10^{-10}$) n = 4
[Phe^{12}]α-MSH	1.53×10^{-7} ($\pm 4.03 \times 10^{-8}$) n = 4	8.76×10^{-8} ($\pm 9.69 \times 10^{-9}$) n = 4
[Asp^{10},Phe^{12}]α-MSH	1.57×10^{-7} ($\pm 1.93 \times 10^{-8}$) n = 3	3.34×10^{-7} ($\pm 7.01 \times 10^{-8}$) n = 4

Peptide	K_i / M (± standard deviation)	EC_{50} / M
[Ala^{11},Ala^{12}]α-MSH	2.81×10^{-7} ($\pm 2.18 \times 10^{-8}$) n = 3	7.63×10^{-8} ($\pm 2.38 \times 10^{-9}$) n = 3
[Ala^{11},Ala^{13}]α-MSH	3.36×10^{-8} ($\pm 8.02 \times 10^{-9}$) n = 4	7.16×10^{-9} ($\pm 6.40 \times 10^{-10}$) n = 3
[Ala^{11},Ala^{12},Ala^{13}]α-MSH	4.48×10^{-7} ($\pm 2.03 \times 10^{-7}$) n = 3	$2.01\ 10^{-7}$ ($\pm 5.73 \times 10^{-8}$) n = 3

Table 4.1. Dissociation constants determined by displacement binding at 0-4°C and EC_{50} values determined by [^{3}H]-cAMP generation at 37°C (± standard deviation) for melanocortin peptide analogue binding to the human MC1 receptor expressed in 293 cells. (n = number of replicate experiments)

Peptide	Relative binding K_i αMSH / K_i	Relative activity EC_{50} αMSH /EC_{50}	$EC_{50rel.}/K_{i\ rel.}$
[Nle^4,DPhe^7]α-MSH	5.3	8.8	1.7
α-MSH	1.0	1.0	1.0
desacetyl-α-MSH	3.8	0.82	0.26
[Asp^{10}]α-MSH	0.38	0.74	2.2
[Phe^{10}]α-MSH	1.09	0.94	0.86
[Phe^{12}]α-MSH	0.20	0.042	0.18
[Asp^{10},Phe^{12}]α-MSH	0.20	0.0096	0.048
[Ala^{11},Ala^{12}]α-MSH	0.11	0.051	0.46
[Ala^{11},Ala^{13}]α-MSH	0.90	0.45	0.5
[Ala^{11},Ala^{12},Ala^{13}]α-MSH	0.067	0.016	0.24

Table 4.2. Relative dissociation and activity of melanocortin analogues as compared to α-MSH together with the relative activity (EC_{50} rel.) to relative dissociation (K_i rel.) constant ratio for each peptide on the human MC1 receptor stably expressed in 293 cells.

4.4.1. Binding and Activity of [Nle^4,DPhe^7]α-MSH, α-MSH & desacetyl-α-MSH

This section investigated the proposed species difference between the murine and human MC1-R in their response to [Nle^4,DPhe^7]α-MSH and α-MSH (Mountjoy, 1994), together with the possibility of desacetyl-α-MSH rather than α-MSH, being the predominant endogenous ligand in man.

All three peptides fully displaced [Nle^4,DPhe^7]α-MSH from the hMC1-R and showed maximum receptor stimulation (Figure 4.6.). α-MSH exhibited a dissociation constant of 30 nM and an EC_{50} value of 3.2 nM (Table 4.1.). [Nle^4,DPhe^7]α-MSH was the most potent ligand with an approximately 5-fold and 9-fold higher affinity and activity, respectively (Table 4.2.). Desacetyl-α-MSH exhibited a significantly higher binding affinity but no significant difference to α-MSH in the stimulation of cAMP production. The higher affinity but similar activity of desacetyl-α-MSH as compared to α-MSH assigns desacetyl-α-MSH a 4-fold lower intrinsic efficacy than α-MSH.

A significant difference was found in the dissociation constant calculated for [Nle^4,DPhe^7]α-MSH (5.74 nM) and its radioiodinated counterpart, [^{125}I-Tyr^2,Nle^4, DPhe^7]α-MSH (0.67 nM) (section 4.3.). A similar difference for the two peptides was observed for the B16 murine MC1 receptor and rat MC3 receptor expressed in 293 cells. It was proposed that the iodination process non-specifically improves affinity by increasing peptide hydrophobicity (Sahm, 1994). However, this affinity difference was not observed for interaction with the human MC1 receptor in COS7 cells (chapter 3). Sargent and Schwyzer (1986) proposed that given the small fraction

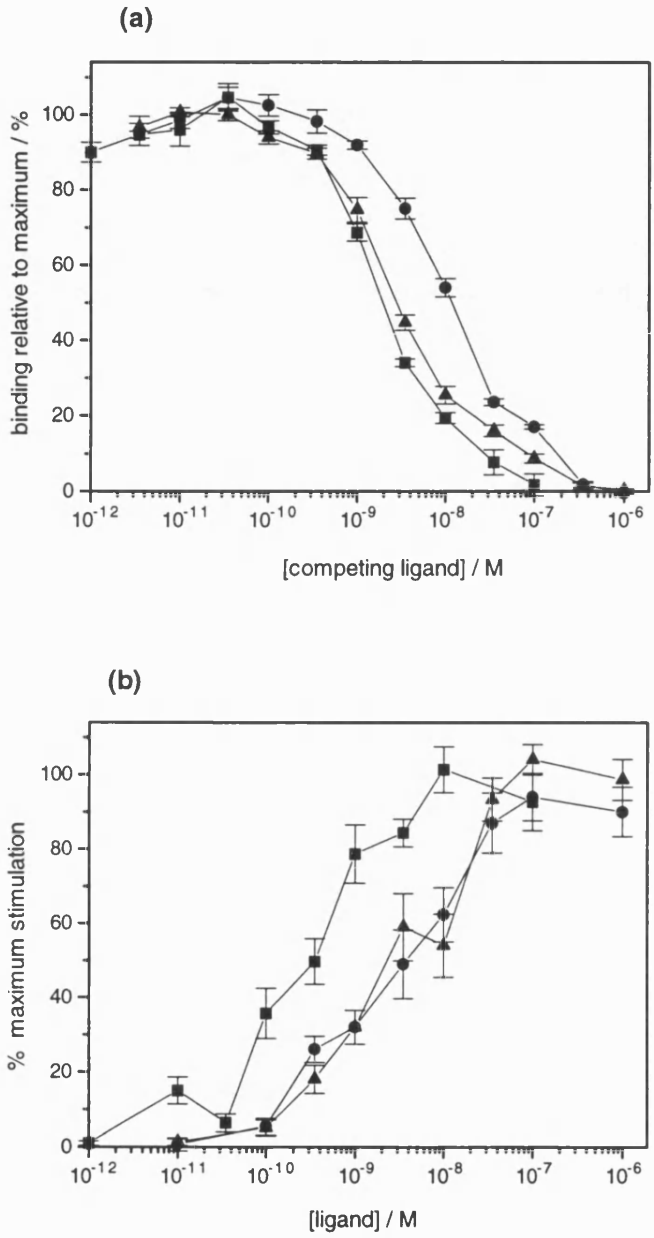

Figure 4.6.(a) Displacement binding at 0-4°C of 0.20 nM [^{125}I-Tyr^2,Nle^4,DPhe^7]α-MSH and **(b)** stimulation at 37°C of cAMP production by α-MSH analogues on the hMC1-R stably expressed in 293 cells.

(■) [Nle^4,DPhe^7]α-MSH; (●) α-MSH; (▲) desacetyl-α-MSH

of cell surface occupied by receptors, the first cellular point of contact of a hormone molecule is likely to be the lipid phase. Any interactions with the lipid bilayer will therefore represent the initial steps of hormone-cell contact. The measured dissociation constant thus becomes a function of the whole cell membrane system rather than the receptor alone. Given the divergence in membrane lipid profiles between cell lines, a particular receptor might be expected to show different binding characteristics according to its local environment.

Affinity and activity constants quoted in the literature for the MC1 receptor vary widely. This is probably a result of different cell lines used as discussed above, together with the different assay methods and conditions employed. For example, Chhajlani and Wikberg (1992) quote dissociation constants of 0.23 pM and 0.92 pM for [Nle^4,DPhe^7]α-MSH and α-MSH, respectively, for transient expression of the hMC1-R in COS7 cells. These figures were calculated after a two hour incubation of the peptide with the receptor at 37°C and are considerably higher than the affinities determined here. However, there is a 4-fold difference in the relative values between the peptides and this is comparable to the ratio of 5.3 determined from this work (Table 4.2.). Haskell-Luevano (1994) quote dissociation constants of 1.2 nM and 6.5 nM for [Nle^4,DPhe^7]α-MSH and α-MSH, respectively, on the human MC1 receptor expressed in L-cells. These figures are in agreement with both the absolute and relative values determined in this work. It is therefore more appropriate to use relative rather than absolute values when comparing data obtained from different laboratories.

In contrast to the murine MC1-R, which has been found to have at least a 10-fold difference in activity between [Nle^4,DPhe^7]α-MSH and α-MSH (Lunec *et al.*,

1992; Mountjoy *et al.*, 1992; Sahm, 1994), Mountjoy (1994) found the two peptides to have comparable activity on the human MC1-R homologue. This observation was supported by the finding of approximate equipotency for these peptides on melanogenesis in cultured human melanocytes (Hunt, 1995). The possibility of a species difference was therefore raised. Such a species specific role would not be unexpected given the 76% sequence homology between the human and murine homologues and the equipotency of ACTH and α-MSH on the former but not the latter (Chhajlani and Wikberg, 1992; Mountjoy *et al.*, 1992; Gantz *et al.*, 1993a). However, the results presented here are at variance with this hypothesis with the determination of an approximate 9-fold difference in activity between the analogues. These data are in broad agreement with the 4-fold and 10-fold difference in activity between [Nle^4,$DPhe^7$]α-MSH and α-MSH reported by Haskell-Luevano *et al.* (1994) and Gantz *et al.* (1993a), respectively for the human MC1 receptor. These conflicting data may be explained by the different behaviour of variant hMC1-R alleles, a phenomenon thought to be responsible for differences in pigmentation in other species (Robbins *et al.*, 1993).

N-terminal acetylations are important in determining the biological activity of many peptide hormones and neurotransmitters (Tsunasawa and Sakiyama, 1984). A modification such as the omission of an acetyl group, whilst a seemingly small alteration may concurrently change several features. A positive charge appears at the amino-terminal end, the hydrophilicity of the region is increased with the loss of the lipophilic methyl group together with a change in the hydrogen-bridge forming ability and the stereochemical relationships of nearby residues. N-terminal

acetylations are important for high affinity binding to the human MC2 receptor (Garren, 1968). The human MC3-R and murine MC1-R however, do not apparently distinguish between acetylated and desacetylated ACTH(1-13) (Miwa *et al.*, 1995; Sahm, 1994). Desacetyl-α-MSH has been located using HPLC and radioimmunological characterisation in both the human foetal and adult pituitary gland (Tilders *et al.* 1981; Brubaker *et al.*, 1982; Bateman *et al.*, 1986) and this peptide also predominates in the hypothalamus (Parker *et al.*, 1981). Early work (section 1.5.1.) showed the effect of acetylation of the N-terminal serine residue to be dependent on the particular amphibian model being investigated with the general conclusion that desacetyl-α-MSH exhibits either equipotency or lower potency than its acetylated counterpart (Eberle, 1988). More recently Mountjoy (1994) and Gantz *et al.* (1993a) found no significant difference between desacetyl-α-MSH and α-MSH in the stimulation of cAMP via the human MC1 receptor. Affinity constants reported for its interaction with the murine MC1 receptor (Eberle, 1988; Sahm, 1994) were not significantly different to values obtained by these workers for α-MSH. The results presented in Table 4.1. assign a significantly higher affinity to desacetyl-α-MSH but agree with the above data in showing no significant difference in activity to α-MSH. The ratio of relative activity to relative affinity assigns desacetyl-α-MSH a lower intrinsic efficacy than α-MSH but its widespread occurrence together with its equipotency with α-MSH supports the possibility of desacetyl-α-MSH being an important natural ligand in man. However, ACTH has also been proposed as having a physiological pigmentary role as human melanocytes have been found to respond to lower concentrations of ACTH than MSH peptides (Hunt, 1995). This raises the

interesting possibility of a combined role for ACTH and the MSH peptides in human skin pigmentation.

4.4.2. Binding of C-terminally-substituted α-MSH Analogues

The C-terminal has long been recognised to play a significant role in the interaction of the melanocortin peptides with their receptors (section 1.5.3.). The two endogenous peptides, α-MSH and γ-MSH show a high degree of conservation except in this C-terminal region (Figure 4.7.). α-MSH has been shown repeatedly to be a high affinity agonist on the human MC1 receptor whereas γ-MSH binds only weakly. For example, Gantz *et al.* (1993a) found γ_2-MSH unable to induce a full cAMP response even at maximal concentrations whereas Chhajlani and Wikberg (1992) found γ-MSH to have approximately ten-fold lower potency than α-MSH on the human MC1 receptor. Mountjoy (1994) found γ_2-MSH to have an approximately four-fold lower activity than [Nle^4,DPhe^7]α-MSH and α-MSH on the human receptor but several orders of magnitude lower on the murine MC1-R.

α-MSH: Ac-Ser-Tyr-Ser-Met-Glu-His-Phe-Arg-Trp-**Gly**-Lys-**Pro**-Val-NH_2

γ_1-MSH: H-Tyr-Val-Met-Gly-His-Phe-Arg-Trp-**Asp**-Arg-**Phe**-OH

Figure 4.7. Amino acid sequences of the endogenous ligands α-MSH and γ_1-MSH. (Major C-terminal differences highlighted.)

Two major structural differences between these endogenous peptides occur at the C-terminal end and these were probed using α-MSH analogues containing the corresponding γ-MSH residues. Aspartic acid was substituted for glycine-10 and phenylalanine for proline-12, numbered with respect to α-MSH. Position 11 of α-MSH is lysine and its equivalent in γ-MSH is arginine. Both residues are basic with comparable size and hydrophobicity (appendix A), therefore it was supposed that the difference in behaviour between the two peptides was unlikely to be due to this conservative change. γ_1-MSH lacks an equivalent residue for valine-13 of α-MSH. The aim of this study was to obtain a clearer understanding of the structural requirements in this region for high affinity binding to and activation of the human MC1 receptor. The importance of the C-terminal region was also more generally probed using multiple alanine-substituted peptides to increase understanding of the combined importance of these residues.

Each investigated peptide was able to displace fully [^{125}I-Tyr^2,Nle^4,DPhe^7]α-MSH from the human MC1 receptor and produce maximum receptor stimulation (Figure 4.8., 4.9.). Neither [Asp^{10}]α-MSH or [Phe^{10}]α-MSH showed any significant difference to α-MSH in binding affinity or activity. [Phe^{12}]α-MSH showed one-fifth of the affinity and only 4% of the activity of the parent peptide. Di-substitution to give [Asp^{10},Phe^{12}]α-MSH did not significantly affect binding affinity as compared to [Phe^{12}]α-MSH but further reduced cAMP production to less than 1% of α-MSH. Both [Phe^{12}]α-MSH and [Asp^{10},Phe^{12}]α-MSH showed lower intrinsic efficacies, displaying EC_{50} rel.:K_i rel. ratios that are 5-fold and 20-fold lower, respectively than

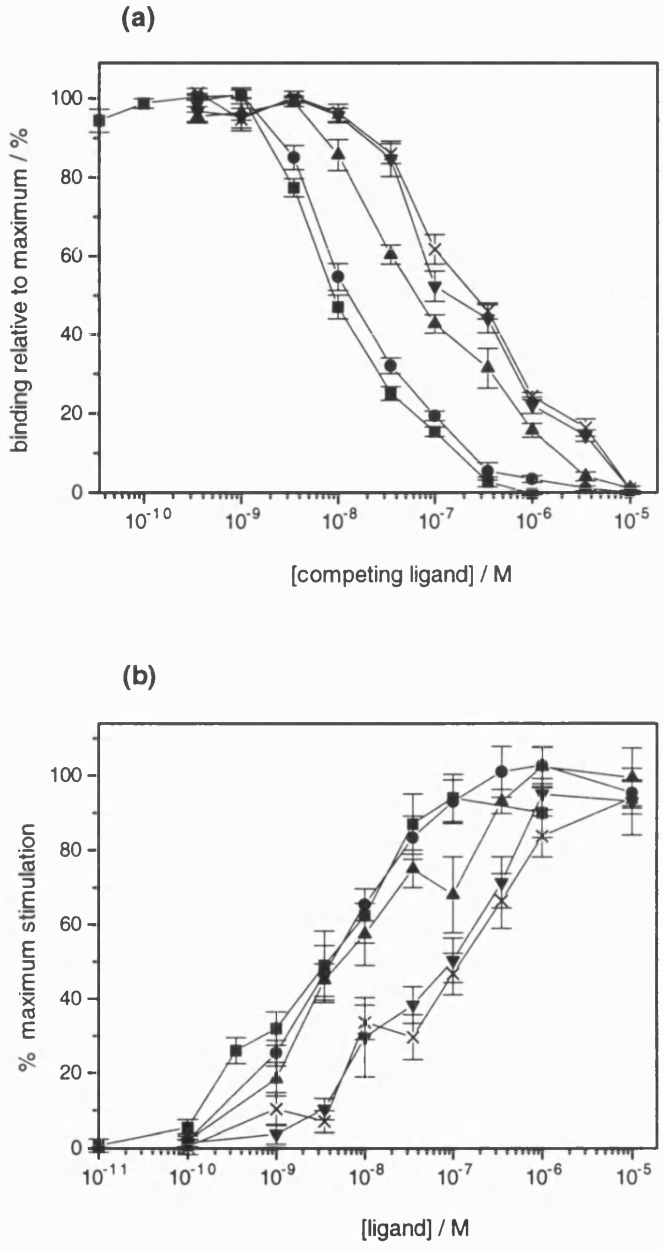

Figure 4.8.(a) Displacement binding at 0-4°C of 0.18 nM [^{125}I-Tyr^{2},Nle^{4},DPhe^{7}]α-MSH and **(b)** stimulation at 37°C of cAMP production by α-MSH analogues on the hMC1-R stably expressed in 293 cells.

(■) α-MSH; (●) [Phe^{10}]α-MSH; (▲) [Asp^{10}]α-MSH; (▼) [Phe^{12}]α-MSH; (×) [Asp^{10},Phe^{12}]α-MSH

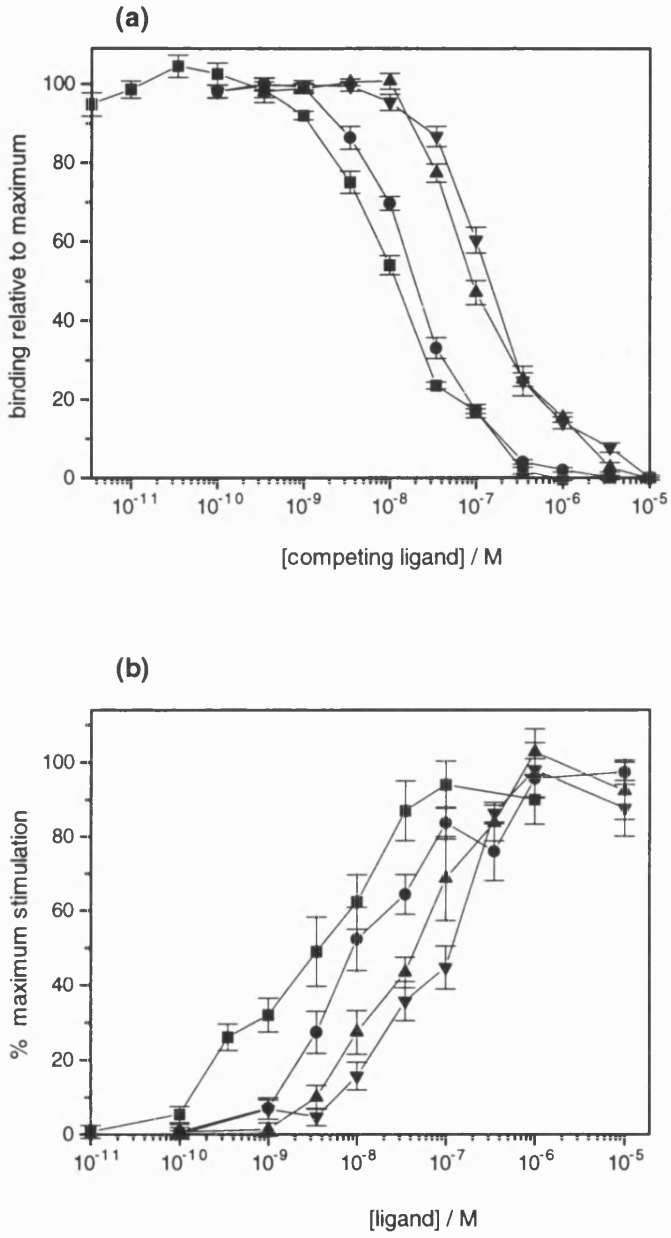

Figure 4.9.(a) Displacement binding at 0-4°C of 0.20 nM [^{125}I-Tyr^{2},Nle^{4},DPhe^{7}]α-MSH and **(b)** stimulation at 37°C of cAMP production by α-MSH analogues on the hMC1-R stably expressed in 293 cells.

(■) α-MSH; (●) [Ala^{11},Ala^{13}]α-MSH; (▲) [Ala^{11},Ala^{12}]α-MSH;

(▼) [Ala^{11},Ala^{12},Ala^{13}]α-MSH

those calculated for α-MSH. [Ala^{11},Ala^{12}]α-MSH showed no significant difference in either binding or activity to [Phe^{12}]α-MSH. [Ala^{11},Ala^{13}]α-MSH produced no significant difference in either binding or activity as compared to the parent compound. Substitution of the terminal tripeptide to give [Ala^{11},Ala^{12},Ala^{13}]α-MSH produced 7% and 1.6% of the binding and activity of the parent peptide, respectively. The activity of this peptide was significantly lower than that of the di-substituted [Ala^{11},Ala^{12}]α-MSH. Multiple alanine substitution within the C-terminal affected biological activity more than binding affinity producing peptides with between 2 to 4-fold lower intrinsic efficacies than α-MSH. The relative binding affinity and activity of each peptide as compared to α-MSH was determined for every assay (Figure 4.10.) to illustrate experimental reproducibility.

The glycine residue at position 10 of α-MSH was originally described as having a "spacer function" (section 1.5.3.) since the presence of an amino acid rather than the nature of the residue itself was thought to be the critical feature (Medzihradsky, 1976). Introduction of residues such as cysteine in c[Cys^{4},Cys^{10}]α-MSH (Sawyer *et al.*, 1980; Eberle, 1988) or lysine in Ac-c[Nle^{4},Glu^{5},DPhe^{7},Lys^{10},Gly^{11}]α-MSH(4-13)-NH_2 and Ac-c[Nle^{4},Asp^{5},DPhe^{7}, Lys^{10},Gly^{11}] α-MSH(4-13)-NH_2 (Al-Obeidi *et al.*, 1989a, b) appears to be possible in both linear and cyclic analogues without a significant effect on peptide action. The data determined here are in agreement with these observations. Replacement of the small neutral glycine molecule with the more bulky phenylalanine produced an analogue with K_i and EC_{50} values remarkably similar to those determined for

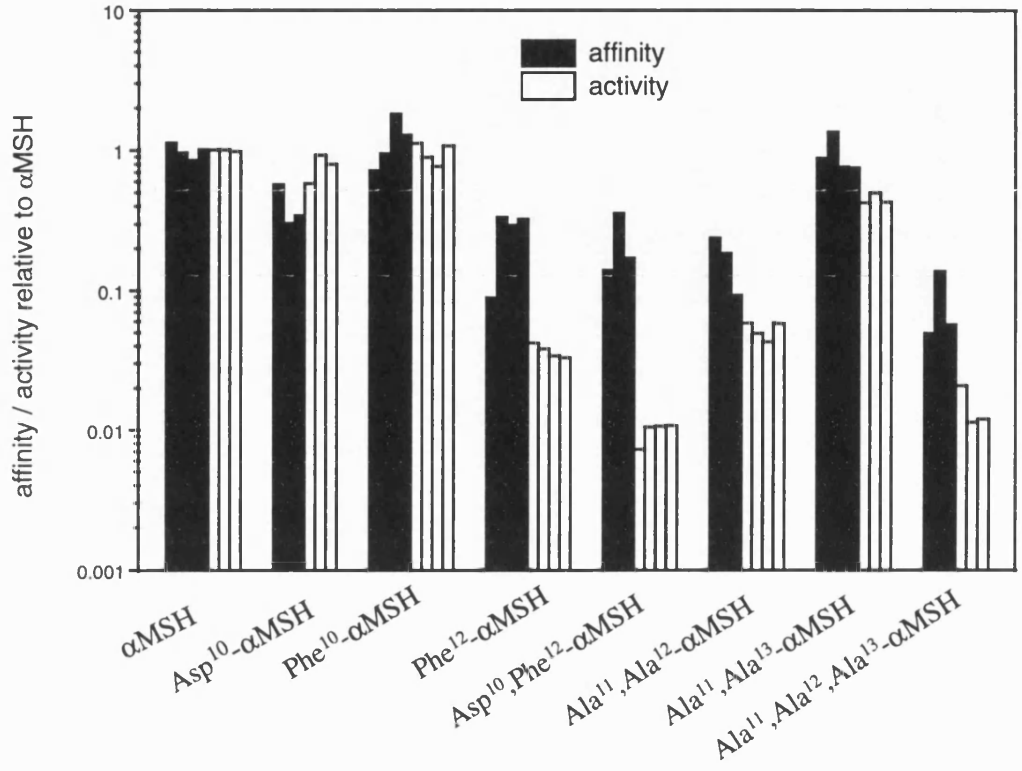

Figure 4.10. Relative affinity and activity of C-terminally substituted α-MSH analogues as compared to α-MSH (log scale). Each column represents a single experiment.

(black: binding affinity; white: cAMP production)

α-MSH. Substitution with aspartic acid produced a small decrease in affinity but no significant difference in activity to α-MSH. The longer side chains of the substituents and charged nature of aspartic acid appear therefore, to have little detrimental effect on the local conformation of the peptide backbone. These data suggest the presence of glycine at position 10 of α-MSH to be relatively unimportant for high affinity binding to the human MC1 receptor. In agreement with the above, replacement of the [Gly^{10}] residue of α-MSH with alanine produced a peptide not significantly different in affinity or activity from α-MSH on the murine MC1 receptor (Sahm 1994). Given the structural similarity of glycine and alanine this result is not unexpected although the methyl side chain of alanine might be expected to limit the conformational freedom of the peptide backbone and increase lipophilicity. However, further work with the murine receptor produced data at variance with the results reported here. [Phe^{10}]α-MSH was found to have 3% of the affinity and 0.7% of the activity whereas [Asp^{10}]α-MSH retained only 1.2% of the affinity and activity of α-MSH (Peng *et al.*, 1996). These data support a proposed species difference between the human and murine MC1 receptors as discussed previously, in which glycine-10 of α-MSH plays a greater role in receptor recognition and stimulation of the murine than the human homologue.

Position 12 of α-MSH is proline whereas the equivalent residue in γ-MSH is phenylalanine. Substitution of proline with its D-stereoisomer, norvaline or glycine has been found to reduce peptide activity significantly in several amphibian assays and in the Cloudman S91 tyrosinase assay, (Eberle, 1988). Sahm (1994) found an insignificant difference in biological activity between [Ala^{12}]α-MSH and its parent

peptide although it exhibited only 10% of the binding affinity of α-MSH. Substitution to give [Phe^{12}]α-MSH had a significantly detrimental effect on both affinity and activity on the murine MC1 receptor (Peng *et al.*, 1996) and is in agreement with the data presented in this work. The significantly lower activity of [Asp^{10},Phe^{12}]α-MSH as compared to [Phe^{12}]α-MSH shows that di-substitution in these positions results in a greater loss of potency than the product of each single change. This may be due to an interaction of the aspartic acid and phenylalanine side chains unfavourably distorting peptide conformation.

The positive charge carried by the lysine residue at position 11 was originally thought to be critical for α-MSH activity (Eberle and Schwyzer, 1975). Its ornithine analogue was found to be almost fully active, whereas the norleucine derivative, with a neutral side chain of comparable length, had 20-fold lower activity than the original hormone as measured by pigment dispersion (Medzihradszky, 1982). Replacement by serine, glycine or glutamic acid reduced biological activity by 20 to 100-fold as measured by pigment dispersion and tyrosinase stimulation in Cloudman S91 cells suggesting the necessary presence of hydrophilicity and the basic side-chain of lysine for optimum effect (Eberle, 1988). Substitution of lysine-11 to arginine-11 within ACTH analogues had no significant effect on corticosteroidogenicity whereas protection of its positive charge diminished potency by 80-fold (Goverde *et al.*, 1993). Other studies refute the importance of this residue with substitution by glycine being found to have an insignificant effect on activity (Al-Obeidi *et al.*, 1989a, b). In this laboratory a photoaffinity label has successfully been attached onto the lysine residue, (Ahmed *et al.* 1992) and replacement with alanine has been made (Sahm,

1994) with neither alteration producing a significant loss of potency on the murine MC1 receptor. Substitution of valine-13 with methionine, its *S*-oxide or *S*-dioxide produced little change in the pigment-dispersing activity of α-MSH(11-13) (Eberle, 1988) and Sahm (1994) found [Ala^{13}]α-MSH to exhibit equipotency with α-MSH on the murine MC1 receptor. These results are in agreement with data obtained in this study showing no significant difference between [Ala^{11},Ala^{13}]α-MSH and α-MSH. This suggests that neither position 11 nor 13 are significant for peptide action. The 9-fold and 20-fold reduction in affinity and activity, respectively seen with [Ala^{11},Ala^{12}]α-MSH as compared to α-MSH, produce similar relative values to those obtained for [Phe^{12}]α-MSH and would appear to agree with the above data for the dispensability of lysine. This suggests that the significant decrease observed for [Ala^{11},Ala^{12}]α-MSH is mostly attributable to alanine-12 substitution. The 15-fold reduction in affinity and 60-fold loss of activity for [Ala^{11},Ala^{12},Ala^{13}]α-MSH is comparable to the results obtained by Sahm (1994) who found the fragment α-MSH(1-10) to have an approximately hundred-fold lower binding affinity and activity than α-MSH in B16 murine melanoma cells. Tri-alanine substitution has a further detrimental effect on activity than its di-substituted counterparts probably as a consequence of the alteration of peptide conformation in this region. These data support the hypothesis of this region containing a second message sequence as proposed by Eberle and Schwyzer (1975).

Taken together these data confirm the importance of the C-terminal region for both high affinity binding to and full activation of the human MC1 receptor.

However, within this sequence proline-12 appears to be most sensitive to alteration and therefore the most critical amino acid for conferring these properties. The relative unimportance of glycine-10 for the human but not the murine receptor lends weight to the proposed species difference between these receptor homologues although the different binding profiles of [Nle^4,DPhe^7]α-MSH and α-MSH to the human and murine MC1 receptors as found by Mountjoy (1994) was not corroborated in this work. These data also infer that the low activity exhibited by the γ-MSH peptide on the MC1 receptor is largely due to the requirement for proline at position 12 rather than the absence of glycine at position 10.

CHAPTER 5: RESULTS and DISCUSSION (Part III)

Binding affinity and biological activity of α-MSH derivatives in 293/hMC4-R cells

Comparison of the hMC1 and hMC4 receptors

Since the recent isolation and cloning of the human melanocortin-4 receptor (section 1.6.4.) relatively few structure-activity data have been reported. Further information would be of interest given the widespread neural distribution of the MC4-R and its possible association with some of the CNS effects attributed to the melanocortins (section 1.4.2.2.).

This chapter investigates α-MSH analogue interaction with the human MC4 receptor subtype. The potency of [Nle^4,$DPhe^7$]α-MSH and the natural ligands α-MSH and desacetyl-α-MSH were once again compared to determine a possible endogenous role. Gantz *et al.* (1993b) reported comparable ligand binding profiles for ACTH, α-MSH and γ-MSH on the MC1 and MC4 receptors and proposed the C-terminal of α-MSH to be important for determining selectivity between these receptors. Use of the same analogues as detailed in the previous chapter enabled an investigation into the role of the C-terminal region for MC4-R binding and activation. It also allowed a direct comparison between the hMC1 and hMC4 receptors with possible delineation of the specific structural requirements of these receptor subtypes.

Degenerate oligonucleotides based on conserved melanocortin sequences in transmembrane domains II and VII were used to probe total rat brain RNA and

resulted in the isolation of a fragment of rat MC4-R. Hybridisation of this fragment with a human genomic DNA library led to the successful identification of the human homologue (Mountjoy *et al.*, 1994). The coding fragment was subsequently subcloned into pcDNA1 Neo and stably transfected into 293 HEK cells as outlined previously for the hMC1-R.

The obtained 293-hMC4 cell line underwent re-selection with geneticin as necessary (section 2.1.2.5.) as discussed in chapter 4.

5.1. Binding Isotherm of [^{125}I-Tyr^2,Nle^4,DPhe^7]α-MSH to the 293 / hMC4-R

The binding affinity of [^{125}I-Tyr^2,Nle^4,DPhe^7]α-MSH for the human MC4 receptor stably expressed in 293 cells was determined from three replicate experiments. Representative data are given in Figure 5.1. and *MINSQ* linear least squares analysis gave a dissociation constant, K_d, of 5.17 ± 0.54 nM. The absence of receptor saturation at the highest working concentration (2 nM) indicates the lower affinity of the ligand for this receptor subtype than for the human MC1-R. The population was shown to be homogenous by Scatchard analysis (Figure 5.2.) with a range of 5000 to 12000 receptors per cell determined by *MINSQ* analysis.

5.2. Binding and Activity of α-MSH Analogues

Absolute and relative K_i and EC_{50} values were determined by *MINSQ* analysis from displacement binding and cAMP assays, respectively (Tables 5.1., 5.2). Average means and standard deviations were determined from three or more experiments. Representative binding curves are given in Figure 5.3a.-5.5a. with standard deviations associated with the replicates being consistently less than 10%.

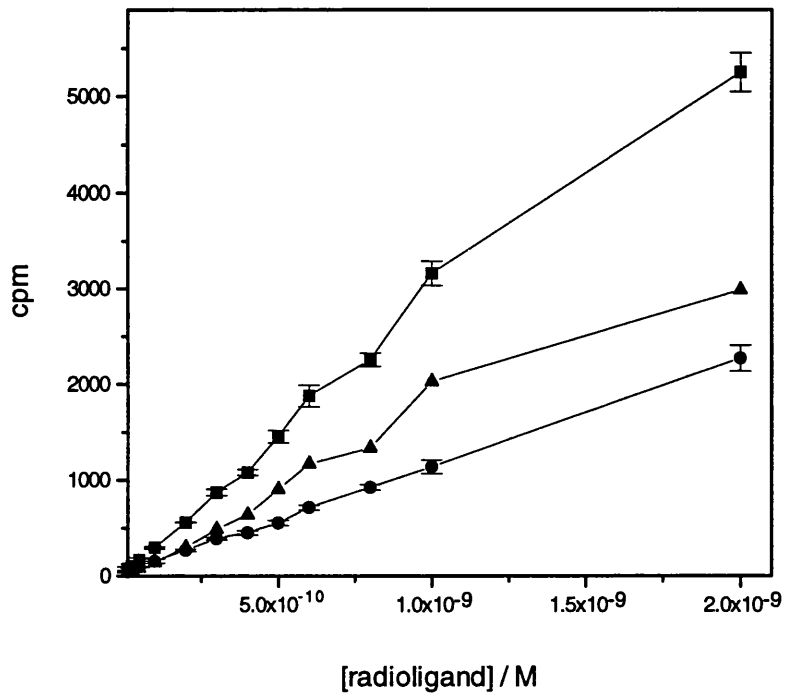

Figure 5.1. Isotherm for the binding at 0-4°C of [^{125}I-Tyr^2,Nle^4,DPhe^7]α-MSH to the hMC4-R stably expressed in 293 cells.

(■) total binding of [^{125}I-Tyr^2,Nle^4,DPhe^7]α-MSH; (●) non-specific binding in the additional presence of 1000x excess non-iodinated [Nle^4,DPhe^7]α-MSH; (▲) specific binding calculated by subtraction.

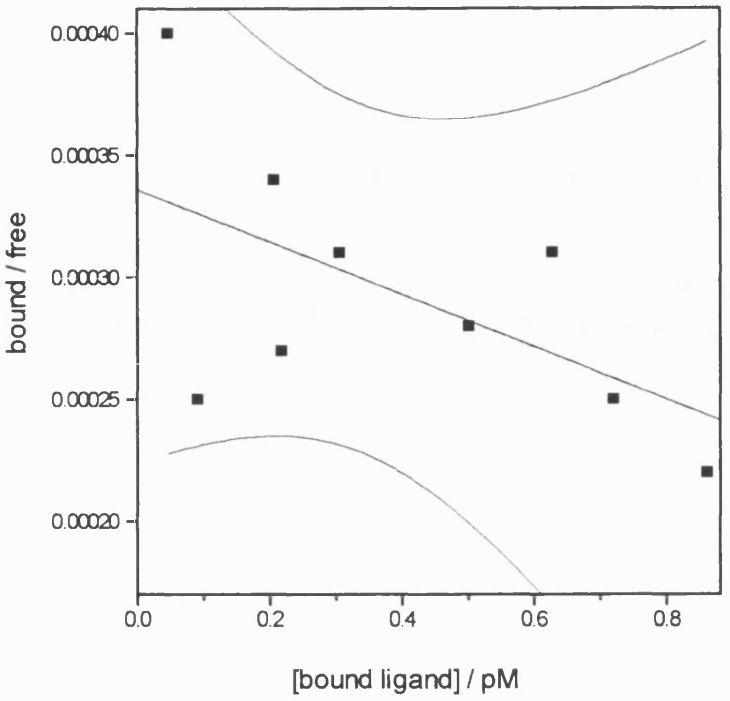

Figure 5.2.. Scatchard plot for the confirmation of a homogeneous melanocortin receptor population in 293 cells transiently transfected with the hMC4-R.

(Curves show 95% confidence intervals.)

Peptide	K_i / M (± standard deviation)	EC_{50} / M (± standard deviation)
[Nle^4,DPhe^7]α-MSH	5.69×10^{-8} ($\pm 6.13 \times 10^{-9}$) n = 5	1.75×10^{-9} ($\pm 8.49 \times 10^{-10}$) n = 6
α-MSH	7.28×10^{-7} ($\pm 5.51 \times 10^{-8}$) n = 6	6.89×10^{-8} ($\pm 7.80 \times 10^{-9}$) n = 3
desacetyl-α-MSH	4.62×10^{-7} ($\pm 3.63 \times 10^{-8}$) n = 3	2.10×10^{-8} ($\pm 8.94 \times 10^{-9}$) n = 3
[Asp^{10}]α-MSH	NA n = 3	2.23×10^{-6} ($\pm 7.73 \times 10^{-7}$) n = 3
[Phe^{10}]α-MSH	1.95×10^{-5} ($\pm 3.52 \times 10^{-6}$) n = 4	3.48×10^{-7} ($\pm 8.57 \times 10^{-8}$) n = 3
[Phe^{12}]α-MSH	2.35×10^{-6} ($\pm 4.56 \times 10^{-7}$) n = 4	5.03×10^{-8} ($\pm 9.40 \times 10^{-9}$) n = 3
[Asp^{10},Phe^{12}]α-MSH	NA n = 3	3.42×10^{-6} ($\pm 5.23 \times 10^{-7}$) n = 3

Peptide	K_i / M (± standard deviation)	EC_{50} / M (± standard deviation)
[Ala^{11},Ala^{12}]α-MSH	2.34×10^{-6} ($\pm 5.74 \times 10^{-7}$) n = 3	2.49×10^{-7} ($\pm 5.92 \times 10^{-8}$) n = 3
[Ala^{11},Ala^{13}]α-MSH	2.52×10^{-6} ($\pm 4.23 \times 10^{-7}$) n = 3	2.10×10^{-7} ($\pm 2.42 \times 10^{-8}$) n = 3
[Ala^{11},Ala^{12},Ala^{13}]α-MSH	4.91×10^{-6} ($\pm 3.97 \times 10^{-7}$) n = 3	9.49×10^{-7} ($\pm 1.16 \times 10^{-7}$) n = 3

Table 5.1. Dissociation constants as determined by displacement binding at 0-4°C and EC_{50} values as determined by [^{3}H]-cAMP generation at 37°C (± standard deviation) for melanocortin peptide analogue binding to the human MC4 receptor expressed in 293 cells.

(NA = 'non-applicable'; indicating too low a peptide affinity for accurate calculation)

(n = number of replicate experiments)

Peptide	Relative binding K_i αMSH / K_i	Relative activity EC_{50} αMSH/EC_{50}	$EC_{50rel.}/K_{i\ rel.}$
[Nle^4,DPhe^7]α-MSH	12.8	39	3.1
α-MSH	1.0	1.0	1.0
desacetyl-α-MSH	1.6	3.3	2.1
[Asp^{10}]α-MSH	NA	0.031	NA
[Phe^{10}]α-MSH	0.037	0.20	5.4
[Phe^{12}]α-MSH	0.31	1.4	4.5
[Asp^{10},Phe^{12}]α-MSH	NA	0.020	NA
[Ala^{11},Ala^{12}]α-MSH	0.31	0.28	0.90
[Ala^{11},Ala^{13}]α-MSH	0.29	0.33	1.1
[Ala^{11},Ala^{12},Ala^{13}]α-MSH	0.15	0.073	0.49

Table 5.2. Relative dissociation and activity of melanocortin analogues as compared to α-MSH together with the relative activity (EC_{50} rel.) to relative dissociation (K_i rel.) constant ratio for each peptide on the human MC4 receptor stably expressed in 293 cells.

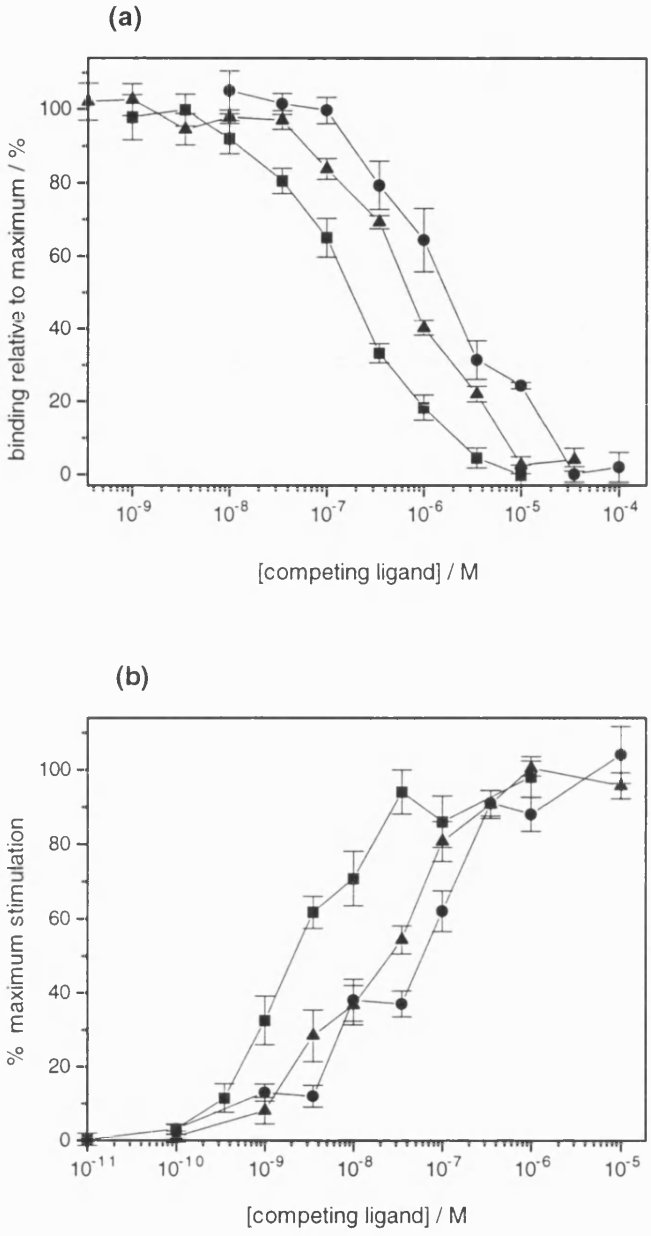

Figure 5.3.(a) Displacement binding at 0-4°C of 0.20 nM [^{125}I-Tyr^{2},Nle^{4},DPhe^{7}]α-MSH and **(b)** stimulation at 37°C of cAMP production by α-MSH analogues on the hMC4-R.

(■) [Nle^{4},DPhe^{7}]α-MSH; (●) α-MSH; (▲) desacetyl-α-MSH

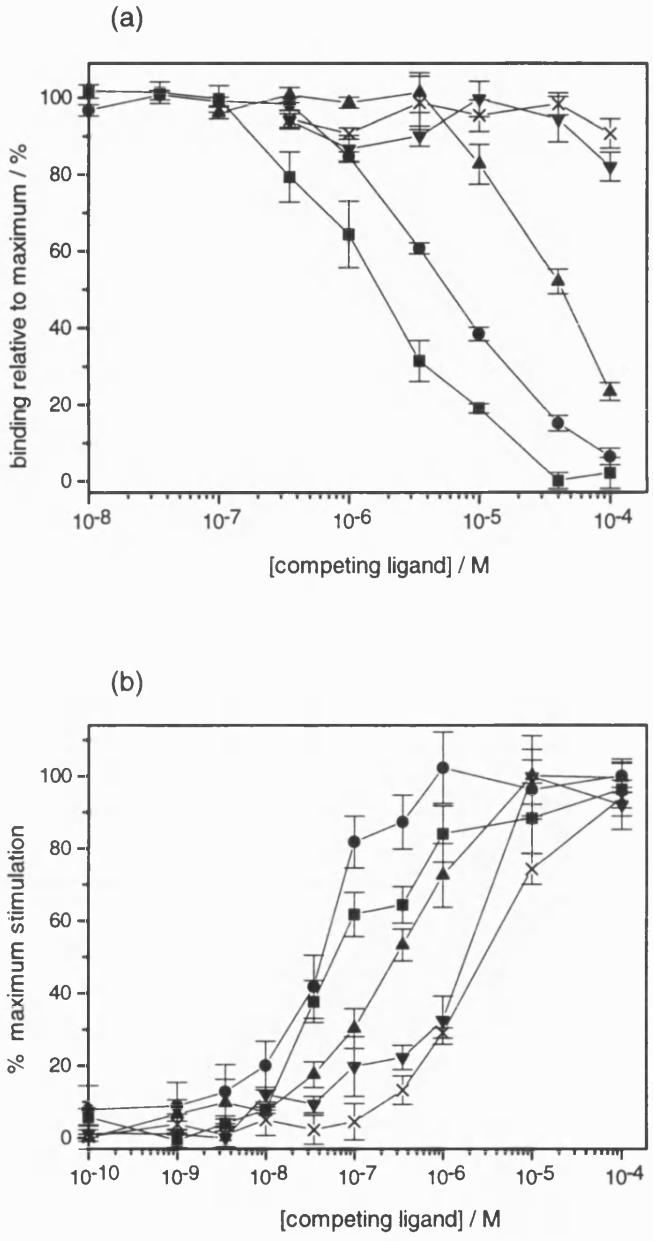

Figure 5.4.(a) Displacement binding at 0-4°C of 0.20 nM [^{125}I-Tyr^{2},Nle^{4},DPhe^{7}]α-MSH and **(b)** stimulation at 37°C of cAMP production by α-MSH analogues on the hMC4-R.

(■) α-MSH; (●) [Phe^{10}]α-MSH; (▲) [Asp^{10}]α-MSH; (▼) [Phe^{12}]α-MSH; (×) [Asp^{10},Phe^{12}]α-MSH

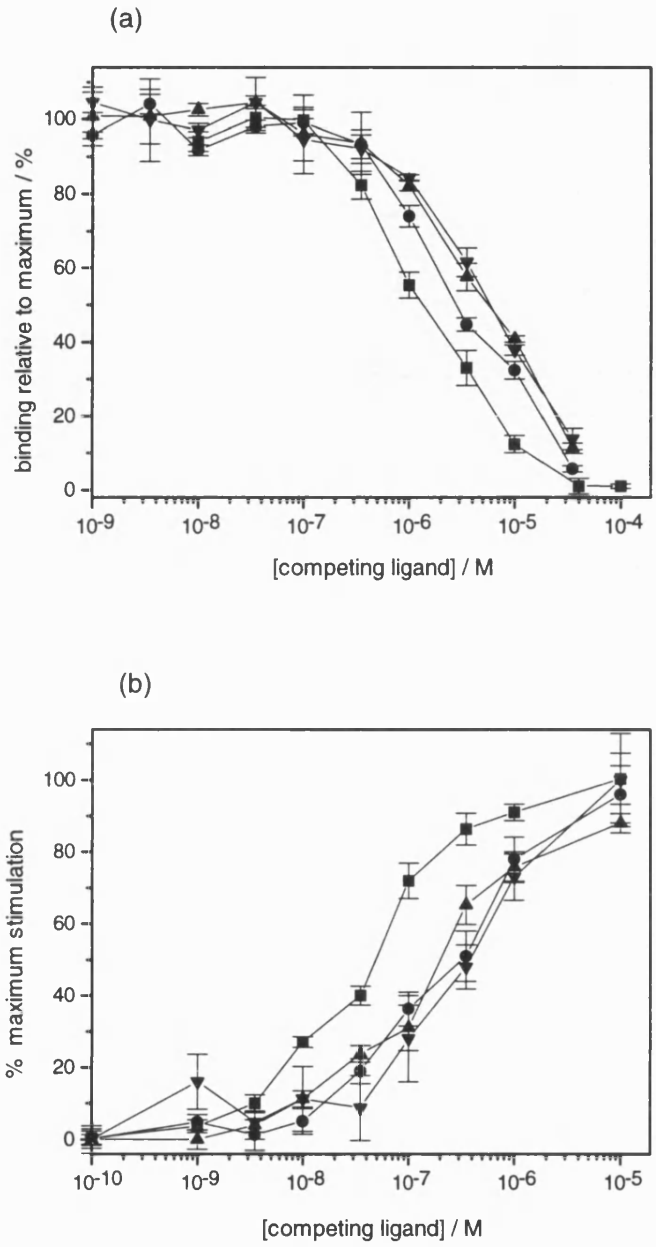

Figure 5.5.(a) Displacement binding at 0-4°C of 0.20 nM [^{125}I-Tyr^{2},Nle^{4},DPhe^{7}]α-MSH and **(b)** stimulation at 37°C of cAMP production by α-MSH analogues on the hMC4-R.

(■) α-MSH; (●) [Ala^{11},Ala^{13}]α-MSH; (▲) [Ala^{11},Ala^{12}]α-MSH; (▼) [Ala^{11},Ala^{12},Ala^{13}]α-MSH

Sigmoidal displacement curves were not obtained for [Asp^{10}]α-MSH and [Asp^{10},Phe^{12}]α-MSH which failed to inhibit completely radioligand binding at maximal concentrations (Figure 5.4a.). Each analogue was capable of maximum receptor stimulation with standard deviations between replicates generally less than 15% (Figure 5.3b.-5.5b). Table 5.2. assigns an EC_{50} rel./K_i rel. constant to each peptide as a measure of intrinsic efficacy.

5.2.1. Binding and Activity of [Nle^4,DPhe^7]α-MSH, α-MSH & desacetyl-α-MSH

α-MSH exhibited an activity of 69 nM as measured by its EC_{50} value with an approximately 11-fold higher dissociation constant of 0.73 μM. [Nle^4,DPhe^7]α-MSH was found to exhibit both higher affinity and activity with constants of 57 nM and 1.8 nM, respectively. Desacetyl-α-MSH exhibited a significantly higher affinity and activity constant than α-MSH but significantly lower values than [Nle^4,DPhe^7]α-MSH. The EC_{50} rel./K_i rel. value for [Nle^4,DPhe^7]α-MSH and desacetyl-α-MSH was found to be approximately 3-fold and 2-fold higher than that of α-MSH, respectively.

The K_i and EC_{50} values reported here for [Nle^4,DPhe^7]α-MSH and α-MSH are approximately one order of magnitude higher than those detailed in the literature (Gantz *et al.*, 1993b; Adan *et al.*, 1994a; Mountjoy *et al.*, 1994; Miwa *et al.*, 1995) for interaction with the human MC4-R. This is in agreement with results obtained from the MC1 (chapter 4) and MC3 (Sahm, 1994) receptors when comparing our assay system to published data. Analysis of the relative values is once again more useful with the finding of Mountjoy *et al.* (1994) that [Nle^4,DPhe^7]α-MSH exhibits approximately two orders of magnitude higher potency than α-MSH. This is

comparable to the value of 39 determined from this work. [Nle^4,DPhe^7]α-MSH shows an approximately 3-fold higher intrinsic efficacy than α-MSH as determined by the ratio of its relative activity and affinity (Table 5.2.). This is in contrast to the reduced efficacy noted at the rat MC3-R (Peng *et al.*, 1996) and approximately 2-fold higher than that determined at the hMC1-R (chapter 4).

The significantly higher activity of desacetyl-α-MSH as compared to α-MSH is in direct agreement with the 3-fold higher activity determined by Mountjoy *et al.* (1994). The hMC4R therefore differs from the hMC1R (chapter 4) and hMC3R (Miwa *et al.*, 1995) which did not distinguish between desacetylated and acetylated ligands as regards potency. The higher intrinsic efficacy of the desacetylated form, its predominance in the human hypothalamus and the hypothalamic localisation of the MC4-R support a role for desacetyl-α-MSH in mediating some of the CNS effects attributed to the melanocortins. Indeed, correlation of potency data from the cloned hMC4-R with melanocortin-induced central effects *in vivo* led Adan *et al.* (1994a) to attribute the excessive grooming behaviour observed in melanocortin-treated rats to MC4 receptor activation. These data, however, contrast with the significantly lower activity determined by Miwa *et al.* (1995) for desacetyl-ACTH(1-13) as compared to ACTH(1-13) and who proposed the requirement for an amino-terminal acetyl group for maximal activity. In the absence of an amidated C-terminal, it therefore appears that desacetylation has a further detrimental effect on activity.

5.2.2. Binding of C-terminally-substituted α-MSH Analogues

The human MC4 receptor, like the human MC1 receptor, has been reported to respond poorly to γ-MSH, being unable to stimulate a full response at maximum concentrations studied (Gantz *et al.* 1993b). As in the previous chapter, the effect of two significant amino acid differences between α-MSH and γ-MSH within the C-terminal region, namely glycine-10 and proline-12 of α-MSH were probed. A more general investigation of the C-terminal importance was undertaken using multiple alanine-substituted peptides.

The relative binding and affinity of each C-terminally-substituted peptide as compared to α-MSH for every assay is given in Figure 5.6. This serves to illustrate assay reproducibility. [Asp^{10}]α-MSH and [Asp^{10},Phe^{12}]α-MSH exhibited extremely low affinities. Displacement of radioligand from the hMC4-R was less than 15% at the maximum working concentration of 0.1 mM (Figure 5.4a). This rendered an accurate calculation of binding affinity impossible, although extrapolation would suggest a value within the millimolar range. Peptide activity was also greatly reduced with [Asp^{10}]α-MSH exhibiting 3% and [Asp^{10},Phe^{12}]α-MSH significantly reducing activity even further to 2% of that determined for α-MSH. Substitution with phenylalanine at position 10 reduced binding affinity to approximately 4% of that calculated for α-MSH although its 5-fold lower activity was not significantly different. [Phe^{12}]α-MSH was not significantly different in either affinity or activity to α-MSH. Both [Phe^{10}]α-MSH and [Phe^{12}]α-MSH showed approximately 5-fold higher intrinsic efficacies than α-MSH as determined by their EC_{50} rel./K_i rel. values.

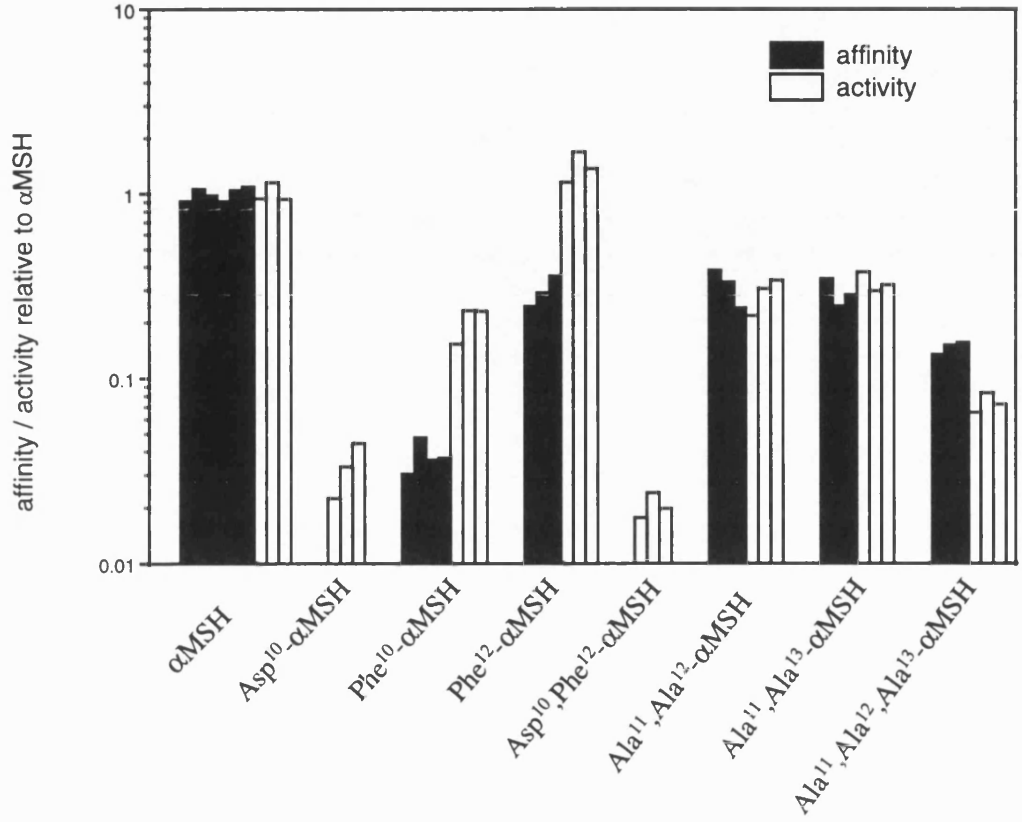

Figure 5.6. Relative affinity and activity of C-terminally-substituted α-MSH analogues as compared to α-MSH (log scale). Each column represents a single experiment.

(black: binding affinity; white: cAMP production)

Di-substitution with alanine in the C-terminal tripeptide to give [Ala^{11},Ala^{12}]α-MSH and [Ala^{11},Ala^{13}]α-MSH produced no significant difference in affinity or activity between them. Both peptides exhibited a significant decrease in affinity to approximately one third of that of α-MSH. A significantly reduced activity was found for [Ala^{11},Ala^{12}]α-MSH but not [Ala^{11},Ala^{13}]α-MSH as compared to the parent peptide. [Ala^{11},Ala^{12},Ala^{13}]α-MSH exhibited significantly reduced binding and activity as compared to its di-substituted counterparts with 15% of the affinity and 7% of the activity of α-MSH. None of these peptides differed greatly in intrinsic activity as compared to α-MSH.

The data presented above assign an important role to position 10 of α-MSH for hMC4-R binding and stimulation. Both [Asp^{10}]α-MSH and [Phe^{10}]α-MSH exhibited low affinity although replacement with aspartic acid but not phenylalanine significantly affected activity. These substituents have comparable masses and are bulkier than the native glycine (appendix A). The reduced affinity may be explained by these bulky residues sterically hindering access of the ligand to the receptor binding pocket. The observed difference in activity between the substituted peptides is most likely due to the negative nature of the aspartic acid moiety which may disrupt the receptor conformational change necessary for G-protein interaction. It therefore appears that amino acid neutrality at position 10 is of greater importance for high potency than residue size. However, the higher intrinsic efficacy attributed to [Phe^{10}]α-MSH suggests a more important role for glycine-10 of α-MSH in receptor recognition than receptor stimulation.

No significant difference in binding and activity was found for [Phe^{12}]α-MSH as compared to α-MSH. This is at variance with the proposal of Gantz *et al.* (1993b) for the specific requirement of proline at position 12 for high potency. They found the truncated peptide ACTH(1-10) to be a partial agonist at the MC4-R and later work assigned [Pro^{12}]γ-MSH a six-fold higher activity than γ-MSH (Miwa *et al.*, 1995). However, this would not fully account for the approximate 100-fold difference in activity between α-MSH and γ-MSH that they first reported (Gantz *et al.* 1993b) supporting a role for other residues in conferring high potency.

The same group also found tyrosine-2 to be an important determinant of activity at the hMC4-R although as this residue is shared by both α-MSH and γ-MSH, it does not explain the lower affinity of the latter. The role of tyrosine-2 is in agreement with findings for the rat MC3-R but contrasts with findings for the mouse MC1-R (Sahm, 1994) and may therefore be a specific requirement for neurally expressed receptors.

The reduction in binding affinity observed with the alanine-substituted analogues emphasises the requirement for the C-terminal tripeptide for high potency. Amino acid substitution at positions 11 and 13 appears to have no detrimental effect on peptide activity indicating the relative unimportance of the nature of these residues. The lower activity observed with [Ala^{11},Ala^{12}]α-MSH shows that substitution at position 12 with a less bulky residue adversely affects activity. Together with the results obtained for [Phe^{12}]α-MSH this suggests that substituent size at position 12 may be more important than side chain structure, with the smaller amino acid side chain of alanine seemingly disrupting the peptide backbone induced

by favourable receptor interaction more so than the bulkier phenyalanine. This importance of correct conformation within the C-terminal tripeptide is emphasised by the greatly adverse effect on both affinity and activity exhibited by the tri-substituted [Ala^{11},Ala^{12},Ala^{13}]α-MSH.

In summary, this chapter demonstrates the requirement for a neutral residue at position 10 of α-MSH for high affinity binding to and activation of the human MC4 receptor. The nature of the C-terminal tripeptide also contributes to peptide activity and within this fragment, residue size at position 12 appears to be a determinant of high potency. These data further suggest that the presence of the aspartic acid residue of γ-MSH is largely responsible for the low potency of this peptide on the hMC4-R. Biological activity of the C-terminally-substituted peptides was less affected in general, than receptor binding leading to peptides with higher intrinsic efficacies than α-MSH. This suggests that the C-terminal region of α-MSH plays a more significant role in receptor binding than stimulation of the human MC4 receptor.

5.3. A Comparison of the hMC1 and hMC4 Receptors

The human MC1 and MC4 receptors show 47% amino acid identity (Mountjoy *et al.*, 1994). Although they are not the most closely related receptors, with the MC4 showing greatest homology to the MC5-R, initial studies reported similar ligand binding profiles (Gantz *et al.*, 1993b). The relatively sparse structure-activity data currently available are unable to account satisfactorily for selectivity between them. Much of this study focused on the largely non-specific knowledge of the importance of the melanocortin C-terminal for biological efficacy and attempted to isolate

differences in melanocortin structure that distinguish between the binding to and activation of these receptor subtypes.

There is a clear difference in the response of each receptor to the tested ligands. Table 5.3. gives the relative affinity of each peptide as compared to the binding of α-MSH to the hMC1-R. Each peptide shows approximately 10 to 100-fold higher affinity and therefore, a higher selectivity for the hMC1-R as compared to the hMC4-R. Figure 5.7. compares the relative activities of each peptide on the two receptors. The synthetic α-MSH analogue, [Nle^4,$DPhe^7$] α-MSH exhibits "superpotency" at both subtypes but shows an approximately 2-fold higher intrinsic efficacy on the hMC4-R than the hMC1-R. The presence of an acetyl group on the N-terminal serine of α-MSH is not required for high potency at either receptor, and indeed, the hMC4-R exhibited a significantly higher activity in its absence. This supports an endogenous role for desacetyl-α-MSH.

Each C-terminally-substituted peptide, with the exception of [Asp^{10}]α-MSH, exhibited a lower intrinsic efficacy for the hMC1-R suggesting that this region is more important for stimulation of the hMC1-R than the hMC4-R. However, the loss of both affinity and activity obtained with [Ala^{11},Ala^{12},Ala^{13}]α-MSH on both subtypes emphasises the important presence of these residues and suggests that the spatial arrangement of the C-terminal tripeptide relative to the central core of α-MSH is decisive for high potency.

The presented data illustrate that although subtype specificity is not conferred solely by any one melanocortin amino acid, certain residues have selective

importance at particular receptor subtypes. The human MC1 and MC4 receptors differ markedly in their response to peptides substituted at positions 10 and 12. The nature of the residue at position 10 is of little consequence at the hMC1-R, but neutrality appears to be critical on the hMC4-R. In contrast, position 12 is the most sensitive amino acid within the C-terminal for human MC1 receptor stimulation but appears to be less significant for activation of the human MC4 receptor.

	MC1	MC4	MC1 / MC4
[Nle^4,DPhe^7]α-MSH	5.3	0.56	9.5
α-MSH	1.0	0.042	23.8
desacetyl-α-MSH	3.8	0.067	56.7
[Asp^{10}]α-MSH	0.38	NA	NA
[Phe^{10}]α-MSH	1.09	0.0016	68.1
[Phe^{12}]α-MSH	0.20	0.013	15.4
[Asp^{10},Phe^{12}]α-MSH	0.20	NA	NA
[Ala^{11},Ala^{12}]α-MSH	0.11	0.013	8.5
[Ala^{11},Ala^{13}]α-MSH	0.90	0.012	75
[Ala^{11},Ala^{12}, Ala^{13}]α-MSH	0.067	0.0063	106

Table 5.3. Comparison of the relative binding affinities of α-MSH and its analogues to the human MC1 and MC4 receptors.

Binding of α-MSH to the hMC1-R = 1.

(NA = "non-applicable"; indicating too low an affinity for accurate calculation.)

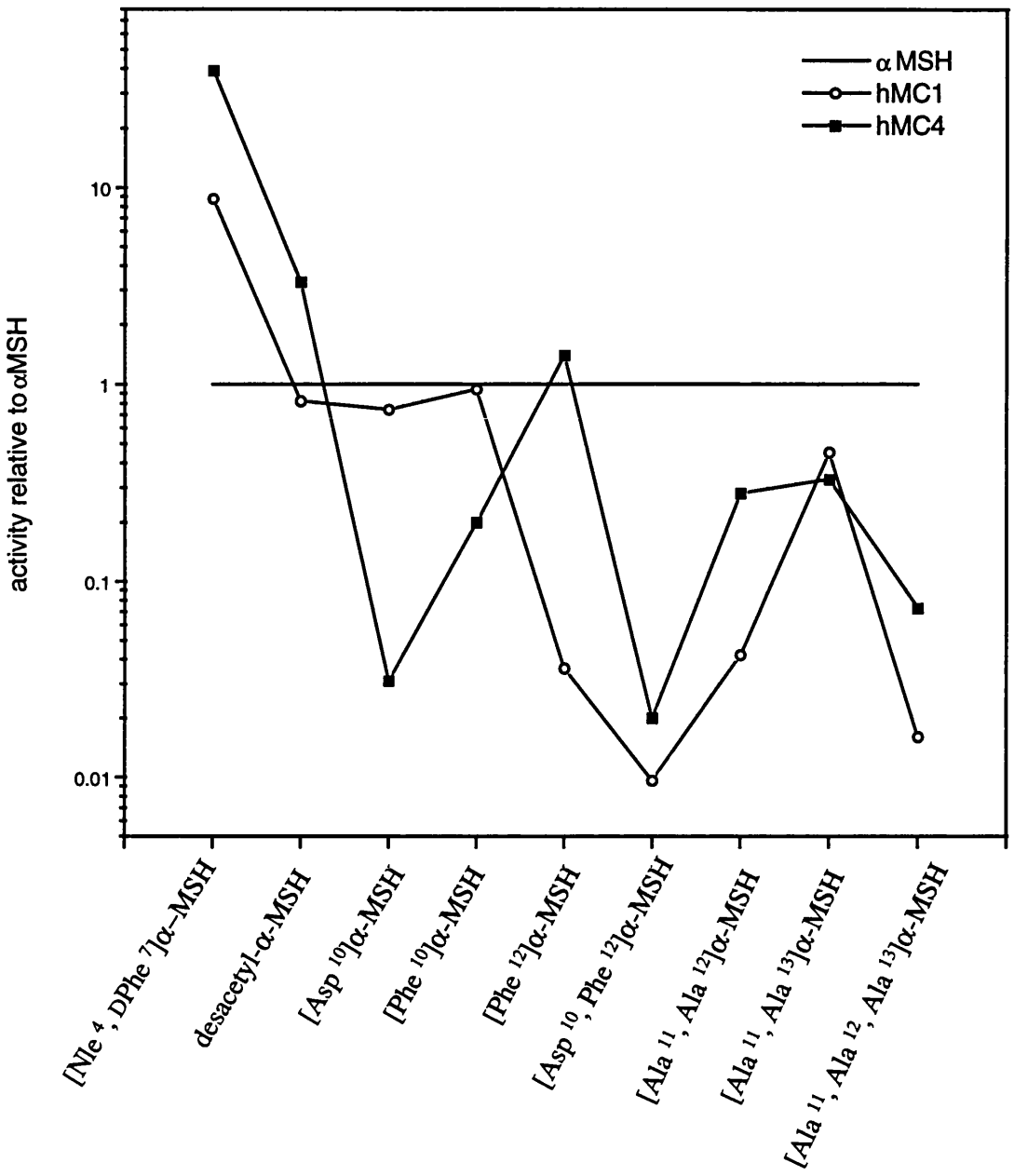

Figure 5.7. Comparison of the relative biological activity of α-MSH analogues on the human MC1 and MC4 receptors.

(Activities expressed relative to α-MSH).

CHAPTER 6: SITE-DIRECTED MUTAGENESIS of the hMC1-R

A thorough understanding of receptor-hormone interaction and cell signalling must necessarily involve knowledge of the mechanism by which ligand binding and receptor activation occurs. To date, very little is known about the binding domains for endogenous agonists of peptidergic G-protein-coupled receptors. It is likely that information gained by the study of one G-protein-coupled receptor family, such as the melanocortin receptors, may be extrapolated to other members of this superfamily.

Current knowledge of the melanocortins and their receptors has led to the proposal of a model in this laboratory for the conformational change occurring during functional coupling of melanocortin receptors to heterotrimeric G-protein complexes. This hypothesis is to be tested using site-directed mutagenesis techniques. The altered receptors will then undergo biological analysis enabling comparison of functional coupling with that of wild-type receptors.

6.1. A Model for Melanocortin Interaction with the MC1 Receptor

A model of the tertiary structure of the MC1 receptor was produced using a universal template for G-protein-coupled receptor structure (Baldwin, 1993) by comparison with the projection structure of bovine rhodopsin (Schertler *et al.*, 1993) (Figure 6.1.). Docking of the conserved melanocortin tetrapeptide His^{a}-Phe^{b}-Arg^{c}-Trp^{d} into the receptor has been performed using molecular computer modelling (Pouton *et al.*, 1994) The determination of energy minima has led to a hypothesis for the conformational changes occurring on receptor activation.

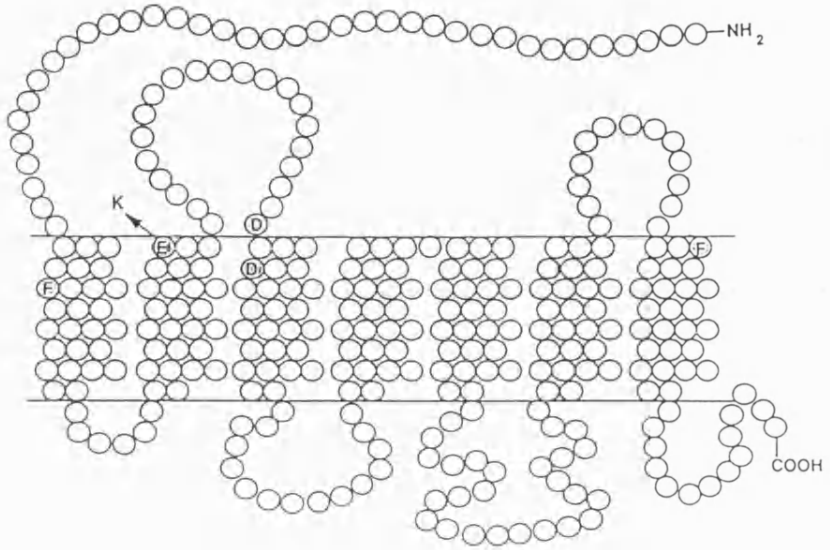

Figure 6.1. Model of the tertiary structure of the human MC1 receptor fitted to the Baldwin template (Baldwin, 1993).

Receptor residues proposed for interaction with the melanocortin tetrapeptide His^{a}-Phe^{b}-Arg^{c}-Trp^{d} are highlighted. "K" indicates the amino acid change from glutamic acid to lysine within the constitutively active $E^{So\text{-}3J}$ murine MC1-R mutant (Robbins *et al.*, 1993).

Based on α-MSH and the human MC1 receptor, this model proposes that [His^6] interacts electrostatically with Asp(117), a residue also proposed to be critical by Prusis *et al.* (1995) or Asp(121) within the third transmembrane helix, [Phe^7] with Phe(279) within the seventh transmembrane helix, [Arg^8] with Glu(94) and [Trp^9] with Phe(45) in the first transmembrane helix (Figure 6.1.). Glu(94) is thought to be a critical residue since a spontaneous point mutation at the equivalent murine residue Glu(92), to lysine produces a highly pigmented black phenotype which is constitutively active in cell culture (section 1.4.2.1.2.; Robbins *et al.*, 1993). This sombre mutant may make a salt bridge in the absence of ligand by the interaction of Lys(92) with one of the aspartic acid residues. This bridging between transmembranes II and III would result in the spatial rearrangement of transmembrane III which contains a highly conserved Asp-Arg-Tyr motif thought to be critical for G-protein binding (Hargrave, 1991). This reorientation would allow the receptor to induce a conformational change in the G-protein α-subunit thereby activating the cellular second messenger system. Such a transformation may be universal to G-protein-coupled receptor function.

6.2. Oligonucleotide Design

If the above hypothesis is valid, biological testing of mutant receptors using melanocortin ligands would produce reduced binding and receptor stimulation. Use of a suitable marker for confirmation of receptor expression is therefore essential. One such system involves the incorporation of a short amino acid sequence to form a

chimera with the recombinant protein. This could serve as an epitope recognised by available antibodies.

The recognition peptide chosen for this work was based on the FLAG sequence (Figure 6.2.), a commercially available octapeptide (IBI-Kodak Ltd.) against which antibodies have been raised. The use of secondary polyclonal antibodies conjugated to such moieties as FITC would enable receptor detection by FACS. Proteins incorporating the FLAG peptide on the N-terminus have been found to be unaffected by its presence, exhibiting no significant difference in dissociation constant from the native receptor (Tate and Blakely, 1994) and retaining a high level of biological activity (Hopp *et al.*, 1988). The small size of this peptide moiety reduces possible disruption of the native protein conformation. Its high hydrophilicity lends the peptide a high surface probability aiding both antibody attachment and antigenicity (Hopp *et al.*, 1988; Prickett *et al.*, 1989).

N-Asp-Tyr-Lys-Asp-Asp-Asp-Asp-Lys-C

5'-GAC TAC AAG GAC GAC GAT GAC AAG-3'

3'-CTG ATG TTC CTG CTG CTA CTG TTC-5'

Figure 6.2. Amino acid and nucleotide sequence of the FLAG recognition peptide.

A unique *Bam*H1 restriction enzyme site five amino acid residues upstream of the native ATG start codon of the hMC1-R gene as revealed by Genbank database searching (section 2.8.1.) was chosen as the point of attachment for the recognition peptide. Oligonucleotide design of the recognition peptide therefore incorporated a *Bam*H1 site for attachment to the MC1-R gene together with an *Eco*R1 recognition

sequence for vector ligation. Both cleavage sites have a high end restriction efficiency which was further optimised by base pair additions to each terminus. Genbank database sequence analysis of pBluescript (SK+) and the hMC1-R gene confirmed the unique nature of these restriction sites. A new ATG initiation codon was incorporated immediately upstream of the FLAG recognition sequence. The synthesised 44-mer oligonucleotide sequence is given in Figure 6.2. and was designed to yield an in-frame peptide after annealing, restriction and ligation into pBluescript / hMC1-R (sections 2.8.6, 2.8.7.).

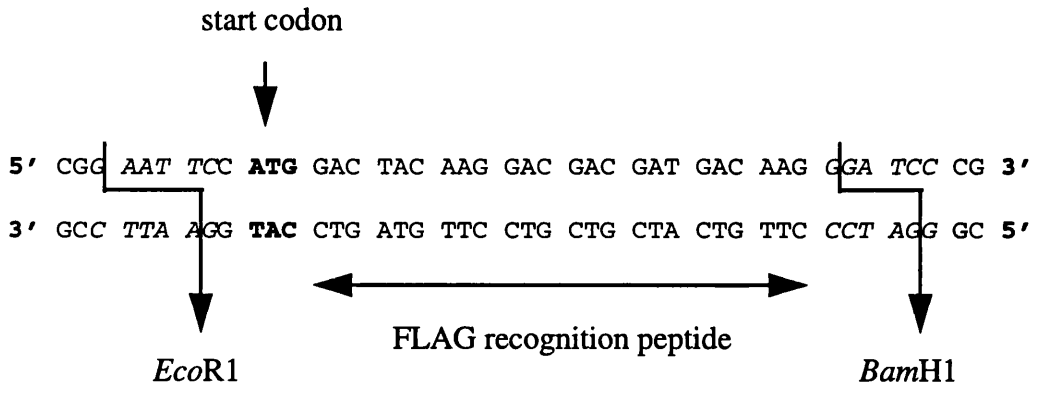

Figure 6.3. Sequence of the single-stranded complementary 44-mer oligonucleotides to form the recognition peptide for attachment to the N-terminus of the hMC1-R.

(Restriction sites italicised)

6.3. Chimera Formation

The strategy involved the excision of the hMC1-R gene from pcDNA1 Neo / hMC1-R plasmid using *Bam*H1 and *Xba*1 endonucleases. The gene was subsequently cloned into similarly digested pBluescript (SK+) (section 2.8.2.). Successful incorporation was confirmed by plasmid DNA preparation, digestion of a sample with *Bam*H1 and *Xba*1 and agarose gel electrophoresis (sections 2.2.4.-2.2.6.).

The modified plasmid (pBluescript / hMC1-R) was re-restricted with *Eco*R1 and *Bam*H1, ligated with the annealed and restricted recognition peptide (section 2.8.6., 2.8.7.) and transformed into *E. coli* XL1-Blue (section 2.8.3.). Transformant selection on antibiotic-supplemented LB agar yielded few colonies. Subsequent restriction and fragment analysis using a high percentage non-denaturing poylacrylamide gel suitable for the detection of low molecular weight base pairs (section 2.8.8.) indicated unsuccessful transformant isolation.

6.4. Trouble-shooting and Future Work

Success of the transformation procedure itself and antibiotic integrity were confirmed by concurrent transformation of wildtype pBluescript and electrocompetent *E. coli* XL1-Blue alone as positive and negative controls, respectively. The probability of successful ligation was optimised by the use of various vector to insert ratios in the reaction mix. Unsuccessful isolation of transformants is therefore a consequence of failure of one or more of the procedures involved in recognition peptide formation from its component oligonucleotides. Isolation of the problem is hindered by an absence of suitable control procedures at

each synthetic step. Further attempts at recognition peptide incorporation would necessarily look to simplify the synthetic protocol.

An alternative strategy would be ligation of the hMC1-R gene into a cloning vector already encoding a recognition epitope and against which antibodies have been raised. This would by-pass the multi-staged process outlined above. An example of such a vector is pSSBS.myc2 which includes unique restriction sites for in-frame fusions at the 3' end of a 10 amino acid recognition epitope (Dr. M. Welham, University of Bath, personal communication). PCR primers specific to the hMC1-R sequence would incorporate appropriate restriction enzyme sites for ligation into the plasmid.

Site-directed mutagenesis of the hMC1-R gene will be performed using a kit based on the method of Deng and Nickoloff (1992). Two oligonucleotide primers will be simultaneously annealed to one strand of denatured double-stranded pBluescript / hMC1-R. One primer will introduce the desired point mutation, the second will mutate a unique restriction site for selection purposes. After DNA elongation using T4 DNA polymerase, ligation and digestion, the mutated and unmutated plasmid mixture will be transformed into a *mutS E. coli* strain defective in mismatch repair. Plasmid DNA prepared from the mixed bacterial population will be subjected to a second selective restriction enzyme digestion. The mutated DNA lacks the selected restriction enzyme site and will therefore be resistant to digestion. Parental DNA will, however, be linearised and rendered 100-fold less efficient to bacterial transformation (Cohen *et al.*, 1972; Conley *et al.*, 1984). A second transformation of the digested DNA should produce efficient recovery of the desired

mutated plasmid. DNA sequencing will be performed to confirm successful mutagenesis.

Initial mutation experiments will investigate whether the five residues referred to above (section 6.1.) are indeed essential for receptor function. Each residue will be mutated in turn with the conservative replacement of Phe(45) and Phe(279) with leucine. The charged residues Glu(94), Asp(117) and Asp(121) are of particular interest given their postulated formation of ionic bridges during receptor activation and the latter will be replaced by the neutral polar serine residue. Each mutant receptor will undergo biological testing to determine the importance of the mutated residue for melanocortin binding and G-protein activation.

CHAPTER 7 CONCLUDING DISCUSSION

7.1. Artificial Melanocortin Receptor Expression - A Valid Model?

Although numerous studies have been carried out using the mouse MC1 receptor, published data for the human homologue have been more limited. This was largely due to variable MC1 receptor expression on human melanoma cells (Libert *et al.*, 1989) and on the strict culture conditions reported to be necessary for the successful growth of melanocytes (Hunt *et al.*, 1994). Indeed, until recently it was debated whether these cells did express the MC1 receptor (Donatien *et al.*, 1992; De Luca *et al.*, 1993). In addition, the predominantly neural distribution of the MC3, MC4 and MC5 receptors and their uncertain cell-specific localisation preclude the study of native expression of these subtypes.

These limitations coupled with the rapid development of molecular biological techniques have led to the now commonplace expression of receptors in alternative cell systems. The MC1-R has been expressed both stably and transiently in a variety of mammalian cell lines including COS, 293 HEK, Hepa, L, CHO and Y1 (Chhajlani and Wikberg, 1992; Gantz *et al.*, 1993a; Gantz *et al.*, 1994a; Griffon *et al.*, 1994; Roselli-Rehfus *et al.*, 1993; Schiöth *et al.*, 1996a). Data obtained from these systems show reasonable correlation to those reported for the endogenously expressed human MC1 receptor on melanocytes. In addition, functional expression in a non-mammalian cell line has recently been demonstrated by Schiöth *et al.* (1996b) using Sf 9 insect cells. Comparable binding constants and potency orders were measured to those obtained with transient expression of the hMC1-R in COS7 cells (Chhajlani

and Wikberg, 1992). These data would appear to validate the use of such artificial expression systems.

However, as outlined in chapter 3 the precise details by which G-protein interaction and subsequent signalling events occur still remain elusive. G-protein structure is extremely diverse and each receptor selectively activates a particular G-protein subtype to produce its specific cellular response (Birnbaumer and Birnbaumer, 1995). Further work detailing the nature of melanocortin-induced cell signalling might therefore be most appropriately performed on receptors in a system as analogous to their endogenous environment as possible. For example, study of the MC1-R in melanocytic or melanoma cells might be expected to induce constitutive activation of the signalling pathway controlling melanogenesis. Indeed, Chluba-de Tapia *et al.* (1996) have transfected the human MC1-R gene into an amelanotic B16 murine melanoma cell line, B16-G4F, previously shown to be MC1-R deficient (Solca *et al.*, 1993) leading to melanogenesis on melanocortin stimulation. The ability to analyse the final response, in this case, melanogenesis, might be expected to reflect more accurately endogenous melanocortin-receptor behaviour.

7.2. [Nle^4,DPhe^7]α-MSH - A Valid Assay Standard?

Since the discovery of the high affinity and prolonged activity of the α-MSH analogue [Nle^4,DPhe^7]α-MSH (Sawyer *et al.*, 1980), its use as a standard in melanocortin work has become commonplace. However, it has been assumed that this closely related synthetic analogue exhibits a comparable binding mechanism to its endogenous counterpart. Some evidence has now been put forward to refute this and different points of attachment for [Nle^4,DPhe^7]α-MSH and α-MSH on the MC1

receptor have been proposed. Substitution of alanine for Asp(117) and His(260) within the hMC1-R sequence produced mutant receptors which exhibited an approximately 100-fold reduced binding affinity for α-MSH as compared to the wild-type receptor whilst that of [Nle^4,DPhe^7]α-MSH remained unchanged (Frändberg *et al.*, 1994). This hypothesis is supported by the observation that C-terminally modified [Nle^4,DPhe^7]α-MSH analogues bound with equal affinity and exhibited comparable biological activities irrespective of amino acid substitution whereas the equivalent α-MSH analogues exhibited a distinct potency order (Peng et *al.*, 1996). The high peptide potency conferred by the [DPhe^7] configuration appears to mask additional changes in binding affinity and biological activity exhibited by substituted [Nle^4,DPhe^7]α-MSH peptides. Taken together these data question the suitability of such an agonist as an assay standard and suggest that use of the lower affinity [Nle^4]α-MSH which maintains the endogenous L-phenylalanine-7 configuration might be more appropriate in further studies.

7.3. Future Directions

Future work with melanocortins in this laboratory is intended to focus on receptor mutagenesis as outlined in chapter 6. The interesting disparity between the murine and human MC1-R homologues in their relative importance of position 10 of α-MSH also warrants further investigation. The development of high-affinity antagonists is ongoing with emphasis being placed on neural melanocortin receptors and the development of highly selective agents. Only in this way can real progress be

made as to how the melanocortins exert their important but subtle and complex effects in the brain.

7.4. The Broader Spectrum

Much progress in the melanocortin field has been made over the last decade, initiated largely by the cloning and characterisation of the majority, indeed, perhaps all of the melanocortin receptor subtypes. However, many mysteries remain unsolved. For example, it would be of interest to elucidate more fully the role of agouti protein in melanocortin regulation and to define the relative importance of ACTH and α-MSH in human pigmentation.

The melanocortin receptors respond differentially to closely related peptide ligands to which are attributed numerous biological responses. Delineation of the structural differences responsible for conferring this specificity will have therapeutic implications. For example, future development of selective melanocortin analogues is foreseeable for use in the control of fever and inflammation, as "neuro-protective" agents for chemotherapy, and by virtue of demonstrated memory-retention effects (chapter 1), for the treatment of such dementia-related disorders as Alzheimer's disease.

Melanocytes and targeted gene therapy

Another interesting possibility involves exploiting current knowledge of the melanin biosynthetic pathway in the treatment of melanoma.

Melanin synthesis is specific to melanocytes which is partly a consequence of transcriptional regulation of tyrosinase and the TRPs (Jackson *et al.*, 1991; Kluppel

et al., 1994). Using the β-galactosidase reporter gene it has been shown that comparatively small encoding fragments of the genes for these enzymes are sufficient to drive expression to both human and murine melanocytes and melanoma cells *in vitro* (Vile and Hart, 1993). Fusion of these promoter regions with a therapeutic gene, such as an immunity-enhancing gene or prodrug-activating gene, should initiate transcription of the latter when introduced into melanocyte-derived cells. When introduced into non-melanocytic cells, however, the absence of specific transcription factors means the promoter remains inactive and the gene is not transcribed. This approach relies on tissue-specific gene transcription in the appropriate cell-type and repression in other tissues (Yavuzer and Goding, 1994). The success of such a concept would represent a major goal in the therapeutic application of gene-mediated delivery.

REFERENCES

Abdel-Malek, Z., Swope, V., Collins, C., Boissy, R., Zhao, H., Nordlund, J. (1993). Contribution of melanogenic peptides to the heterogeneous pigmentation of human melanocytes. *Journal of Cell Science*, **106**, 1323-1331.

Abdel-Malek, Z., Swope, V.B., Suzuki, I., Akcali, C., Harriger, M.D., Boyce, S.T., Ùrabe, K., Hearing, V.J. (1995). Mitogenic and melanogenic stimulation of normal human melanocytes by melanotropic peptides. *Proceedings of the National Academy of Sciences of the USA*, **92**, 1789-1793.

Abe, K., Island, D.P., Liddle, G.W., Fleischer, N., Nicholson, W.E. (1967). Radioimmunological evidence of α-MSH (melanocyte-stimulating hormone) in human pituitary and tumour tissues. *Journal of Clinical Endocrinology and Metabolism*, **27**, 46-52.

Adams, G. (1993). Internalisation of α-MSH to B16 murine melanoma cells via the α-MSH receptor. PhD thesis, University of Bath.

Adan, R.A.H., Cone, R.D., Burbach, J.P.H., Gispen, W.H. (1994a). Differential effects of melanocortin peptides on neural melanocortin receptors. *Molecular Pharmacology*, **46**, 1182-1190.

Adan, R.A.H., Oosterom, J., Ludvigsdottir, G., Brakkee, J.H., Burbach, J.P.H., Gispen, W.H. (1994b). Identification of antagonists for melanocortin MC3, MC4 and MC5 receptors. *European Journal of Pharmacology (Molecular Pharmacology Section)*, **269**, 331-337.

Ahmed, A.R.H., Olivier, G.W.J., Adams, G., Erskine, M.E., Kinsman, R.G., Branch, S.K., Moss, S.H., Notoriani, L.J., Pouton, C.W. (1992). Isolation and partial purification of a melanocyte-stimulating hormone receptor from B16 murine melanoma cells. *Biochemical Journal*, **286**, 377-382.

Al-Obeidi, F., de Lauro Castrucci, A.M., Hadley, M.E., Hruby, V.J. (1989a). Potent and prolonged acting cyclic lactam analogues of α-melanotropin.: design based on molecular dynamics. *Journal of Medicinal Chemistry*, **32**, 2555-2561.

Al-Obeidi, F., Hruby, V.J., de Lauro Castrucci, A., Hadley, M.E. (1989b). Design of potent linear α-melanotropin 4-10 analogues modified in positions 5 and 10. *Journal of Medicinal Chemistry*, **323**, 174-179.

Al-Obeidi, F., Hruby, V.J., Hadley, M.E., Sawyer, T.K., de Lauro Castrucci, A.M. (1990). Design, synthesis and biological activities of a potent and selective α-melanotropin antagonist. *International Journal of Peptide and Protein Research*, **35**, 228-234.

Alberts, B., Bray, D., Lewis, J., Raff, M., Roberts, K., Watson, J.D. (1994). Molecular Biology of the Cell (3rd ed.). Garland Publishing Inc., NewYork.

Andreason, G.L., Evans, G.A. (1989). Optimization of electroporation for transfection of mammalian cell lines. *Analytical Biochemistry*, **180**, 2, 269-275.

Applebury, M.L., Hargrave, P.A. (1986). Molecular biology of the visual pigments. *Vision Research*, **26**, 1881-1895.

Arnould, R., Dubois, J., Abikhalil, F., Libert, A., Ghanem, G., Atassi, G., Hancoq, M., Lejeune, F.J. (1990). Comparison of two cytotoxicity assays - tetrazolium derivative reduction (MTT) and tritiated thymidine uptake on three malignant mouse cell lines using chemotherapeutic agents and investigational drugs. *Anticancer Research*, **10**, 145-154.

Atherton, E., Sheppard, R.C. (1989). Solid-phase peptide synthesis - a practical approach, IRL Press, Oxford.

Baldwin, J. (1993). The probable arrangement of the helices in G-protein-coupled receptors. *EMBO Journal*, **12**, 1693-1703.

Banerjee, P., Berry-Kravis, E., Bonafede-Chhabra, D., Dawson, G. (1993). Heterologous expression of the serotonin 5-HT_{1A} receptor in neural and non-neural cell lines. *Bichemical and Biophysical Research Communications*, **192**, 104-110.

Bard, D.R., Knight, C.G., Page-Thomas, D.P. (1990). A chelating derivative of α-melanocyte-stimulating hormone as a potential imaging agent for malignant melanoma. *British Journal of Cancer*, **62**, 919-922.

Barrett, P., MacDonald, A., Helliwell, R., Davidson, G., Morgan, P. (1994). Cloning and expression of a new member of the melanocyte-stimulating hormone receptor family. *Journal of Molecular Endocrinology*, **12**, 203-213.

Bateman, A., Dell, A., Whotehouse, B.J., Vinson, G.P. (1986). Non-ACTH components of adult pituitary extracts which stimulate adrenal steroidogenesis. *Neuropeptides*, **7**, 381-390.

Bertagna, X., Lenne, F., Comar, D., Massias, J.F., Wajcman, H., Baudin, V., Luton, J.P., Girard, F. (1986). Human β-melanocyte-stimulating hormone revisited. *Proceedings of the National Academy Sciences of the USA*, **83**, 9719-9723.

Biijlsma, W.A., Jennekens, F.G.I., Schotman, P., Gispen, W.H. (1981). Effects of corticotrophin (ACTH) on recovery of sensorimotor function in the rat: structure-activity study. *European Journal of Pharmacology*, **76**, 73.

Birnbaumer, L., Birnbaumer, M. (1995). Signal transduction by G-proteins: 1994 edition. *Journal of Receptor and Signal Transduction*, **15**, 1-4, 213-252.

Birnboim, H.C., Doly, J. (1979). A rapid alkaline extraction procedure for screening recombinant plasmid DNA. *Nucleic Acids Research*, **7**, 6, 1513-1523.

Bitensky, M.W., Demopoulos, H.B. (1970). Activation of melanoma adenyl cyclase by MSH. *Journal of Investigative Dermatology*, **54**, 83.

Blanchard, S.G., Harris, C.O., Ittoop, O.R.R., Nichols, J.S., Parks, D.J., Truesdale, A.T., Wilkison, W.O. (1995). Agouti antagonism of melanocortin binding and action in the $B_{16}F_{10}$ murine melanoma cell line. *Biochemistry*, **34**, 10406-10411.

Böhlen, P., Esch, F., Shibasaki, T., Baird, A., Ling, N., Guillemin, R. (1981). Isolation and characterisation of a γ_1-melanotropin-like peptide from bovine neurointermediate pituitary. *FEBS Letters*, **128**, 1, 67-70.

Bolognia, J., Murray, M., Pawelek, J. (1989). UVB-induced melanogenesis may be mediated through the MSH-receptor system. *Journal of Investigative Dermatology*, **92**, 651-656.

Boston, B.A., Cone, R.D. (1996). Characterization of melanocortin receptor subtype expression in murine adipose tissues and in the 3T3-L1 cell line. *Endocrinology*, **137**, 5, 2043-2050.

Brubaker, P.L., Baird, A.C., Bennett, H.P.J., Browne, C.A., Solomon, S. (1982). Corticotropic peptides in the human fetal pituitary. *Endocrinology*, **111**, 1150-1155.

Buffey, J.A., Hill, S.E., Bleehen, S.S., MacNeil, S.S. (1991). Evidence for calcium / calmodulin involvement in density-dependent melanogenesis in murine B16 melanoma cells. *Pigment Cell Research*, **4**, 112-119.

Buffey, J.A, Thody, A.J., Bleehen, S.S., MacNeil, S. (1992). α-melanocyte-stimulating hormone stimulates protein kinase C activity in murine B16 melanoma. *Journal of Endocrinology*, **133**, 333-340.

Bultman, S.J., Michaud, E.J., Woychik, R.P. (1992). Molecular characterisation of the mouse agouti locus. *Cell*, **71**, 1195-1204.

Cammas, F.M., Kapas, S., Barker, S., Clark, A.J.L. (1995). Cloning, characterisation and expression of a functional mouse ACTH receptor. *Biochemical and Biophysical Research Communications*, **212**, 3, 912-918.

Cannon J.G., Tatro, J.B., Reichlin, S., Dinarello, C.A. (1986). α-melanocyte stimulating hormone inhibits immunostimulatory and inflammatory actions of interleukin 1. *Journal of Immunology*, **137**, 7, 2232-2236.

Carter, R.J., Shuster, S. (1978). A sensitive new in vitro bioassay for melanocyte-stimulating hormone activity using the skin of Anolis carolinensis. *Journal of Investigative Dermatology*, **71**, 229-232.

Catania, A., Gerloni, V., Procaccia, S., Airaghi, L., Manfredi, M.G., Lomater, C., Grossi, L., Lipton, J.M. (1994). The neuropeptide α-MSH in synovial fluid of patients with rheumatic diseases: comparisons with other anticytokine molecules. *NeuroImmunoModulation*, **1**, 321-328.

Catania, A., Rajora, N., Capsoni, F., Minonzio, F., Star, R.A., Lipton. J.M. (1996). The neuropeptide α-MSH has specific receptors on neutrophils and reduces chemotaxis in vitro. *Peptides*, **17**, 4, 675-679.

Ceriani, G., Macaluso, A., Catania, A., Lipton, J.M. (1994). Central neurogenic anti-inflammatory action of αMSH: modulation of peripheral inflammation induced by cytokines and other mediators of inflammation. *Neuroendocrinology*, **59**, 138-143.

Chakraborty, A., Slominski, A., Ermak, G., Hwang, J., Pawelek, J. (1995). Ultraviolet B and melanocyte-stimulating hormone, (MSH), stimulate mRNA production for αMSH receptors and proopiomelanocortin-derived peptides in mouse melanoma cells and transformed keratinocytes. (1995). *Journal of Investigative Dermatology*, **105**, 655-659.

Chan, N.C., Branch, S.K., Moss, S.H., Pouton, C.W. (1995). Molecular modelling of β-turns in a cyclic melanotropin. *Journal of Pharmacy and Pharmacology*, **48**, 218-222.

Chang, A.C.Y., Cochet, M., Cohen, S.N. (1980). Structural organisation of human genomic DNA encoding the pro-opiomelanocortin peptide. *Proceedings of the National Academy of Sciences of the USA*, **77**, 4890-4894.

Chen, C.L.C., Chang, C.C., Krieger, D.T., Bardin. C.W. (1986). Expression and regulation of proopiomelanocortin-like gene in the ovary and placenta: comparison with the testis. *Endocrinology*, **118**, 2382-2389.

Chhajlani, V. (1996). Characterisation of a putative α-MSH antagonist 153N-6 at melanocortin receptor subtypes by radioligand binding. *Peptides*, **17**, 2, 349-351.

Chhajlani, V., Muceniece, R., Wikberg, J.E.S., (1993). Molecular cloning of a novel human melanocortin receptor. *Biochemical and Biophysical Research Communications*, **195**, 2, 866-873.

Chhajlani, V., Wikberg, J.E.S. (1992). Molecular cloning and expression of the human melanocyte stimulating hormone receptor cDNA. *FEBS 11553*, **309**, 3, 417-420.

Chluba-de Tapia, Bagutti, C., Cotti, R., Eberle, A.N. (1996). Induction of constitutive melanogenesis in amelanotic mouse melanoma cells by transfection of the human melanocortin-1 receptor gene. *Journal of Cell Science*, **109**, 2023-2030.

Chu, G., Hayakawa, H., Berg, P. (1987). Electroporation for the efficient transfection of mammalian-cells with DNA. *Nucleic Acids Research*, **15**, 3, 1311-1326.

Chung, D., Li, C.H. (1967). The synthesis of D-tryptophanyl-D-arginyl-D-phenylalanyl-D-histidyl-D-glutamic acid and its effect on melanotropic activity. *Biochimica et Biophysica Acta*, **136**, 570-571.

Clark, D., Thody, A.J., Shuster, S., Bowers, H. (1978). Immunoreactive alpha-MSH in human plasma in pregnancy. *Nature*, **273**, 163-164.

Cody, W.L., Mahoney, M., Knittel, J., Hruby, V.J., de Lauro Castrucci, A.M., Hadley, M.E. (1985). Cyclic melanotropins. 9. 7-D-phenylalanine analogues of the active site sequence. *Journal of Medicinal Chemistry*, **28**, 5, 583-588.

Cohen, S.N., Chang, A.C.Y., Hsu, L. (1972). Nonchromosomal antibiotic resistance in bacteria: genetic transformation of *Escherichia coli* by R-factor DNA. *Proceedings of the National Academy of Sciences of the USA*, **69**, 2110.

Cone, R.D., Lu, D., Koppula, S., Vage, D.I., Klungland, H., Boston, B., Chen, W., Orth, D.N., Pouton, C., Kesterton, R.A. (1996). The melanocortin receptors: agonists, antagonists and the hormonal control of pigmentation. (Submitted).

Conklin, B.R., Bourne, H.R. (1993). Mouse coat colour reconsidered. *Nature*, **364**, 110.

Conley, E.C., Saunders, J.R. (1984). Recombination-dependent recircularisation of linearized pBR322 plasmid DNA following transformation of *Escherichia coli*. *Molecular and General Genetics*, **194**, 211.

Daniel, P.M., Pritchard, M.M.L. (1975). Studies of the hypothalamus and the pituitary gland. *Acta Endocrinology*, suppl. **201**, 1-205.

de Graan, P.N.E., Brussaard, A.B., Gamboni, G., Girard, J., Eberle, A.N. (1987). α-MSH-induced changes in protein phosphorylation of Cloudman S91 mouse melanoma cells. *Molecular and Cellular Endocrinology*, **51**, 87-93.

De Luca, M., Siegrist, W., Bondanza, S., Mathor, M., Cancedda, R., Eberle, A.N. (1993). α melanocyte stimulating hormone (αMSH) stimulates normal human melanocyte growth by binding to high-affinity receptors. *Journal of Cell Science*, **105**, 1079-1084.

de Wied, D. (1964). Influence of anterior pituitaries on avoidance learning and escape behaviour. *American Journal of Physiology*, **207**, 255-259.

de Wied, D. (1965). The influence of the posterior and intermediate lobe of the pituitary on a conditioned avoidance response in rats. *International Journal of Neuropharmacology*, **4**, 157-167.

de Wied, D. (1966). Inhibitory effect of ACTH and related peptides on extinction of conditioned avoidance behaviour in rats. *Proceedings of the Society for Experimental Biology and Medicine*, **122**, 28-32.

de Wied, D., Jolles, J. (1982). Neuropeptides derived from pro-opiocortin: behavioral, physiological and neurochemical effects. *Physiological Reviews*, **62**, 3, 976-1059.

Deeter, L.B., Martin, W.W., Lipton, J.M. (1988). Antipyretic properties of centrally administered αMSH fragments in rabbit. *Peptides*, **9**, 991-995.

Deng, W.P., Nickoloff, J.A. (1992). Site-directed mutagenesis of virtually any plasmid by eliminating a unique site. *Analytical Biochemistry*, **200**, 81-88.

Desarnaud, F., Labbé, O., Eggerickx, D., Vassart, G., Parmentier, M. (1994). Molecular cloning, functional expression and pharmacological characterisation of a mouse melanocortin receptor gene. *Biochemical Journal*, **299**, 367-373.

Dixon, R.A.F., Sigal, I.S., Candelore, M.R. (1987). Structural features required for ligand binding to the β-adrenergic receptor. *EMBO Journal*, **6**, 3269-3275.

Donatien, P.D., Hunt, G., Pieron, C., Lunec, J., Taieb, A., Thody, A.J. (1992). The expression of functional MSH receptors on cultured human melanocytes. *Archives of Dermatological Research*, **284**, 424-426.

Dores, R.M. (1990). The proopiomelanocortin family. *Progress in Comparative Endocrinology*, 22-27.

Dorr, R.T., Lines, R., Levine, N., Brooks, C., Xiang, L., Hruby, V., Hadley, M. (1996). Evaluation of melanotan-II, a superpotent cyclic melanotropic peptide in a pilot phase-I clinical study. *Life Sciences*, **58**, 20, 1777-1784.

Dower, W.J., Miller, J.F. (1988). High efficiency transformation of *E. coli* by high voltage electroporation. *Nucleic Acids Research*, **16**, 13, 6127-6145.

Dyer, J.K., Ahmed, A., Olivier, G.W.J., Pouton, C.W., Haynes, L.W. (1993). Solubilisation and partial characterisation of the αMSH receptor on primary rat Schwann cells. *FEBS 13384*, **336**, 1, 103-106.

Dyer, J.K., Philipsen, H.L.A., Tonnaer, A.D.M., Hermkens, P.H.H., Haynes, L. (1995). Melanocortin analogue Org2766 binds to rat Schwann cells, upregulates NGF low-affinity receptor p75, and releases neurotrophic activity. *Peptides*, **16**, 3, 515-522.

Eberle, A.N. (1988). The Melanotropins: Chemistry, Physiology and Mechanisms of Action, Karger, Basel.

Eberle, A.N., de Graan, P.N.E., Baumann, J.B., Girard, J., van Hees, G., van de Veerdonk, F.C.G. (1984). Structural requirements of αMSH for the stimulation of MSH receptors on different pigment cells. *Yale Journal of Biological Medicine*, **57**, 353-354.

Eberle, A.N., Hübscher, W. (1979). α-melanotropin labelled at its tyrosine^2 residue: synthesis and biological activities of 3'-iodotyrosine^2-, 3'-^{125}iodotyrosine^2-, 3',5'-diiodotyrosine^2- and (3',5'-$^3H_2$)-tyrosine^2-α-melanotropin, and of related peptides. *Helvetica Chimica Acta.*, **62**, 2460-2483.

Eberle, A.N., Schwyzer, R. (1975). Hormone-receptor interactions. Demonstration of two message sequence (active sites) in α-melanotropin. *Helvetica Chimica Acta*, **58**, 1528-1535.

Eberle, A.N., Schwyzer, R. (1979). Divergent melanophore-dispersing and tyrosinase-stimulating activity of synthetic leucine^9-α-melanotropin. *Helvetica Chimica Acta*, **62**, 2452-2459.

Edwards, P.M., van der Zee, C.E.E.M., Verhaagen, J., Schotman, P., Jennekens, F.G.I., Gispen, W.H. (1984). Evidence that the neurotrophic actions of α-MSH may derive from its ability to mimic the actions of a peptide formed in degenerating nerve stumps. *Journal of the Neurological Sciences,* **64**, 333-340.

Eipper, B.A., Mains, R.E. (1980). Structure and function of adrenocorticotropin / endorphin and related peptides. *Endocrinology Review*, **1**, 247-262.

Engelman, D.M., Steitz, T.A., Goldman, A. (1986). Identifying nonpolar transbilayer helices in amino acid sequences of membrane proteins. *Annual Review of Biophysics and Biophysical Chemistry*, **15**, 321-353.

Estivariz, F.E., Hope, J., McLean, C., Lowry, P.J. (1980). Purification and characterisation of a γ-melanotropin precursor from frozen human pituitary glands. *Biochemical Journal*, **191**, 125-132.

Everard, D., Wilson, C.A., Thody, A.J. (1977). Effect of melanocyte-stimulating hormone on sexual behavior in the female rat. *Journal of Endocrinology,* **73**, 32P.

Fathi, Z., Iben, L.G., Parker, E.M. (1995). Cloning, expression and tissue distribution of a fifth melanocortin receptor subtype. *Neurochemical Research*, **20**, 1, 107-113.

Ferrari, W. (1958). Behavioural changes in animals after intracisternal injection with adrenocorticotropic hormone and melanocyte-stimulating hormone. *Nature*, **181**, 925-926.

Ferrari, W., Gessa, G.L., Vargiu, L. (1963). Behavioral effects induced by intracisternally injected ACTH and MSH. *Annals of the New York Academy of Sciences*, **104**, 330-345.

Feurle, G.E., Weber, U., Helmstaedter, V. (1980). Corticotropin-like substances in human gastric antrum and pancreas. *Biochemical and Biophysical Research Communications*, **95**, 1656-1662.

Frändberg, P-A., Muceniece, R., Prusis, P., Wikberg, J., Chhajlani, V. (1995). Evidence for alternate points of attachment for α-MSH and its stereoisomer [Nle^4,DPhe^7]-αMSH at the melanocortin-1 receptor. *Biochemical and Biophysical Research Communications*, **202**, 3, 1266-1271.

Fuchs, R.F. (1912). Die physiologische Funktion des Chromatophorsystems als Organ der Waermeregulierung der Poikilothermin. *Sitzungberichte der Physikalisch-medizinischen Sozietaet Erlangen*, **44**, 134-177.

Fuller, B.B. and Lebowitz, J., (1980). Decay of hormone responsiveness in mouse melanoma cells in culture as a function of cell density. *Journal of Cellular Physiology*, **103**, 279-287.

Fuller, B.B., Lunsford, J.B., Iman, D.S. (1987). α-melanocyte-stimulating hormone regulation of tyrosinase in Cloudman S91 mouse melanoma cell cultures. *Journal of Biological Chemistry*, **262**, 9, 4024-4033.

Gantz, I., Konda, Y., Tashiro, T., Simoto, Y., Miwa, H., Munzert, G., Watson, S.J., DelValle, J., Yamada, T. (1993a). Molecular cloning of a novel melanocortin receptor. *Journal of Biological Chemistry*, **268**, 11, 8246-8250.

Gantz, I., Miwa, H., Konda, Y., Shimoto, Y., Tashiro, T., Watson, S.J., DelValle, J., Yamada, T. (1993b). Molecular cloning, expression and gene localisation of a fourth melanocortin receptor. *Journal of Biological Chemistry*, **268**, 20, 15174-15179.

Gantz, I., Shimoto, Y., Konda, Y., Miwa, H., Dickinson, C.J., Yamada, T. (1994a). Molecular cloning, expression and characterisation of a fifth melanocortin receptor. *Biochemical and Biophysical Research Communications*, **200**, 3, 1214-1220.

Gantz, I., Tashiro, T., Barcroft, C., Konda, Y., Shimoto, Y., Miwa, H., Glover, T., Munzert, G., Yamada, T. (1993c). Localisation of the genes encoding the melanocortin-2 (adrenocorticotropic hormone) and melanocortin-3 receptors to chromosomes 18p11.2 and 20q13.2-q13.3 by fluorescence in situ hybridisation. *Genomics*, **18**, 166-167.

Gantz, I., Yamada, T., Tashiro, T., Konda, Y., Shimoto, Y., Miwa, H., Trent, J.M. (1994b). Mapping of the gene encoding the melanocortin-1 (α-melanocyte stimulating hormone) receptor (MC1R) to human chromosome 16q24.3 by fluorescence in situ hybridisation. *Genomics*, **19**, 394-395.

García-Bórron, J., Solano, F., Martinez-Liarte, J., Jara, J., Lozano, J., Ghanem, G. (1992). Binding and subcellular distribution of [^{125}I]-[Nle^{4},DPhe^{7}]-αMSH in B16/F10 mouse melanoma cells. *Life Science Advances (Biochemistry Series)*, **11**, 273-277.

Garren, L.D. (1968). The mechanism of action of ACTH. *Vitamins and Hormones*, **26**, 119-141.

Gerst, J.E., Sole, J., Hazum, E., Salomon, Y. (1988). Identification and characterization of melanotropin binding proteins from M2R melanoma cells by covalent photoaffinity labeling. *Endocrinology*, **123**, 1792-1797.

Ghanem, G., Comunale, J., Libert, A., Vercammen, A., Lejeune, F. (1988). Evidence for alpha-melanocyte-stimulating hormone (alpha-MSH) receptors on human malignant melanoma cells. *International Journal of Cancer*, **41**, 248-255.

Ghanem, G., Liénard, D., Hanson, P., Lejeune, F., Frühling, J. (1986). Increased serum α-melanocyte stimulating hormone (α-MSH) in human malignant melanoma. *European Journal of Cancer and Clinical Endocrinology*, **22**, 535-536.

Gispen, W.H., Wiegant, V.M. (1976). Opiate antagonists suppress ACTH(1-24)-induced excessive grooming in the rat. *Neuroscience Letters*, **2**, 159-164.

Gispen, W.H., Wiegant, V.M., Greven, H.N., de Wied, D. (1975). The induction of excessive grooming in the rat by intraventricular application of peptides derived from ACTH: structure-activity studies. *Life Sciences*, **17**, 645-652.

Glatt, C.E., Snyder, S.H. (1993). Cloning and expression of an adenylyl cyclase localised to the corpus striatum. *Nature*, **361**, 536-538.

Glembotski, C.C. (1982). Characterisation of the peptide acetyltransferase activity in bovine and rat intermediate pituitaries responsible for the acetylation of β-endorphin and α-melanotropin. *Journal of Biological Chemistry*, **257**, 10510-10519.

Gluzman, Y. (1981). SV40-transformed simian cells support the replication of early SV40 mutants. *Cell*, **23**, 175-182.

Goldsmith, L.A. (1991). Physiology, Biochemistry and Molecular Biology of the Skin. Oxford University Press, New York.

Gordon, P.R., Mansur, C.P., Gilchrest, B.A. (1989). Regulation of human melanocyte growth, dendricity and melanization by keratinocyte derived factors. *Journal of Investigative Dermatology*, **92**, 565-572.

Goverde, H.J.M., Pesman, G.J., Smals, A.G.H. (1993). Major contribution of the basic amino acid lysine at position 11 to the bioactivity of ACTH in purified isolated rat adrenocortical cells. *Biochemical and Biophysical Research Communications*, **190**, 3, 1060-1065.

Graziadei, L., Burfeind, P., Bar-Sagi, D. (1991). Introduction of unlabeled proteins into living cells by electroporation and isolation of viable protein-loaded cells using dextran-FITC as a marker for protein uptake. *Analytical Biochemistry*, **194**, 1, 198-203.

Griffon, N., Mignon, V., Facchinetti, P., Diaz, J., Schwartz, J-C., Sokoloff, P. (1994). Molecular cloning and characterisation of the rat fifth melanocortin receptor. *Biochemical and Biophysical Research Communications*, **200**, 2, 1007-1014.

Hadley, M.E., Anderson, B., Heward, C.B., Sawyer, T.K., Hruby, V.J. (1981). Calcium-dependent prolonged effects on melanophores of [4-norleucine, 7-D-phenylalanine]-α-melanotropin. *Science*, **213**, 1025-1027.

Halaban, R., Pomerantz, S.H., Marshall, S., Lambert, D.T., Lerner, A.B. (1983). Regulation of tyrosinase in human melanocytes grown in culture. *The Journal of Cell Biology*, **97**, 480-488.

Halaban, R., Pomerantz, S.H., Marshall, S., Lerner, A.B. (1984). Tyrosinase activity and abundance in Cloudman melanoma cells. *Archives of Biochemistry and Biophysics*, **230**, 1, 383-387.

Hargrave, P.A. (1991). Seven-helix receptors. *Current Opinions in Structural Biology*, **1**, 575-581.

Harris, J.I. (1959). Structure of α-melanocyte-stimulating hormone from the pituitary gland. *Nature*, **184**, 167-169.

Harris, J.I., Lerner, A.B. (1957). Amino acid sequence of the α-melanocyte-stimulating hormone. *Nature*, **179**, 1346-1347.

Haskell-Luevano, C., Boteju, L.W., Miwa, H., Dickinson, C., Gantz, I., Yamada, T., Hadley, M.E., Hruby, V.J. (1995a). Topographical modification of melanotropin peptide analogues with β-methyltryptophan isomers at position 9 leads to differential potencies and prolonged biological activities. *Journal of Medicinal Chemistry*, **38**, 4720-4729.

Haskell-Luevano, C., Miwa, H., Dickinson, C., Hadley, M.E., Hruby, V.J., Yamada, T., Gantz, I. (1996). Characterizations of the unusual dissociation properties of melanotropin peptides from the melanocortin receptor, hMC1R. *Journal of Medicinal Chemistry*, **39**, 432-435.

Haskell-Luevano, C., Miwa, H., Dickinson, C., Hruby, V.J., Yamada, T., Gantz, I. (1994). Binding and cAMP studies of melanotropin peptides with the cloned human peripheral melanocortin receptor, hMC1R. *Biochemical and Biophysical Research Communications*, **204**, 3, 1137-1142.

Haskell-Luevano, C., Shenderovich, M.D., Sharma, S.D., Nikiforovich, G.V., Hadley, M.E., Hruby, V.J. (1995b). Design, synthesis, biology and conformations of bicyclic α-melanotropin analogues. *Journal of Medicinal Chemistry*, **38**, 1736-1750.

Hauschka, T.S., Jacobs, B.B., Holdridge, B.A. (1968). Recessive yellow and its interaction with belted in the mouse. *Journal of Heredity*, **59**, 339-341.

Hearing, V.J., Tsukamoto, K. (1991). Enzymatic control of pigmentation in mammals. *The FASEB Journal*, **5**, 2902-2909.

Hiltz, M.E., Catania, A., Lipton, J.M. (1991). Anti-inflammatory activity of αMSH(11-13) analogs: influences of alteration in stereochemistry. *Peptides*, **12**, 767-771.

Hoganson, G.E., Ledwitz-Rigby, F., Davidson, R.L., Fuller, B.B. (1989). Regulation of tyrosinase mRNA levels in mouse melanoma cell clones by MSH and cAMP. *Somatic Cell and Molecular Genetics*, **15**, 255-263.

Hopp, T.P., Prickett, K.S., Price, V.L., Libby, R.T., March, C.J., Cerretti, D.P., Urdal, D.L., Conlon, P.J. (1988). A short polypeptide marker sequence for recombinant protein identification and purification. *Biotechnology*, **6**, 1204-1210.

Hruby, V.J., Lu, D., Sharma, S.D, de Lauro Castrucci, A., Kesterton, R.A., Al-Obeidi, F., Hadley, M.E., Cone, R.D. (1995). Cyclic lactam α-melanotropin analogues of Ac-Nle^4-cyclo[Asp^5,DPhe^7,Lys^{10}]α-melanocyte stimulating hormone-(4-10)-NH_2 with bulky aromatic amino acids at position 7 show high antagonist potency and selectivity at specific melanocortin receptors. *Journal of Medicinal Chemistry*, **38**, 3454-3461.

Hruby, V.J., Wilkes, B.C., Hadley, M.E., Al-Obeidi, F.A., Sawyer, T.K., Staples, D.J., deVaux, A.E., Dym, O., de L. Castrucci, A.M., Hintz., M.F., Riehm, J.P., Rao, K.R. (1987). α-melanotropin : the minimal active sequence in the frog skin bioassay. *Journal of Medicinal Chemistry*, **30**, 2126-2130.

Hunt, G. (1995). Melanocyte-stimulating hormone: a regulator of human melanocyte physiology. *Pathobiology*, **63**, 12-21.

Hunt, G., Thody, A.J. (1995). Agouti protein can act independently of melanocyte-stimulating hormone to inhibit melanogenesis. *Journal of Endocrinology*, **147**, R1-R4.

Hunt, G., Todd, C., Cresswell, J.E., Thody, A.J. (1994). α-melanocyte-stimulating hormone and its analogue [Nle^{4}DPhe^7]α-MSH affect morphology, tyrosinase activity and melanogenesis in cultured human melanocytes. *Journal of Cell Science*, **107**, 205-211.

Jackson, I.J. (1993). More to colour than meets the eye. *Current Biology*, **3**, 8, 518-521.

Jackson, I.J., Chambers, D.M., Budd, P.S., Johnson, R. (1991). The tyrosinase-related protein-1 gene has a structure and promoter sequence very different from tyrosinase. *Nucleic Acids Research*, **19**, 3798-3804.

Jayawickreme, C.K., Quillan, J.M., Graminski, G.F., Lerner, M.R. (1994). Discovery and structure-function analysis of α-melanocyte-stimulating hormone antagonists. *Journal of Biological Chemistry*, **269**, 47, 29846-29854.

Jiang, J., Sharma, S.D., Nakamura, S., Lai, J-Y., Fink, J.L., Hruby, V.J., Hadley, M.E. (1995). The melanotropic peptide, [Nle^4,D-Phe^7]α-MSH, stimulates human melanoma tyrosinase activity and inhibits cell proliferation. *Pigment Cell Research*, **8**, 314-323.

Jiménez, M., Kameyama, K., Maloy, W.L., Tomita, Y., Hearing, V.J. (1988). Mammalian tyrosinase: biosynthesis, processing and modulation by melanocyte-stimulating hormone. *Proceedings of the National Academy of Sciences of the USA*, **85**, 3830-3834.

Jiménez-Cervantes, C., Solano, F., Kobayashi, T., Urabe, K., Hearing, V.J., Lozano, J.A., García-Borrón, J.C. (1994). A new enzymatic function in the melanogenic pathway. *Journal of Biological Chemistry*, **269**, 27, 17993-18001.

Johnson, R.A., Salomon, Y. (1991). Assay of adenylyl cyclase catalytic activity. *Methods in Enzymology*, **195**, 3-21.

Kapas, S., Cammas, F.M., Hinson, J.P., Clark, A.J.L. (1996). Agonist and receptor binding properties of adrenocorticotropin peptides using the cloned mouse adrenocorticotropin receptor expressed in a stably transfected HeLa cell line. *Endocrinology*, **137**, 8, 3291-3294.

Karnik, S.S., Sakmann, J.P., Chen, H.B., Khorana, H.G. (1988). Cysteine residues 110 and 187 are essential for the formation of correct structure in bovine rhodopsin. *Proceedings of the National Academy of Sciences of the USA*, **85**, 8459-8463.

Kawai, Y., Inagaki, S., Shioska, S., Shibasaki, T., Ling, N., Tohyama, M., Shiotani, Y. (1984) The distribution and projection of gamma-melanocyte-stimulating hormone in the rat brain: an immunohistochemical analysis. *Brain Research*, **297**, 21-32.

Klebig, M.L., Wilkinson, J.E., Woychik, R.P. (1994) Molecular and Genetic Aspects of Obesity Bray, G. (ed.) LSU Press, Baton Rouge. LA.

Kluppel, M., Beermann, F., Puppert, S., Schmid, E., Hummler, E., Schutz, G. (1991). The mouse tyrosinase promoter is sufficient for expression in melanocytes and in the pigmented epithelium of the retina. *Proceedings of the National Academy of Sciences of the USA*, **88**, 3777-3781.

Konda, Y., Gantz, I., DelValle, J., Shimoto, Y., Miwa, H., Yamada, T. (1994). Interaction of dual intracellular signaling pathways activated by the melanocortin-3 receptor. *Journal of Biological Chemistry*, **269**, 18, 13162-13166.

Körner, A., Pawelek, J. (1982). Mammalian tyrosinase catalyses three reactions in the biosynthesis of melanin. *Science*, **217**, 1163-1164.

Kreiner, P.W., Gold, C.J., Keirns, J.J., Brock, W.A., Bitensky, M.W. (1973). Hormonal control of melanocytes: MSH-sensitive adenyl cyclase in the Cloudman melanoma. *Yale Journal of Biology and Medicine*, **46**, 583-591.

Krishnan, A. (1975). Rapid flow cytoflurometric analysis of mammalian cell cycle by propidium iodide staining. *The Journal of Cell Biology*, **66**, 188-193.

Kwon, B.S., Haq, A.K., Pomerantz, S.H., Halaban, R. (1987). Isolation and sequence of a cDNA clone for human tyrosinase that maps at the mouse c-albino locus. *Proceedings of the National Academy of Sciences of the USA*, **84**, 7473-7477.

Kwon, B.S., Wakulchik, M., Haq, A.Q., Halaban, R., Kestler, D. (1988). Sequence analysis of mouse tyrosinase cDNA and the effect of melanotropin on its gene expression. *Biochemical and Biophysical Research Communications*, **153**, 1301-1309.

Kwon, H.Y., Bultman, S.J., Löffler, C., Chen, W-J., Furdon, P.J., Powell, J.G., Usala, A-L., Wilkison, W., Hansmann, I., Woychik, R.P. (1994). Molecular structure and chromosomal mapping of the human homologue of the agouti gene. *Proceedings of the National Academy of Sciences of the USA*, **91**, 9760-9764.

Kyte, J., Doolittle, R.F. (1982). A simple method for displaying the hydropathic character of a protein. *Journal of Molecular Biology*, **157**, 105-132.

Labbé, O., Desarnaud, F., Eggerickx, D., Vassart, G., Parmentier, M. (1994). Molecular cloning of a mouse melanocortin 5 receptor gene widely expressed in peripheral tissues. *Biochemistry*, **33**, 4543-4549.

Lameh, J., Cone, R.I., Maeda, S., Philip, M., Corbani, M., Naderdi, L., Ramachandran, J., Smith, G.M., Sadee, W. (1990). Structure and function of G-protein coupled receptors. *Pharmaceutical Research*, **7**, 12, 1213-1221.

Lee, T.H., Buettner-Janusch, V. (1963). On the mechanism of sodium hydroxide modification of α-melanocyte-stimulating hormone. *Journal of Biological Chemistry*, **238**, 2021-2015.

Lefkowitz, R.J., Caron, M.G. (1988). Adrenergic receptors: models for the study of receptors coupled to guanine nucleotide regulatory proteins. *Journal of Biological Chemistry*, **263**, 11, 4993-4996.

Legros, F., Coel, J., Doyen, A., Hanson, P., van Tieghem, N., Vercammen-Grandjean, A., Fruhling, J., Lejeune, F.J. (1981). α-melanocyte-stimulating hormone binding and biological activity in a human melanoma cell line. *Cancer Research*, **41**, 1539-1544.

Leppert, M., Anderson, V.F., Quattlebaum, T., Stauffer, D., O'Connel, P., Lathrop, G.M., Lalouel, J,M., White, R. (1989). Benign familial neonatal convulsions linked to genetic markers on chromosome 20. *Nature*, **337**, 647-648.

Lerner, A.B., McGuire, J.S. (1961). Effect of alpha- and beta-melanocyte-stimulating hormone on the skin colour of man. *Nature*, **189**, 176-179.

Lerner, A.B., Shizume, K., Bunding, I. (1954). The mechanism of endocrine control of melanin pigmentation. *Journal of Clinical and Endocrinological Metabolism*, **14**, 1463-1490.

Libert, A., Ghanem, G., Arnould, R., Lejeune, F. (1989). Use of an alpha-melanocyte-stimulating hormone analogue to improve α-MSH-receptor-binding assay in human melanoma. *Pigment Cell Research*, **2**, 510-518.

Ling, N., Ying, S., Minick, S., Guillemin, R. (1979). Synthesis and biological activity of four γ-melanotropin peptides derived from the cryptic region of the adrenocorticotropin / β-lipotropin precursor. *Life Sciences*, **25**, 1773-1780.

Liotta, A., Krieger, D.T. (1980). *In vitro* biosynthesis and post-translational processing of immunoreactive precursor corticotropin / β-endorphin by human placental and pituitary cells. *Endocrinology*, **106**, 1504-1511.

Lu, D., Willard, D., Patel, I.R., Kadwell, S., Overton, L., Kost, T., Luther, M., Chen, W., Woychik, R.P., Wilkison, W.O., Cone, R.D. (1994). Agouti protein is an antagonist of the melanocyte-stimulating-hormone receptor. *Nature*, **371**, 799-802.

Lunec, J., Pieron, C., Thody, A.J. (1992). MSH receptor expression and the relationship to melanogenesis and metastatic activity in B16 melanoma. *Melanoma Research*, **2**, 5-12.

Macaluso, A, McCoy, D., Ceriani, G., Watanabe, T., Biltz, J., Catania, A., Lipton, J.M. (1994). Anti-inflammatory influences of αMSH molecules: central neurogenic and peripheral actions. *The Journal of Neuroscience*, **14**, 4, 2377-2382.

MacGregor, G.R., Nolan, G.P., Fiering, S., Roederer, M., Herzenberg, L.A. (1991). Use of *E. coli lacZ* (β-galactosidase) as a reporter gene. *Methods in Molecular Biology*, **7**, 217-235.

Magenis, R.E., Smith, L., Nadeau, J.H., Johnson, K.R., Mountjoy, K.G., Cone, R.D. (1994). Mapping of the ACTH, MSH and neural (MC3 and MC4) melanocortin receptors in the mouse and human. *Mammalian Genome*, **5**, 503-508.

McLoughlin, L., Lowry, P.J., Ratter, S.J., Besser, G.M., Rees, L.H. (1980). β-endorphin and β-MSH in human plasma. *Clinical Endocrinology*, **12**, 287-292.

Medzihradsky, K. (1982). The bio-organic chemistry of α-melanotropin. *Medicinal Research Reviews*, **2**, 3, 247-270.

Medzihradszky, K. (1976). Synthesis and biological activity of adrenocorticotropic and melanotropic hormones. In Bognár, R. *et al.* (eds.). Recent developments in the chemistry of natural carbon compounds, **7**, 117-250. Akadémi Kiadó, Budapest.

Medzihradszky, K., Magyar, A., Pakdi-Haris, P., Medzihradszky-Schweiger, H. (1979). Synthesis of melanotropin fragments and analogues for the study of the mechanism of hormone action. In Siemion, I.Z., Kupryszewski, G. (eds.). Peptides, 593-596. Wroclaw University Press, Wroclaw.

Miwa, H., Gantz., I., Konda, Y., Shimoto, Y., Yamada, T. (1995). Structural determinants of the melanocortin peptides required for activation of melanocortin-3 and melanocortin-4 receptors. *The Journal of Pharmacology and Experimental Therapeutics*, **273**, 367-372.

Morandini, R., Süli-Vargha, H., Libert, A., Loir, B., Botyánszki, J., Medzihradszky, K., Ghanem, G. (1994). Receptor-mediated cytotoxicity of α-MSH fragments containing melphalan in a human melanoma cell line. *International Journal of Cancer*, **56**, 129-133.

Mosmann, T. (1983). Rapid colorimetric assay for cellular growth and survival: application to proliferation and cytotoxicity assays. *Journal of Immunological Methods*, **65**, 55-63.

Mountjoy, K.G. (1994). The human melanocyte stimulating hormone has evolved to become "super-sensitive" to melanocortin peptides. *Molecular and Cellular Endocrinology*, **102**, R7-R11.

Mountjoy, K.G., Mortrud, M.T., Low, M.J., Simerly, R.B., Cone, R.D. (1994). Localization of the melanocortin-4 receptor (MC4-R) in neuroendocrine and autonomic control circuits in the brain. *Molecular Endocrinology*, **8**, 1298-1308.

Mountjoy, K.G., Robbins, L.S., Mortrud, M.T., Cone, R.D. (1992). The cloning of a family of genes that encode the melanocortin receptors. *Science*, **257**, 1248-1251.

Nakanishi, S., Inoue, A., Kita, T., Nakmura, M., Chang, A.Y., Cohen, S.N., Numa, S. (1979). Nucleotide sequence of cloned cDNA for bovine corticotrphin-β-lipotrophin precursor. *Nature*, **278**, 423-427.

Neumann, E., Schaeferridder, M., Wang, Y., Hofschneider, P.H. (1982). Gene-transfer into mouse lyoma cells by electroporation in high electric-fields. *EMBO Journal*, **1**, 7, 841-845.

O'Donohue, T.L. Dorsa, D.M. (1982). The opiomelanotropinergic neuronal and endocrine systems. *Peptides*, **3**, 353-395.

O'Dowd, B.F. (1989). Structure and function of G protein-coupled receptors. *Annual Review of Neurosciences*, **12**, 67-83.

Oelofsen, W., Ramachandran, J. (1983). Studies of corticotropin receptors on rat adipocytes. *Archives of Biochemistry and Biophysics*, **225**, 414-421.

Oliver, J.M., Richard, D., Davies, B.H. (1984). Use of horseradish peroxidase and fluorescent dextrans to study fluid pinocytosis in leukocytes. *Methods in Enzymology*, **108**, 336-347.

Olivera, B.M., Miljanich, G.P., Ramachandran, J., Adams, M.E. (1994). Calcium channel diversity and neurotransmitter release: the ω-conotoxins and ω-agatoxins. *Annual Review of Biochemistry*, **63**, 823-867.

Orci, L., Ravazzola, M., Amherdt, M., Madsen, O., Perrelet, A., Vassalli, J.D., Andersen, R.G.W., (1986). Conversion of pro-insulin to insulin occurs coordinately with acidification of maturing secretory vesicles. *The Journal of Cell Biology*, **103**, 2273-2281.

Orlow, S.J., Boissy, R.E., Moran, D.J., Pifko-Hirst, S. (1993). Subcellular distribution of tyrosinase and tyrosinase-related protein-1: implications for melanosomal biogenesis. *Journal of Investigative Dermatology*, **100**, 55-64.

Orlow, S.J., Hotchkiss, S., Pawelek, J.M. (1990). Internal binding sites for MSH: analyses in wild-type and variant Cloudman melanoma cells. *Journal of Cellular Physiology*, **142**, 129-136.

Otsuka, H., Inouye, K. (1964). Synthesis of peptides related to the N-terminal structure of corticotropin. III. The synthesis of L-histidyl-L-phenylalanyl-L-arginyl-L-tryptophan, the smallest peptide exhibiting the melanocyte-stimulating and the lipolytic activities. *Bulletin of the Chemical Society of Japan*, **37**, 1465.

Parker, C.R., Barnea, A., Tilders, F.J.H., Porter, J.C. (1981). Characterization of immunoreactive α-melanocyte-stimulating hormone (α-MSH_i) in human brain tissue. *Brain Research Bulletin*, **6**, 275-280.

Peng, P-J., Sahm, U.G., Doherty, R.V.M., Kinsman, R.G., Moss, S.H., Pouton, C.W. (1996). Binding and biological activity of C-terminally modified peptides: a comparison between MC1 and MC3 receptors. (Submitted).

Perry, W.L., Nakamura, T., Swing, D.A., Secrest, L., Eagleson, B., Hustad, C.M., Copeland, N.G., Jenkins, N.A. (1996). Coupled site-directed mutagenesis / transgenesis identifies important functional domains of the mouse agouti protein. *Genetics*, **144**, 255-264.

Plantinga, L.C., Verhaagen, J., Edwards, P.M., Hali, M., Brakkee, J.H., Gispen, W.H. (1995). Pharmacological evidence for the involvement of endogenous αMSH-like peptides in peripheral nerve regeneration. *Peptides*, **16**, 2, 319-324.

Potter, H. (1988). Electroporation in biology: methods, applications and instrumentation. *Analytical Biochemistry*, **174**, 361-373.

Pouton, C.W., Chan, N.C., Branch, S.K., Moss, S.H. (1994). Proposed mechanism of functional coupling of melanocortin receptors with ligand and heterotrimeric G-protein complexes. Proceedings 3rd Ukaps Annual Conference, p65.

Prickett, K.S. Amberg, D.C., Hopp, T.P. (1989). A calcium dependent antibody for identification and purification of recombinant proteins. *BioTechniques*, **7**, 580-589.

Probst, W.C., Snyder, L.A., Schuster, D.I., Brosius, J., Sealfon, S.C. (1992). Sequence alignment of the G-protein coupled receptor superfamily. *DNA Cell Biology*, **11**, 1-20.

Prota, G. (1980). Recent advances in the chemistry of melanogenesis in mammals. *Journal of Investigative Dermatology*, **75**, 122-127.

Prusis, P., Frändberg, P-A., Muceniece, R., Kalvinsh, I., Wikberg, J.E.S. (1995). A three dimensional model for the interaction of MSH with the melanocortin-1 receptor. *Biochemical and Biophysical Research Communications*, **210**, 205-210.

Quillan, J.M., Jayawickreme, C.K., Lerner, M.R. (1995). Combinatorial diffusion assay used to identify topically active melanocyte-stimulating hormone antagonists. *Proceedings of the National Academy of Sciences of the USA*, **92**, 2894-2898.

Richards, D.B., Lipton, J.M. (1984). Effect of αMSH(11-13) (lysine-proline-valine) on fever in the rabbit. *Peptides*, **5**, 815-817.

Robbins, L.S., Nadeau, J.H., Johnson, K.R., Kelly, M.A., Roselli-Rehfus, L., Baack, E., Mountjoy, K.G., Cone, R.D. (1993). Pigmentation phenotypes of variant extension locus alleles result from point mutations that alter MSH receptor function. *Cell*, **72**, 827-834.

Roselli-Rehfus, L., Mountjoy, K.G., Robbins, L.S., Mortrud, M.T., Low, M.J., Tatro, J.B., Entwistle, M.L., Simerly, R.B., Cone, R.D. (1993). Identification of a receptor for γ-melanotropin and other proopiomelanocortin peptides in the hypothalamus and limbic system. *Proceedings of the National Academy of Sciences of the USA*, **90**, 8856-8860.

Rudman, D., Del Rio, A.E., Hollins, B.M., Houser, D.H., Keeling, M.E., Sutin, J., Scott, J.W., Sears, R.A., Rosenberg, M.Z. (1973). Melanotropic-lipolytic peptides in various regions of bovine, simian and human brain and cerebrospinal fluid. *Endocrinology*, **92**, 372-379.

Sahm, U.G. (1994). Interaction of naturally occurring and synthetic MSH peptides with peripheral and CNS melanocortin receptors. PhD thesis. University of Bath.

Sahm, U.G., Olivier, G.W.J., Branch, S.K., Moss, S.H., Pouton, C.W. (1996). Receptor binding affinities and biological activities of linear and cyclic melanocortins in B16 murine melanoma cells expressing the native MC1 receptor. *Journal of Pharmacy and Pharmacology*, **48**, 197-200.

Sahm, U.G., Qarawi, M.A., Olivier, G.O., Ahmed, A.R.H., Branch, S.K., Moss, S.H., Pouton, C.W. (1994). The melanocortin (MC3) receptor from rat hypothalamus: photoaffinity labelling and binding of alanine-substituted α-MSH analogues. *FEBS 14339*, 29-32.

Salomon, Y. (1991). Cellular responsiveness to hormone and neurotransmitters: conversion of [^{3}H]adenine to [^{3}H]cAMP in cell monolayers, cell suspensions and tissue slices. *Methods in Enzymology*, **195**, 22-28.

Sambrook, J., Fritsch, E.F., Maniatis, T. (1989). Molecular cloning: a laboratory manual (2nd edition) Cold Spring Harbour Press, USA.

Sargent, D.F., Schwyzer, R. (1986). Membrane lipid phase as catalyst for peptide-receptor interactions. *Proceedings of the National Academy of Sciences of the USA*, **83**, 5774-5778.

Sasaki, D.T., Dumas, S.E., Engleman, E.G. (1987). Discrimination of viable and non-viable cells using propidium iodide in two color immunofluorescence. *Cytometry*, **8**, 413-420.

Sawyer, T.K., Hruby, V.J., Darman, P.S., Hadley, M.E. (1982). [half-Cys^4,half-Cys^{10}]-α-melanocyte-stimulating hormone: a cyclic α-melanotropin exhibiting superagonist biological activity. *Proceedings of the National Academy of Sciences of the USA*, **79**, 1751-1755.

Sawyer, T.K., Sanfilippo, P.J., Hruby, V.J., Engel, M.H., Heward, C.B., Burnett, J.B., Hadley, M.E. (1980). 4-Norleucine,-7-D-phenylalanine-α-melanocyte stimulating hormone: a highly potent α-melanotropin with ultralong biological activity. *Proceedings of the National Academy of Sciences of the USA*, **77**, 10, 5754-5758.

Sawyer, T.K., Staples, D.J., de L. Castrucci, A.M., Hadley, M.E., Al-Obeidi, F.A., Cody, W.L., Hruby, V.J. (1990). α- melanocyte stimulating hormone message and inhibitory sequences: comparative structure-activity studies on melanocytes. *Peptides*, **11**, 351-357.

Scatchard, G. (1949). The attraction of proteins for small molecules and iron. *Annals of the New York Academy of Sciences*, **51**, 660-672.

Schertler, G.F.X., Villa, C., Henderson, R. (1993). Projection structure of rhodopsin. *Nature*, **362**, 770-772.

Schiöth, H.B., Chhajlani, V., Muceniece, R., Klusa, V., Wikberg, J.E.S. (1996a). Major pharmacological distinction of the ACTH receptor from other melanocortin receptors. *Life Sciences*, **59**, 10, 797-801.

Schiöth, H.B., Kuusinen, A., Muceniece, R., Szardenings, M., Keinänen, K., Wikberg, J.E.S. (1996b). Expression of functional melanocortin 1 receptors in insect cells. *Biochemical and Biophysical Research Communications*, **221**, 807-814.

Scott, A.P., Lowry, P.J. (1974). Adrenocorticotrophic and melanocyte-stimulating peptides in the human pituitary. *Biochemical Journal*, **139**, 593-602.

Sharma, S.D., Granberry, M.E., Jiang, J., Leong, S.P.L., Hadley, M.E., Hruby, V.J. (1994). Multivalent melanotropic peptides and fluorescent macromolecular conjugates: new reagents for characterisation of melanotropin receptors. *Bioconjugate Chemistry*, **5**, 6, 591-601.

Siegrist, W., Bagutti, C., Solca, J., Girard, J., Eberle, A.N. (1992). MSH receptors on mouse and human melanoma cells: receptor identification, analysis and quantification. *Progress in Histo- and Cytochemistry*, **26**, 110-118.

Siegrist, W., Östreicher, M., Stutz, S., Girard, J., Eberle, A.N. (1988). Radioreceptor assay for α-MSH using mouse B16 melanoma cells. *Journal of Receptor Research*, **8**, 323-343.

Siegrist, W., Solca, F., Stutz, S., Giuffrè, L., Carrel, S., Girard, J., Eberle, A.N. (1989). Characterisation of receptors for α-melanocyte-stimulating hormone on human melanoma cells. *Cancer Research*, **49**, 6352-6358.

Siegrist, W., Willard, D.H., Wilkison, W.O., Eberle, A.N. (1996). Agouti protein inhibits growth of B16 melanoma cells *in vitro* by acting through melanocortin receptors. *Biochemical and Biophysical Research Communications*, **218**, 171-175.

Slominski, A., Paus, R., Wortsman, J. (1993). On the potential role of proopiomelanocortin in skin physiology and pathology. *Molecular and Cellular Endocrinology*, **93**, C1-C6.

Solca, F., Siegrist, W., Drozdz, R., Girard, J., Eberle, A.N. (1989). The receptor for α-melanotropin of mouse and human melanoma cells. *Journal of Biological Chemistry*, **264**, 24, 14277-14281.

Star, R.A., Rajora, N., Huang, J., Stock, R.C., Catania, A., Lipton, J.M. (1995). Evidence of autocrine modulation of macrophage nitric oxide synthase by α-melanocyte stimulating hormone. *Proceedings of the National Academy of Sciences of the USA*, **92**, 8016-8020.

Strand, F.L., Kung, T.T. (1980). ACTH accelerates recovery of neuromuscular function following crushing of peripheral nerves. *Peptides*, **1**, 135-138.

Sugg, E.E., Cody, W.L., Abdel-Malek, Z., Hadley, M.E., Hruby, V.J. (1986). D-isomeric replacements within the 6-9 core sequence of Ac-[Nle^4]-α-MSH(4-11)-NH_2: a topological model for the solution conformation of α-melanotropin. *Biopolymers*, **25**, 2029-2042.

Süli-Vargha, H., Csukas, I., Botyanszki, J., Jeney, A., Kopper, L., Lapis, K. (1990). Anti-tumor action and mutagenicity of melphalan-containing α-MSH fragments. *Journal of Cancer Research and Clinical Endocrinology*, **116**, 939.

Suzuki, I., Cone, R.D, Im, S., Nordlund, J., Abdel-Malek, Z.A. (1996). Binding of melanotropic hormones to the melanocortin receptor MC1R on human melanocytes stimulates proliferation and melanogenesis. *Endocrinology*, **137**, 5, 1627-1633.

Tanaka, I., Nakai, Y., Jingami, H., Fukata, J., Nakao, K., Oki, S., Nakanishi, S., Numa, S., Imura, H. (1980). Existence of γ-melanotropin (γ-MSH)-like immunoreactivity in bovine and human pituitary glands. *Biochemical and Biophysical Research Communications*, **94**, 1, 211-217.

Tate, C.G., Blakely, R.A. (1994). The effect of *N*-linked glycosylation on activity of the Na^+ and Cl^- dependent serotonin transporter expressed using recombinant baculovirus in insect cells. *Journal of Biological Chemistry*, **269**, 42, 26303-26310.

Tatro, J., Wen, Z., Entwistle, M., Atkins, M., Smith, T., Reichlin, S., Murphy, J. (1992). Interaction of an α-MSH -diphtheria toxin fusion protein with melanotropin receptors in human melanoma metastases. *Cancer Research*, **52**, 2545-2548.

Tatro, J.B., Entwistle, M.L. (1994). Heterogeneity of brain melanocortin receptors as suggested by differential ligand binding in situ. *Brain Research*, **635**, 148-158.

Tatro, J.B., Entwistle, M.L., Lester, B.R., Reichlin, S. (1990). Melanotropin receptors of murine melanoma characterised in cultured cells and demonstrated in experimental tumours *in situ*. *Cancer Research*, **50**, 1237-1242.

Thody, A.J. (1995). Epidermal melanocytes: their regulation and role in skin pigmentation. *European Journal of Dermatology*, **5**, 558-565.

Thody, A.J., Ridley, K., Penny, R.J., Chalmers, R., Fisher, C., Shuster, S. (1983). MSH peptides are present in mammalian skin. *Peptides*, **4**, 813-816.

Thody, A.J., Wilson, C.A., Everard, D. (1979). Facilitation and inhibition of sexual receptivity in the female rat by alpha-MSH. *Physiology and Behaviour*, **22**, 447-450.

Tilders, F.J.H., Mulder, A.H., Smelik, P.G. (1975). Re-introduction and evaluation of an accurate high capacity bioassay for melanocyte-stimulating hormone using the skin of Anolis carolinensis in vitro. *Journal of Endocrinology*, **66**, 165-175.

Tilders, F.J.H., Parker, C.R., Barnea, A., Porter, J.C. (1981). The major immunoreactive α-melanocyte-stimulating hormone (α-MSH)-like substance found in human foetal pituitary tissue is not αMSH but may be desacetyl-αMSH (adrenocorticotropin$_{1\text{-}13}$NH$_2$). *Journal of Clinical Endocrinology and Metabolism*, **52**, 319-323.

Tobin, D., Quinn, A.G., Ito, S., Thody, A.J. (1994). The presence of tyrosinase and related proteins in epidermis and their relationship to melanin type. *Pigment Cell Research*, **7**, 204-209.

Tsukamoto, K., Jackson, I.J., Urabe, K., Montague, P.M., Hearing, V.J. (1992). A second tyrosinase-related protein, TRP-2, is a melanogenic enzyme termed DOPAchrome-tautomerase, *EMBO Journal*, **11**, 519-526.

Tsunasawa, S., Sakiyama, F. (1984). Amino-terminal acetylation of proteins: an overview. *Methods in Enzymology*, **106**, 165-170.

Valverde, P., García-Borrón, J.C., Martínez-Liarte, J.H., Solano, F., Lozano, J.A. (1992). Melanocyte stimulating hormone activation of tyrosinase in B16 mouse melanoma cells: evidence for a differential induction of two distinct isoenzymes. *FEBS 11129*, **304**, 114-118.

Van Nispen, J,W., Smeets, P.J.H., Poll, E.H.A., Tesser, G.I. (1977). Investigation of the role of tryptophan in α-MSH. *International Journal of Peptide Protein Research*, **9**, 203-212.

Vanetti, M., Schönrock, C., Meyerhof, W., Höllt, V. (1994). Molecular cloning of a bovine MSH receptor which is highly expressed in the testis. *FEBS Letters*, **348**, 268-272.

Varga, J.M., Asato, N., Lande, S., Lerner, A.B. (1977). Melanotropin-daunomycin conjugate shows receptor-mediated cytotoxicity in cultured murine melanoma cells. *Nature,* **267**, 56-58.

Vaudry, H., Tonon, M.C., Delarue, R., Vaillant, R., Kraicer, J. (1978). Biological and radioimmunological evidence for the melanocyte stimulating hormones (MSH) of extrapituitary origin in the rat brain. *Neuroendocrinology*, **27**, 9-24.

Vile, R.G., Hart, I.R. (1993). In vitro and in vivo targeting of gene expression to melanoma cells. *Cancer Research*, **53**, 962-967.

Watson, S., Arkinstall, S. (1994). The G-protein linked receptor factsbook. Academic Press Limited, London.

Weber, A., Kapas, S., Hinson, J., Grant, D.B., Grossman, A., Clark, A.L. (1993). Functional characterisation of the cloned human ACTH receptor: impaired responsiveness of a mutant receptor in familial glucocorticoid deficiency. *Biochemical and Biophysical Research Communications*, **197**, 1, 172-178.

Wiegant, V.M., Cools, A.R., Gispen, W.H. (1977). ACTH-induced grooming involves brain dopamine. *European Journal of Pharmacology*, **41**, 343-345.

Willard, D.H., Bodnar, W., Harris, C., Kiefer, L., Nichols, J.S., Blanchard, S., Hoffman, C., Moyer, M., Burkhart, W., Weiel, J., Luther, M.A., Wilkison, W.O., Rocque, W.J. (1995). Agouti structure and function: characterisation of a potent αMSH receptor antagonist. *Biochemistry*, **34**, 12341-12346.

Wilson, B.D., Ollman, M.M., Kang, L., Stoffel, M., Bell, G.I., Barsh, G.S. (1995). Structure and function of *ASP*, the human homologue of the mouse agouti gene. *Human Molecular Genetics*, **4**, 2, 223-230.

Winterbourne, D.J., Thomas, S., Hermon-Taylor, J., Hussain, I., Johnstone, A.P. (1988). Electric-shock-mediated transfection of cells: characterization and optimisation of electrical parameters. *Biochemical Journal*, **251**, 427-434.

Wintzen, M., Yaar, M., Burbach, J.P.H., Gilchrest, B.A. (1996). Proopiomelanocortin gene product regulation in keratinocytes. *Journal of Investigative Dermatology*, **106**, 4, 673-678.

Wolff, G.L. (1987). Bodyweight and cancer. *American Journal of Clinical Nutrition*, **45**, 1, 168-180.

Wolff, G.L., Roberts, D.W., Galbraith, D.B. (1986). Prenatal determination of obesity, tumour susceptibility and coat colour pattern in viable yellow (AVY/A) mice - the yellow mouse syndrome. *Journal of Heredity*, **77**, 3, 151-158.

Wong, G., Pawelek, J, (1973). Control of phenotypic expression of cultured melanoma cells by melanocyte stimulating hormone. *Nature*, **241**, 213-215.

Wong, G., Pawelek, J. (1975). Melanocyte-stimulating hormone promotes activation of pre-existing tyrosinase molecules in Cloudman S91 melanoma cells. *Nature*, **255**, 644-646.

Wong, T.K., Neumann, E. (1982). Electric-field mediated gene-transfer. *Biochemical and Biophysical Research Communications*, **107**, 2, 584-587.

Wood, J.M., Schallreuter, K.U. (1991). Studies on the reaction between human tyrosinase, superoxide anion, hydrogen peroxide and thiols. *Biochimica et Biophysica Acta*, **1074**, 378-385.

Xia, Y., Skoog, V., Muceniece, R., Chhajlani, V., Wikberg, J.E.S. (1995a). Polyclonal antibodies against human melanocortin MC1 receptor: preliminary immunohistochemical localisation of melanocortin MC1 receptor to malignant melanoma cells. *European Journal of Pharmacology: Molecular Pharmacology Section*, **288**, 277-283.

Xia, Y., Wikberg, J.E.S., Chhajlani, V. (1995b). Expression of melanocortin 1 receptor in periaqueductal gray matter. *Molecular Neuroscience*, **6**, 2193-2196.

Yajima, H., Kubo, K., Kinomura, Y. (1967). Studies on Peptides XIII. Contribution of the arginine residue in L-histidyl-L-phenylalanyl-L-arginyl-L-tryptophyl-glycine to its melanotropic activity. *Chemical and Pharmaceutical Bulletin*, **15**, 4, 504-510.

Yajima, H., Kubo, K., Okada, Y. (1965). Studies on Peptides VI. Synthesis of three stereoisomeric pentapeptides of histidyl-phenylalanyl-arginyl-tryptophyl-glycine possessing D-phenylalanyl-D-arginyl moiety within the sequence, and their melanocyte-stimulating activities *in vitro*. *Chemical and Pharmaceutical Bulletin*, **13**, 11, 1326-1331.

Yajima, H., Kubo, K., Oshima, T., Hano, K., Koida, M. (1966). Studies on Peptides VII. Synthesis of three stereoisomeric pentapeptides of histidyl-phenylalanyl-arginyl-tryptophyl-glycine and their melanocyte-stimulating activities *in vitro*. *Chemical and Pharmaceutical Bulletin,* **14**, 7, 775-776.

Yavuzer, U., Goding, C.R. (1994). Melanocyte-specific gene expression: role of repression and identification of a melanocyte-specific factor, MSF. *Molecular Cell Biology*, **14**, 3494-3508.

Yen, T.T., Gill, A.M., Frigeri, L.G., Barsh, G.S., Wolff, G.L. (1994). Obesity, diabetes, and neoplasia in yellow A^{vy} /- mice: ectopic expression of the *agouti* gene. *The FASEB Journal*, **8**, 479-488.

Zemel, M.B., Kim, J.H., Woychik, R.P., Michaud, E.J., Kadwell, S.H., Patel, I.R., Wilkison, W.O. (1995). Agouti regulation of intracellular calcium: role in the insulin resistance of viable yellow mice. *Proceedings of the National Academy of Sciences of the USA,* **92**, 4733-4735.

Zimmerman, M., Mumford, R.A., Steiner, D.F. (eds.) (1980). Precursor processing in the biosynthesis of proteins. *Annals of the New York Academy of Sciences*, **343**, 1-449.

APPENDIX A: Amino Acids

Amino acid	Abbrev.	Code letter	Mass	Properties	Hydropathy Index (1)	Hydropathy Index (2)
Alanine	Ala	A	89.09	neutral	1.8	-1.6
Arginine	Arg	R	174.2	basic	-4.5	12.3
Asparagine	Asn	N	132.1	neutral	-3.5	4.8
Aspartic acid	Asp	D	133.1	acidic	-3.5	9.2
Cysteine	Cys	C	121.1	neutral	2.5	-2.0
Glutamic acid	Glu	E	147.1	acidic	-3.5	8.2
Glutamine	Gln	Q	146.1	neutral	-3.5	4.1
Glycine	Gly	G	75.07	neutral	-0.4	1.0
Histidine	His	H	155.2	basic	-3.2	3.0
Isoleucine	Ile	I	131.2	neutral	3.8	-3.1
Leucine	Leu	L	131.2	neutral	3.8	-2.8
Lysine	Lys	K	146.2	basic	-3.9	8.8
Methionine	Met	M	149.2	neutral	1.9	-3.4
Phenyalanine	Phe	F	165.2	neutral	2.8	-3.7
Proline	Pro	P	115.1	neutral	-1.6	0.2
Serine	Ser	S	105.1	neutral	-0.8	-0.6
Threonine	Thr	T	119.1	neutral	-0.7	-1.2
Tryptophan	Trp	W	204.2	neutral	-0.9	-1.9
Tyrosine	Tyr	Y	181.2	neutral	-1.3	0.7
Valine	Val	V	177.2	neutral	4.2	-2.6

Hydropathy index according to:

(1) Kyte and Doolittle (1982) and (2) Engelman *et al.* (1986).

APPENDIX B: Media and Solutions

Where appropriate, media and solutions were sterilised by autoclaving at 15 lbs/sq. inch (121°C) for 15 minutes on a liquid cycle.

Buffer P1: 50 mM Tris-Cl, 10 mM EDTA, pH 8.0, 100 μg/ml RNAase A.

Buffer P2: 200 mM NaOH, 1% SDS.

Buffer P3: 3.0M potassium acetate, pH 5.5.

Buffer QBT: 7 50 mM NaCl, 50 mM MOPS, 15% ethanol, 0.15% Triton X-100

Buffer QC: 1M NaCl, 50 mM MOPS, 15% ethanol.

Buffer QF: 1.25M NaCl, 50 mM MOPS, 15% ethanol.

Chloroform:isoamyl alcohol: Chloroform mixed with isoamyl alcohol 24:1 (Amresco)

DNA loading buffer: 50 mM EDTA, 0.2% SDS, 0.05% bromophenol blue, 50% glycerol.

ethidium bromide: 1 mg/ml in double distilled water

Phosphate buffered saline (PBS): 137 mM NaCl, 2.7 mM KCl, 4.3 mM Na_2HPO_4, 1.4 mM KH_2PO_4, pH 7.3.

LB medium: (Luria-Bertani medium): (per litre) 10g Bacto-tryptone (Difco), 5g Bacto yeast extract (Difco), 10g NaCl, adjusted to pH 7.0. with NaOH.

LB agar: LB medium plus 20g agar (Difco).

Phenol:chloroform: Tris-phenol : chloroform : isoamyl alcohol 25:24:1 (Amresco)

RNAase A: 10 mg/ml pancreatic ribonuclease A (Sigma) in STE.
Heated to 100°C for 5 minutes and allowed to cool to room temperature.

SOC medium: 2% Bacto-tryptone (Difco), 0.5% Bacto yeast extract (Difco), 10 mM NaCl, 2.5 mM KCl, 10 mM $MgCl_2$, 1 mM $MgSO_4$, 20 mM glucose.

STE: 10 mM tris-Cl, 15 mM NaCl, pH 7.5.

TBE buffer (1x): 10.8g Tris base, 5.5g boric acid, 0.93g $Na_2EDTA.H_2O$, pH 8.3

TE buffer: 10 mM Tris-Cl, 1mM EDTA, pH 8.0.

APPENDIX C: Molecular Weight Markers

For agarose gel electrophoresis, markers consisted of *Hin*dIII-cut lambda DNA (Sigma). The digest consists of DNA fragments of the following sizes (base pairs):

1.	23130	5.	2322
2.	9416	6.	2027
3.	6557	7.	564
4.	4361	8.	125

For non-denaturing PAGE, markers consisted of *Hae*III-cut pBR322 (Sigma). The digest consists of DNA fragments of the following sizes (base pairs):

1.	587	9.	192	17.	57
2.	540	10.	184	18.	51
3.	504	11.	124	19.	21
4.	458	12.	123	20.	18
5.	434	13.	104	21.	11
6.	267	14.	89	22.	8
7.	234	15.	80		
8.	213	16.	64		

APPENDIX D: FACS Data

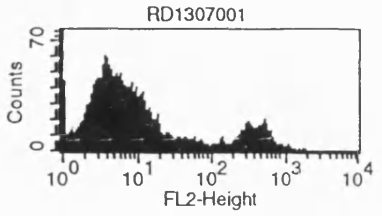

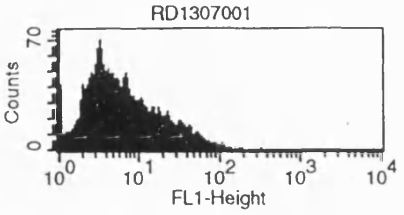

CONTROL COS7

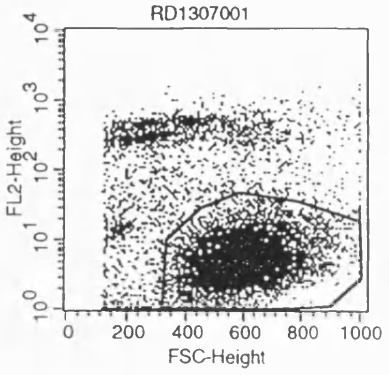

File: RD1307001 Sample ID: CONTROL
X Parameter: FL1-H FL1-Height (Log)

Mean	Peak Ch
9.98	1

File: RD1307001 Sample ID: CONTROL
Gated Events: 10000

Events	% Gated
7684	76.84

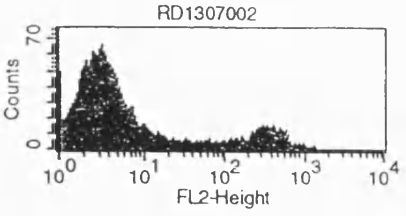

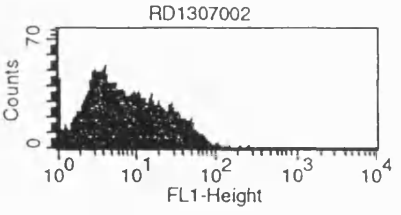

125/100V

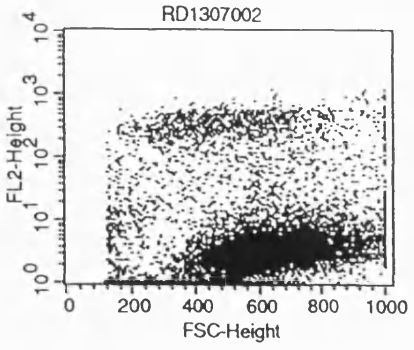

File: RD1307002 Sample ID: 125/100
X Parameter: FL1-H FL1-Height (Log)

Mean	Peak Ch
11.43	1

File: RD1307002 Sample ID: 125/100
Gated Events: 10000

Events	% Gated
7878	78.78

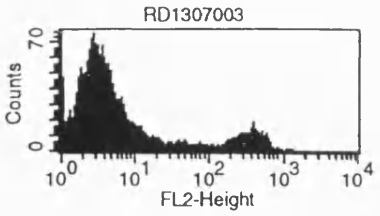

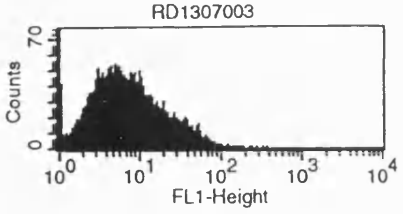

125/200V

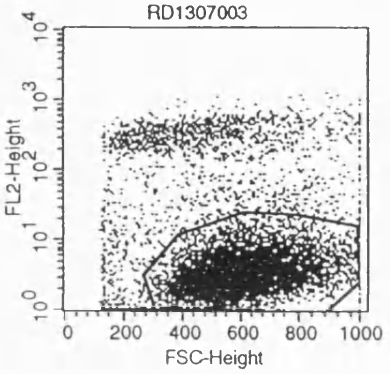

File: RD1307003 Sample ID: 125/200
X Parameter: FL1-H FL1-Height (Log)

Mean	Peak Ch
10.86	1

File: RD1307003 Sample ID: 125/200
Gated Events: 10000

Events	% Gated
8064	80.64

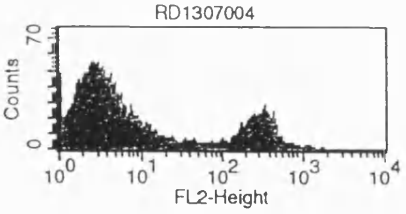

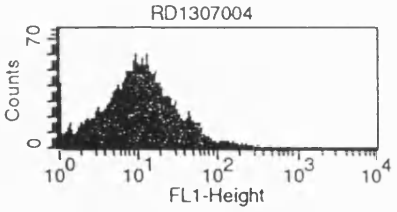

125/300V

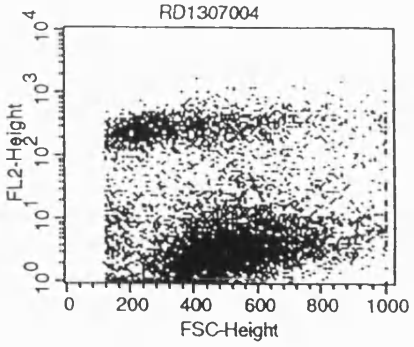

File: RD1307004 Sample ID: 125/300
X Parameter: FL1-H FL1-Height (Log)

Mean	Peak Ch
15.07	1

File: RD1307004 Sample ID: 125/300
Gated Events: 10000

Events	% Gated
6709	67.09

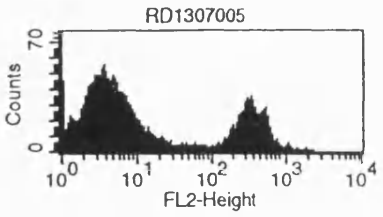

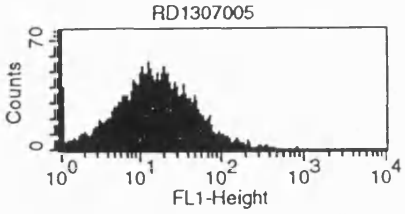

125/350V

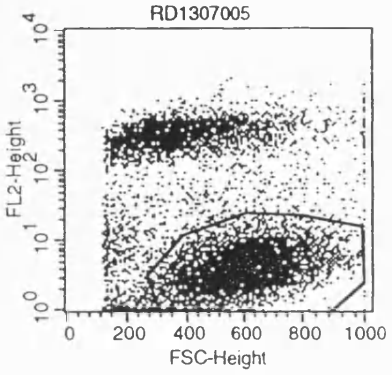

File: RD1307005 Sample ID: 125/350
X Parameter: FL1-H FL1-Height (Log)

Mean	Peak Ch
22.78	1

File: RD1307005 Sample ID: 125/350
Gated Events: 10000

Events	% Gated
6193	61.93

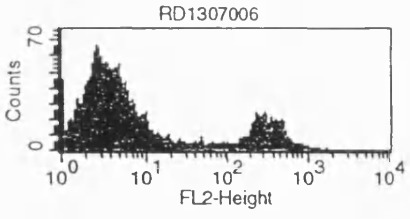

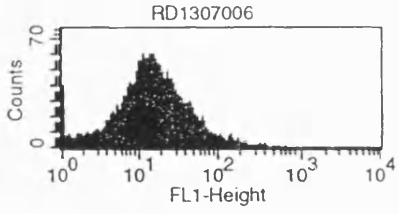

125/400V

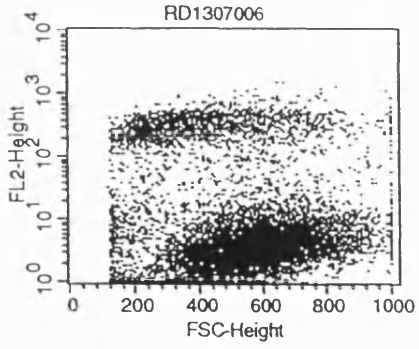

File: RD1307006 Sample ID: 125/400
X Parameter: FL1-H FL1-Height (Log)

Mean	Peak Ch
21.29	1

File: RD1307006 Sample ID: 125/400
Gated Events: 10000

Events	% Gated
7266	72.66

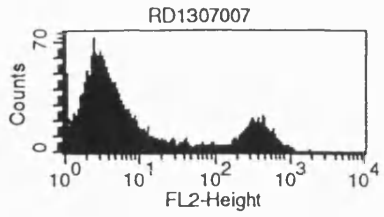

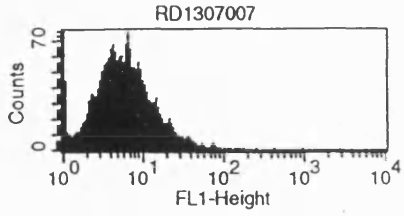

250/100V

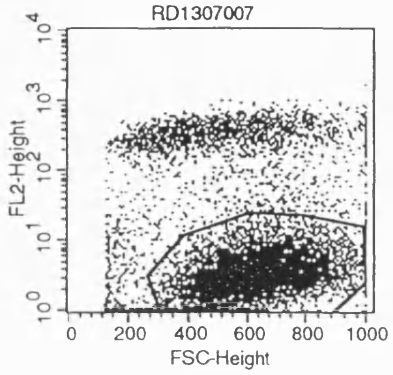

File: RD1307007 Sample ID: 250/100
X Parameter: FL1-H FL1-Height (Log)

Mean	Peak Ch
7.66	1

File: RD1307007 Sample ID: 250/100
Gated Events: 10000

Events	% Gated
7341	73.41

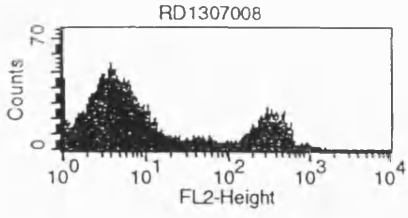

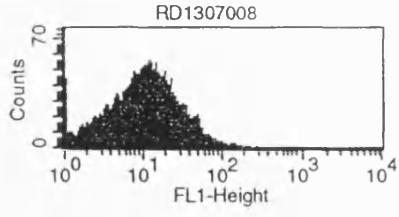

250/200V

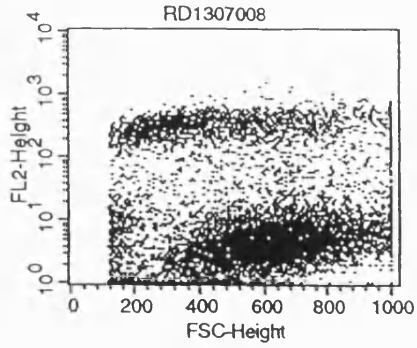

File: RD1307008 Sample ID: 250/200
X Parameter: FL1-H FL1-Height (Log)

Mean	Peak Ch
14.46	1

File: RD1307008 Sample ID: 250/200
Gated Events: 10000

Events	% Gated
6446	64.46

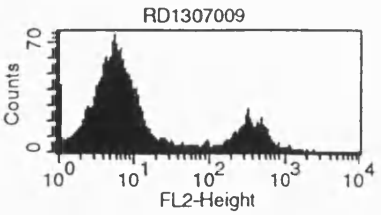

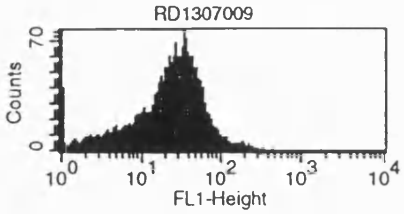

250/300V

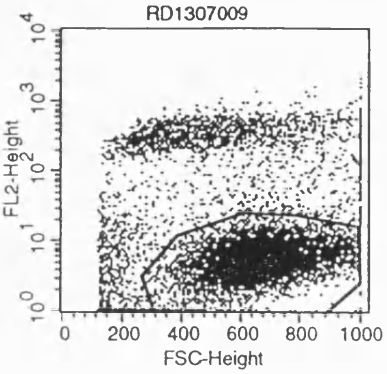

File: RD1307009 Sample ID: 250/300
X Parameter: FL1-H FL1-Height (Log)

Mean	Peak Ch
30.34	1

File: RD1307009 Sample ID: 250/300
Gated Events: 10000

Events	% Gated
7086	70.86

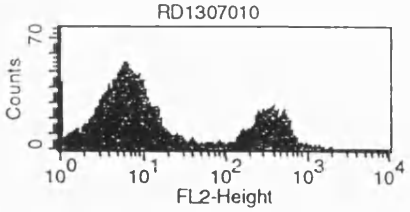

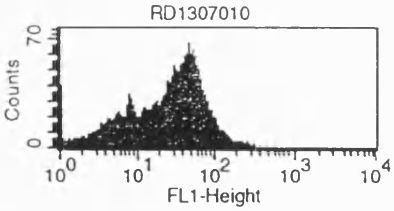

250/350V

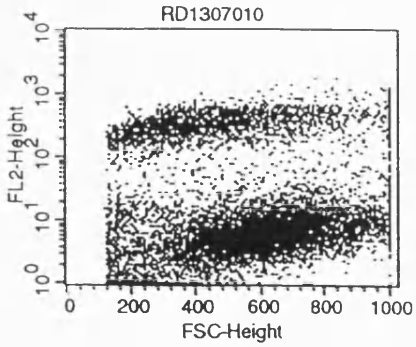

File: RD1307010 Sample ID: 250/350
X Parameter: FL1-H FL1-Height (Log)

Mean	Peak Ch
34.44	1

File: RD1307010 Sample ID: 250/350
Gated Events: 10000

Events	% Gated
6208	62.08

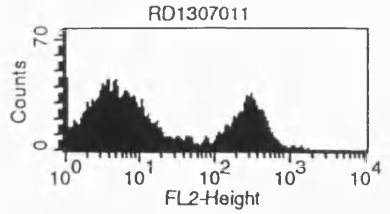

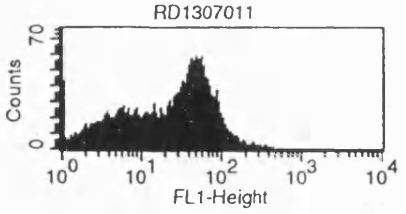

250/400V

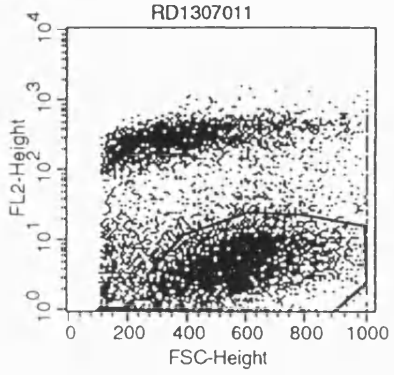

File: RD1307011 Sample ID: 250/4000
X Parameter: FL1-H FL1-Height (Log)

Mean	Peak Ch
35.25	1

File: RD1307011 Sample ID: 250/4000
Gated Events: 10000

Events	% Gated
5265	52.65

APPENDIX E: Statistical Analysis of Binding and cAMP Assay Data

COS7-hMC1R BINDING DATA
AMSH, NLDP, DTRP9, PHE9, TYR9

```
6.300 1
7.450 1
6.040 1
0.753 2
0.517 2
0.775 2
1.730 3
1.280 3
1.520 3
1.750 4
2.130 4
1.580 4
8.600 5
14.400 5
11.300 5

MTB > Oneway c8 c9;
SUBC>   Tukey 5;
SUBC>   Fisher 5.
One-Way Analysis of Variance

Analysis of Variance on C8
Source     DF        SS        MS        F        p
C9          4    249.38     62.35    34.12    0.000
Error      10     18.27      1.83
Total      14    267.66
                                    Individual 95% CIs For Mean
                                    Based on Pooled StDev
 Level      N      Mean     StDev  ---+---------+---------+---------+---
     1      3     6.597     0.750                (---*----)
     2      3     0.682     0.143  (----*---)
     3      3     1.510     0.225    (----*---)
     4      3     1.820     0.282     (----*---)
     5      3    11.433     2.902                              (----*---)
                                    ---+---------+---------+---------+---
Pooled StDev =    1.352              0.0       4.0       8.0      12.0

Tukey's pairwise comparisons
    Family error rate = 0.0500
Individual error rate = 0.00819

Critical value = 4.65

Intervals for (column level mean) - (row level mean)

               1         2         3         4

     2     2.286
           9.544

     3     1.458    -4.457
           8.716     2.801

     4     1.148    -4.767    -3.939
           8.406     2.491     3.319

     5    -8.466   -14.381   -13.552   -13.242
          -1.208    -7.123    -6.294    -5.984
```

```
Fisher's pairwise comparisons

    Family error rate = 0.245
Individual error rate = 0.0500

Critical value = 2.228

Intervals for (column level mean) - (row level mean)

               1         2         3         4

     2     3.456
           8.374

     3     2.628    -3.287
           7.546     1.631

     4     2.318    -3.597    -2.769
           7.236     1.321     2.149

     5    -7.296   -13.211   -12.382   -12.072
          -2.378    -8.293    -7.464    -7.154
```

COS7-hMC1R BINDING DATA
AMSH, THR9, ALA9

```
0.8   1
0.5   1
0.8   1
3420.0      2
3460.0      2
1220.0      2
1590.0      2
32500.0     3
19000.0     3
19400.0     3
32800.0     3

SUBC>   Tukey 5;
SUBC>   Fisher 5.

One-Way Analysis of Variance

Analysis of Variance on C35
Source     DF        SS        MS        F        p
C36         2 1.543E+09 771504832    33.32    0.000
Error       8 185237968  23154746
Total      10 1.728E+09
                                  Individual 95% CIs For Mean
                                  Based on Pooled StDev
 Level      N      Mean     StDev  ------+---------+---------+---------+
     1      3         1         0   (----*----)
     2      4      2423      1185     (----*----)
     3      4     25925      7768                          (----*---)
                                  ------+---------+---------+---------+
Pooled StDev =     4812                0     12000     24000     36000

Tukey's pairwise comparisons

    Family error rate = 0.0500
Individual error rate = 0.0212
```

Critical value = 4.04

Intervals for (column level mean) - (row level mean)

	1	2
2	-12921 8077	
3	-36423 -15425	-33223 -13782

Fisher's pairwise comparisons

Family error rate = 0.112
Individual error rate = 0.0500

Critical value = 2.306

Intervals for (column level mean) - (row level mean)

	1	2
2	-10897 6053	
3	-34399 -17449	-31349 -15656

293-hMC1R: BINDING DATA
NLDP, AMSH, desacetyl-AMSH

```
26.20 1
30.70 1
34.60 1
29.20 1
6.62  2
5.58  2
5.12  2
5.40  2
7.69  2
7.21  2
5.39  2
4.54  2
4.11  2
8.23  3
7.64  3
8.22  3
```

One-Way Analysis of Variance
Analysis of Variance on C23

Source	DF	SS	MS	F	p
C24	2	1720.06	860.03	231.39	0.000
Error	13	48.32	3.72		
Total	15	1768.37			

```
                                    Individual 95% CIs For Mean
                                     Based on Pooled StDev
 Level      N      Mean      StDev  -----+---------+---------+---------+-
     1      4    30.175      3.493                                 (--*-)
     2      9     5.740      1.198  (-*-)
     3      3     8.030      0.338    (--*--)
                                    -----+---------+---------+---------+-
Pooled StDev =    1.928               8.0      16.0      24.0      32.0

Tukey's pairwise comparisons

    Family error rate = 0.0500
Individual error rate = 0.0205

Critical value = 3.73

Intervals for (column level mean) - (row level mean)

               1         2

     2    21.379
          27.491

     3    18.261    -5.680
          26.029     1.100



Fisher's pairwise comparisons

    Family error rate = 0.116
Individual error rate = 0.0500

Critical value = 2.160

Intervals for (column level mean) - (row level mean)

               1         2

     2    21.933
          26.937

     3    18.964    -5.066
          25.326     0.486
```

293-hMC1R BINDING DATA
AMSH, ASP10, PHE10, PHE12, ASP10,PHE12

```
26.2  1
30.7  1
34.6  1
29.2  1
52.4  2
97.8  2
85.6  2
41.6  3
31.6  3
25.7  3
16.4  3
22.8  3
198.0 4
164.0 4
101.0 4
149.0 4
```

```
136.0 5
161.0 5
174.0 5

MTB > Stack ('n' ) ('ASP10') ('PHE10') ('PHE12') ('ASPPHE') (c25);
SUBC>   Subscripts c26.
MTB > Oneway c25 c26;
SUBC>   Tukey 5;
SUBC>   Fisher 5.

One-Way Analysis of Variance

Analysis of Variance on C25
Source     DF        SS        MS        F        p
C26         4     62583     15646    30.78    0.000
Error      14      7117       508
Total      18     69699
                                    Individual 95% CIs For Mean
                                    Based on Pooled StDev
 Level      N      Mean     StDev  ---------+---------+---------+-------
     1      4     30.17      3.49  (----*----)
     2      3     78.60     23.50            (-----*----)
     3      5     27.62      9.54  (----*---)
     4      4    153.00     40.27                          (----*---)
     5      3    157.00     19.31                          (----*-----)
                                    ---------+---------+---------+-------
Pooled StDev =    22.55                    50        100       150

Tukey's pairwise comparisons

    Family error rate = 0.0500
Individual error rate = 0.00755

Critical value = 4.41

Intervals for (column level mean) - (row level mean)

               1         2         3         4

     2    -102.1
             5.3

     3     -44.6      -0.4
            49.7     102.3

     4    -172.5    -128.1    -172.5
           -73.1     -20.7     -78.2

     5    -180.5    -135.8    -180.7     -57.7
           -73.1     -21.0     -78.0      49.7


Fisher's pairwise comparisons

    Family error rate = 0.256
Individual error rate = 0.0500

Critical value = 2.145
```

```
Intervals for (column level mean) - (row level mean)

               1         2         3         4

     2     -85.4
           -11.5

     3     -29.9      15.7
            35.0      86.3

     4    -157.0    -111.3    -157.8
           -88.6     -37.5     -92.9

     5    -163.8    -117.9    -164.7     -40.9
           -89.9     -38.9     -94.1      32.9
```

293-hMC1R BINDING DATA
AMSH, ALA11,ALA12, ALA11,ALA13, ALA11,12,13

```
26.2  1
30.7  1
34.6  1
29.2  1
256.0 2
291.0 2
296.0 2
33.8  3
22.2  3
38.8  3
39.6  3
603.0 4
218.0 4
523.0 4

MTB > Stack ('n' ) ('ALA112') ('ALA113') ('ALA123') (c27);
SUBC>   Subscripts c28.
MTB > Oneway c27 c28;
SUBC>   Tukey 5;
SUBC>   Fisher 5.

One-Way Analysis of Variance

Analysis of Variance on C27
Source     DF        SS        MS        F        p
C28         3    421164    140388    16.77    0.000
Error      10     83730      8373
Total      13    504893
                                    Individual 95% CIs For Mean
                                    Based on Pooled StDev
 Level      N      Mean     StDev  ----+---------+---------+---------+--
     1      4     30.17      3.49  (-----*----)
     2      3    281.00     21.79              (-----*-----)
     3      4     33.60      8.02   (----*----)
     4      3    448.00    203.16                        (----*-----)
                                    ----+---------+---------+---------+--
Pooled StDev =    91.50               0       200       400       600

Tukey's pairwise comparisons

    Family error rate = 0.0500
Individual error rate = 0.0120

Critical value = 4.33
```

```
Intervals for (column level mean) - (row level mean)

               1         2         3

     2    -464.8
           -36.8

     3    -201.5      33.4
           194.7     461.4

     4    -631.8    -395.8    -628.4
          -203.8      61.8    -200.4


Fisher's pairwise comparisons

    Family error rate = 0.181
Individual error rate = 0.0500

Critical value = 2.228

Intervals for (column level mean) - (row level mean)

               1         2         3

     2    -406.5
           -95.1

     3    -147.6      91.7
           140.7     403.1

     4    -573.5    -333.5    -570.1
          -262.1      -0.5    -258.7
```

293-hMC1R cAMP DATA
NLDP, AMSH, desacetyl-AMSH

```
0.210 1
0.652 1
0.229 1
0.324 1
0.405 1
3.170 2
3.150 2
3.250 2
4.160 3
3.190 3
4.260 3

MTB > Stack ('nldp') ('amsh') ('des') (c4);
SUBC>   Subscripts c5.
MTB > Oneway c4 c5.

One-Way Analysis of Variance

Analysis of Variance on C4
Source     DF        SS        MS        F        p
C5          2    28.031    14.015   134.70    0.000
Error       8     0.832     0.104
Total      10    28.863

                                  Individual 95% CIs For Mean
                                  Based on Pooled StDev
```

```
 Level      N      Mean     StDev  ----------+---------+---------+------
     1      5    0.3640    0.1790  (--*--)
     2      3    3.1900    0.0529                      (---*--)
     3      3    3.8700    0.5910                            (--*---)
                                   ----------+---------+---------+------
Pooled StDev =   0.3226                1.2       2.4       3.6
MTB > Oneway c4 c5;
SUBC>   Tukey 5;
SUBC>   Fisher 5.


Tukey's pairwise comparisons

    Family error rate = 0.0500
Individual error rate = 0.0212

Critical value = 4.04

Intervals for (column level mean) - (row level mean)

               1         2

     2   -3.4989
         -2.1531

     3   -4.1789   -1.4324
         -2.8331    0.0724
```

293-hMC1R cAMP DATA
AMSH, ASP10, PHE10, PHE12, ASP10,PHE12

```
3.17  1
3.15  1
3.25  1
5.47  2
3.48  2
4.01  2
2.85  3
3.57  3
4.12  3
2.98  3
75.80 4
83.90 4
93.30 4
97.40 4
439.00      5
304.00      5
298.00      5
295.00      5

MTB > Stack ('amsh') ('asp10') ('phe10') ('phe12') ('aspphe') (c10);
SUBC>   Subscripts c11.
MTB > Oneway c10 c11;
SUBC>   Tukey 5;
SUBC>   Fisher 5.


One-Way Analysis of Variance


Analysis of Variance on C10
Source     DF        SS        MS        F        p
C11         4    312227     78057    67.53    0.000
Error      13     15027      1156
```

```
Total      17    327254

                                    Individual 95% CIs For Mean
                                    Based on Pooled StDev
 Level      N      Mean     StDev  ----+---------+---------+---------+--
     1      3      3.19      0.05   (--*---)
     2      3      4.32      1.03   (--*---)
     3      4      3.38      0.58   (--*--)
     4      4     87.60      9.69          (--*--)
     5      4    334.00     70.10                          (--*--)
                                    ----+---------+---------+---------+--
Pooled StDev =    34.00               0        120       240       360

Tukey's pairwise comparisons

    Family error rate = 0.0500
Individual error rate = 0.00772

Critical value = 4.45

Intervals for (column level mean) - (row level mean)

               1         2         3         4

     2     -88.5
            86.2

     3     -81.9     -80.8
            81.5      82.6

     4    -166.1    -165.0    -159.9
           -2.7      -1.6      -8.6

     5    -412.5    -411.4    -406.3    -322.0
          -249.1    -248.0    -255.0    -170.8


Fisher's pairwise comparisons

    Family error rate = 0.254
Individual error rate = 0.0500

Critical value = 2.160

Intervals for (column level mean) - (row level mean)

               1         2         3         4

     2     -61.1
            58.8

     3     -56.3     -55.1
            55.9      57.0

     4    -140.5    -139.4    -136.1
           -28.3     -27.2     -32.3

     5    -386.9    -385.8    -382.5    -298.3
          -274.7    -273.6    -278.7    -194.5
```

293-hMC1R cAMP DATA
AMSH, ALA112, ALA113, ALA11,12,13

```
3.17  1
3.15  1
3.25  1
79.00 2
75.40 2
74.50 2
7.56  3
6.42  3
7.50  3
155.00      4
182.00      4
265.00      4

MTB > Stack (c1 ) (c3) (c4) (c5) (c27);
SUBC>   Subscripts c28.
MTB > Oneway c27 c28;
SUBC>   Tukey 5;
SUBC>   Fisher 5.

One-Way Analysis of Variance

Analysis of Variance on C27
Source     DF        SS        MS        F        p
C28         3     76538     25513    31.00    0.000
Error       8      6585       823
Total      11     83122
                                    Individual 95% CIs For Mean
                                    Based on Pooled StDev
 Level      N      Mean     StDev  -----+---------+---------+---------+-
     1      3      3.19      0.05   (---*----)
     2      3     76.30      2.38             (----*---)
     3      3      7.16      0.64   (----*----)
     4      3    200.67     57.33                          (----*----)
                                    -----+---------+---------+---------+-
Pooled StDev =    28.69                 0         80        160       240

Tukey's pairwise comparisons

    Family error rate = 0.0500
Individual error rate = 0.0126

Critical value = 4.53

Intervals for (column level mean) - (row level mean)

               1         2         3

     2    -148.1
            1.9

     3     -79.0      -5.9
            71.1     144.2

     4    -272.5    -199.4    -268.5
          -122.4     -49.3    -118.5



Fisher's pairwise comparisons

    Family error rate = 0.176
Individual error rate = 0.0500
```

```
Critical value = 2.306

Intervals for (column level mean) - (row level mean)

               1         2         3

     2    -127.1
           -19.1

     3     -58.0      15.1
            50.0     123.2

     4    -251.5    -178.4    -247.5
          -143.5     -70.3    -139.5
```

293-hMC1R BINDING DATA
PHE12, ASP10,PHE12, ALA11,12, ALA11,12,13

```
198   1
164   1
101   1
149   1
136   2
161   2
174   2
256   3
291   3
296   3
603   4
218   4
523   4

SUBC>   Subscripts c42.
MTB > Oneway c41 c42;
SUBC>   Tukey 5;
SUBC>   Fisher 5.

One-Way Analysis of Variance

Analysis of Variance on C41
Source     DF        SS        MS        F        p
C42         3    184047     61349     6.20    0.014
Error       9     89112      9901
Total      12    273159
                                  Individual 95% CIs For Mean
                                  Based on Pooled StDev
 Level      N      Mean     StDev  ---------+---------+---------+-------
     1      4    153.00     40.27    (------*-------)
     2      3    157.00     19.31   (-------*--------)
     3      3    281.00     21.79           (--------*-------)
     4      3    448.00    203.16                     (--------*--------
                                  ---------+---------+---------+-------
Pooled StDev =    99.51                  150       300       450

Tukey's pairwise comparisons

    Family error rate = 0.0500
Individual error rate = 0.0122

Critical value = 4.42
```

```
Intervals for (column level mean) - (row level mean)
               1         2         3

     2    -241.5
           233.5

     3    -365.5    -377.9
           109.5     129.9

     4    -532.5    -544.9    -420.9
           -57.5     -37.1      86.9



Fisher's pairwise comparisons

    Family error rate = 0.178
Individual error rate = 0.0500

Critical value = 2.262

Intervals for (column level mean) - (row level mean)

               1         2         3

     2    -175.9
           167.9

     3    -299.9    -307.8
            43.9      59.8

     4    -466.9    -474.8    -350.8
           -123.1    -107.2      16.8
```

293-hMC1R cAMP DATA
PHE12, ASP10,PHE12, ALA11,12, ALA11,12,13

```
75.8  1
83.9  1
93.3  1
97.4  1
439.0 2
304.0 2
298.0 2
295.0 2
79.0  3
75.4  3
74.5  3
155.0 4
182.0 4
265.0 4

MTB > Oneway c47 c48;
SUBC>   Tukey 5;
SUBC>   Fisher 5.


One-Way Analysis of Variance

Analysis of Variance on C47
Source     DF        SS        MS        F        p
C48         3    162557     54186    25.08    0.000
Error      10     21607      2161
Total      13    184164
```

```
                                    Individual 95% CIs For Mean
                                    Based on Pooled StDev
 Level      N      Mean      StDev  ---------+---------+---------+-------
     1      4     87.60       9.69     (----*----)
     2      4    334.00      70.10                               (----*-----
     3      3     76.30       2.38   (-----*-----)
     4      3    200.67      57.33                (-----*-----)
                                    ---------+---------+---------+-------
Pooled StDev =    46.48                    100       200       300

Tukey's pairwise comparisons

    Family error rate = 0.0500
Individual error rate = 0.0120

Critical value = 4.33

Intervals for (column level mean) - (row level mean)

               1         2         3

     2    -347.0
          -145.8

     3     -97.4     149.0
           120.0     366.4

     4    -221.8      24.6    -240.6
           -4.4     242.0      -8.2


Fisher's pairwise comparisons

    Family error rate = 0.181
Individual error rate = 0.0500

Critical value = 2.228

Intervals for (column level mean) - (row level mean)

               1         2         3

     2    -319.6
          -173.2

     3     -67.8     178.6
           90.4     336.8

     4    -192.2      54.2    -208.9
          -34.0     212.4     -39.8
```

293-hMC4R BINDING DATA
NLDP, AMSH, desacetyl-AMSH

```
0.583 1
0.513 1
0.497 1
0.629 1
0.623 1
7.880 2
6.770 2
7.340 2
```

```
7.890 2
7.240 2
6.560 2
4.490 3
5.030 3
4.340 3

MTB > Stack ('n') ('a') ('des') (c4);
SUBC>   Subscripts c5.
MTB > Oneway c4 c5;
SUBC>   Tukey 5;
SUBC>   Fisher 5.

One-Way Analysis of Variance

Analysis of Variance on C4
Source     DF        SS        MS        F        p
C5          2   123.189    61.594   377.62    0.000
Error      11     1.794     0.163
Total      13   124.983
                                    Individual 95% CIs For Mean
                                    Based on Pooled StDev
 Level      N      Mean     StDev  ----------+---------+---------+------
     1      5    0.5690    0.0613   (*-)
     2      6    7.2800    0.5506                                (*-)
     3      3    4.6200    0.3629                     (-*--)
                                    ----------+---------+---------+------
Pooled StDev =   0.4039                    2.5       5.0       7.5

Tukey's pairwise comparisons

    Family error rate = 0.0500
Individual error rate = 0.0206

Critical value = 3.82

Intervals for (column level mean) - (row level mean)

               1         2

     2   -7.3716
         -6.0504

     3   -4.8477    1.8886
         -3.2543    3.4314



Fisher's pairwise comparisons

    Family error rate = 0.115
Individual error rate = 0.0500

Critical value = 2.201
Intervals for (column level mean) - (row level mean)

               1         2

     2   -7.2493
         -6.1727

     3   -4.7002    2.0314
         -3.4018    3.2886
```

293-hMC4R BINDING DATA
AMSH, (ASP10), PHE10, PHE12, (ASP10,PHE12)

```
0.583 1
0.513 1
7.88  1
6.77  1
7.34  1
7.89  1
7.24  1
6.56  1
237.00      2
151.00      2
199.00      2
193.00      2
29.40 3
24.80 3
19.70 3
20.10 3

MTB > Oneway c9 c10;
SUBC>   Tukey 5;
SUBC>   Fisher 5.

One-Way Analysis of Variance

Analysis of Variance on C9
Source     DF        SS        MS        F        p
C10         2     94474     47237   137.32    0.000
Error      11      3784       344
Total      13     98258
                                    Individual 95% CIs For Mean
                                    Based on Pooled StDev
 Level      N      Mean     StDev  --+---------+---------+---------+----
     1      6      7.28      0.55   (-*-)
     2      4    195.00     35.21                              (--*--)
     3      4     23.50      4.56    (--*--)
                                    --+---------+---------+---------+----
Pooled StDev =    18.55               0         70        140       210

Tukey's pairwise comparisons

    Family error rate = 0.0500
Individual error rate = 0.0206

Critical value = 3.82



Intervals for (column level mean) - (row level mean)

               1         2

     2   -220.06
         -155.38

     3    -48.56    136.07
           16.12    206.93



Fisher's pairwise comparisons

    Family error rate = 0.115
```

```
Individual error rate = 0.0500

Critical value = 2.201

Intervals for (column level mean) - (row level mean)

               1         2

     2   -214.07
         -161.37

     3    -42.57    142.63
           10.13    200.37
```

293-hMC4R BINDING DATA
AMSH, ALA11,12, ALA11,13, ALA11,12,13

```
7.88  1
6.77  1
7.34  1
7.89  1
7.24  1
6.56  1
18.70 2
21.70 2
29.80 2
20.80 3
29.30 3
25.50 3
53.60 4
47.60 4
46.10 4

MTB > Stack ('a') (C11) (C12) (C13) (c14);
SUBC>   Subscripts c15.
MTB > Oneway c14 c15;
SUBC>   Tukey 5;
SUBC>   Fisher 5.

One-Way Analysis of Variance

Analysis of Variance on C14
Source     DF        SS        MS        F        p
C15         3    3536.8    1178.9    95.91    0.000
Error      11     135.2      12.3
Total      14    3672.1
                                    Individual 95% CIs For Mean
                                    Based on Pooled StDev
 Level      N      Mean     StDev  --------+---------+---------+--------
     1      6     7.280     0.551   (-*-)
     2      3    23.400     5.742             (--*--)
     3      3    25.200     4.258              (--*--)
     4      3    49.100     3.969                               (--*--)
                                    --------+---------+---------+--------
Pooled StDev =    3.506              15        30        45

Tukey's pairwise comparisons

    Family error rate = 0.0500
Individual error rate = 0.0118

Critical value = 4.26

Intervals for (column level mean) - (row level mean)
```

```
              1         2         3

     2   -23.588
          -8.652

     3   -25.388   -10.423
         -10.452     6.823

     4   -49.288   -34.323   -32.523
         -34.352   -17.077   -15.277


Fisher's pairwise comparisons

    Family error rate = 0.183
Individual error rate = 0.0500

Critical value = 2.201

Intervals for (column level mean) - (row level mean)

              1         2         3

     2   -21.577
         -10.663

     3   -23.377    -8.101
         -12.463     4.501

     4   -47.277   -32.001   -30.201
         -36.363   -19.399   -17.599
```

293-hMC4R cAMP DATA
NLDP, AMSH, desacetyl-AMSH

```
0.201 1
0.317 1
0.206 1
0.105 1
0.137 1
0.086 1
7.310 2
5.990 2
7.370 2
1.160 3
2.200 3
2.940 3

MTB > Stack (C16) (C17) (C18) (c19);
SUBC>   Subscripts c20.
MTB > Oneway c19 c20;
SUBC>   Tukey 5;
SUBC>   Fisher 5.

One-Way Analysis of Variance

Analysis of Variance on C19
Source     DF        SS        MS        F        p
C20         2    90.395    45.197   142.63    0.000
Error       9     2.852     0.317
Total      11    93.247
                                  Individual 95% CIs For Mean
                                  Based on Pooled StDev
```

```
 Level      N      Mean     StDev  --+---------+---------+---------+----
     1      6    0.1753    0.0849   (-*-)
     2      3    6.8900    0.7800                              (--*--)
     3      3    2.1000    0.8942          (--*--)
                                    --+---------+---------+---------+----
Pooled StDev =    0.5629            0.0       2.5       5.0       7.5

Tukey's pairwise comparisons

    Family error rate = 0.0500
Individual error rate = 0.0209

Critical value = 3.95

Intervals for (column level mean) - (row level mean)

               1         2

     2   -7.8265
         -5.6029

     3   -3.0365    3.5062
         -0.8129    6.0738



Fisher's pairwise comparisons

    Family error rate = 0.113
Individual error rate = 0.0500

Critical value = 2.262

Intervals for (column level mean) - (row level mean)

               1         2

     2   -7.6151
         -5.8143

     3   -2.8251    3.7503
         -1.0243    5.8297
```

293-hMC4R cAMP DATA
AMSH, ASP10, PHE10, PHE12, ASP10,PHE12

```
7.31  1
5.99  1
7.37  1
307.00      2
207.00      2
155.00      2
44.70 3
29.70 3
30.00 3
5.97  4
4.09  4
5.03  4
391.00      5
287.00      5
348.00      5
```

```
MTB > Stack (C17) (C21) (C22) (C23) (C24) (c25);
SUBC>   Subscripts c26.
MTB > Oneway c25 c26;
SUBC>   Tukey 5;
SUBC>   Fisher 5.

One-Way Analysis of Variance

Analysis of Variance on C25
Source     DF        SS        MS        F        p
C26         4    279410     69852    39.81    0.000
Error      10     17548      1755
Total      14    296958

                                    Individual 95% CIs For Mean
                                    Based on Pooled StDev
 Level      N      Mean     StDev  ----+---------+---------+---------+--
     1      3      6.89      0.78   (--*---)
     2      3    223.00     77.25                (---*--)
     3      3     34.80      8.57     (--*---)
     4      3      5.03      0.94   (--*---)
     5      3    342.00     52.26                        (---*--)
                                    ----+---------+---------+---------+--
Pooled StDev =    41.89               0       150       300       450

Tukey's pairwise comparisons

    Family error rate = 0.0500
Individual error rate = 0.00819

Critical value = 4.65

Intervals for (column level mean) - (row level mean)

               1         2         3         4

     2    -328.6
          -103.6

     3    -140.4      75.7
            84.6     300.7

     4    -110.6     105.5     -82.7
           114.3     330.4     142.2

     5    -447.6    -231.5    -419.7    -449.4
          -222.6      -6.5    -194.7    -224.5


Fisher's pairwise comparisons

    Family error rate = 0.245
Individual error rate = 0.0500

Critical value = 2.228

Intervals for (column level mean) - (row level mean)

               1         2         3         4

     2    -292.3
          -139.9

     3    -104.1     112.0
            48.3     264.4
```

```
     4     -74.3      141.8      -46.4
            78.1      294.2      106.0

     5    -411.3     -195.2     -383.4     -413.2
          -258.9      -42.8     -231.0     -260.8
```

293-hMC4R cAMP DATA
AMSH, ALA11,12, ALA11,13, ALA11,12,13

```
7.31  1
5.99  1
7.37  1
31.60 2
22.70 2
20.40 2
18.40 3
23.20 3
21.40 3
106.00      4
82.90 4
95.80 4

MTB > Stack (C1) (C2) (C3) (C4) (c5);
SUBC>   Subscripts c6.
MTB > Oneway c5 c6;
SUBC>   Tukey 5;
SUBC>   Fisher 5.

One-Way Analysis of Variance

Analysis of Variance on C5
Source     DF        SS        MS        F        p
C6          3   13984.2    4661.4   106.25    0.000
Error       8     351.0      43.9
Total      11   14335.2
                                  Individual 95% CIs For Mean
                                  Based on Pooled StDev
 Level      N      Mean     StDev  -+---------+---------+---------+-----
     1      3      6.89      0.78  (--*--)
     2      3     24.90      5.92        (--*--)
     3      3     21.00      2.42      (--*--)
     4      3     94.90     11.58                                (--*--)
                                  -+---------+---------+---------+-----
Pooled StDev =     6.62             0         30        60        90

Tukey's pairwise comparisons

    Family error rate = 0.0500
Individual error rate = 0.0126

Critical value = 4.53

Intervals for (column level mean) - (row level mean)

               1         2         3

     2    -35.33
           -0.69

     3    -31.43    -13.42
            3.21     21.22

     4   -105.33    -87.32    -91.22
          -70.69    -52.68    -56.58
```

```
Fisher's pairwise comparisons

    Family error rate = 0.176
Individual error rate = 0.0500

Critical value = 2.306

Intervals for (column level mean) - (row level mean)

               1         2         3

     2    -30.48
           -5.54

     3    -26.58     -8.57
           -1.64     16.37

     4   -100.48    -82.47    -86.37
          -75.54    -57.53    -61.43
```